

May 27, 2022

Madison County Seismic and Liquefaction Hazard Maps
(HUD Grant Year Five Products)

Chris H. Cramer, Roy B. Van Arsdale, Valarie Harrison, David Arellano, Hamed Tohidi, Roshan Bhattarai, Shahram Pezeshk, and Mohsen Senejani

Abstract

A five-year seismic and liquefaction hazard mapping project for five western Tennessee counties began in 2017 under a Disaster Resilience Competition grant from the U.S. Department of Housing and Urban Development to the State of Tennessee. The project supports natural hazard (flood and earthquake) mitigation efforts in these five counties. The seismic hazard maps for Madison County in western Tennessee were completed in 2022. Additional geological, seismological, and geotechnical information has been gathered in Madison Co. to improve the base northern Mississippi Embayment hazard maps of Dhar and Cramer (2018). Information gathered includes additional geological and geotechnical subsurface exploration logs, water table level data collection and measurements, and new measurements of shallow shear-wave velocity (V_s) profiles. Improvements were made in the 3D geological model, water table model, and the geotechnical liquefaction probability curves, and the V_s correlation with lithology model for Madison County. Resulting improved soil response amplification distributions on a 0.5 km grid were combined with the 2014 U.S. Geological Survey seismic hazard model (Petersen et al., 2014) sources and attenuation models to add the effect of local geology for Madison Co. Resulting products are an improved 3D-geology, geotechnical, seismic hazard, and liquefaction hazard models and maps for Madison Co. Seismic hazard maps at PGA and 1.0 s show a 50% decrease to 100% increase in hazard at short periods and a 0-100% increase at long periods compared with 2014 USGS NSHMP maps.

Introduction

As part of the 2015 Disaster Resilience Competition, the State of Tennessee received funds from the Department of Housing and Urban Development (HUD) for several grants for flood hazard mitigation efforts. The University of Memphis received one of the grants for flood and seismic hazard mapping efforts in five western Tennessee counties (Figure 1) covering a five-year period starting in 2017. The fifth-year seismic hazard mapping effort is for Madison County seismic and liquefaction hazard maps (this report).

The goal for the seismic hazard mapping project is to develop seismic and liquefaction hazard maps for use in flood hazard mitigation efforts in other portions of the HUD grant effort via the University of Memphis. The hazard maps will also be useful for other earthquake hazard mitigation efforts in the five western Tennessee counties.

HUD Project Counties

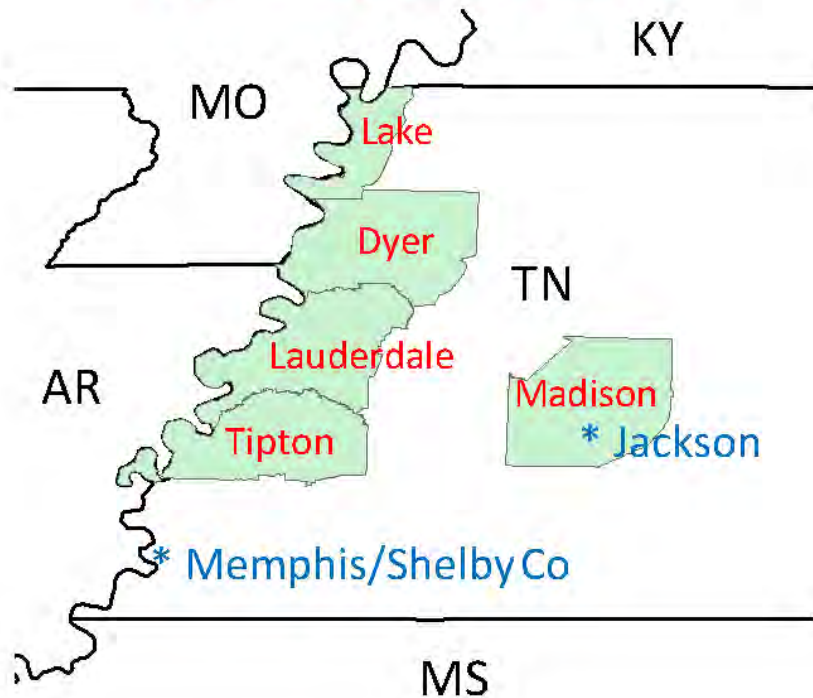


Figure 1: Five western Tennessee counties of the HUD grant supported seismic hazard study. AR – Arkansas, KY – Kentucky, MO – Missouri, MS – Mississippi, and TN – Tennessee.

The major elements to the seismic and liquefaction hazard mapping in this project are (1) geological 3D model development, (2) geotechnical (soil response to ground motions) model development, and (3) hazard maps generation. The 3D geological model of sediments above bedrock involves the gathering and interpretation of boring logs, entering geological information into a geographic information system (GIS), and developing maps of the depth to the tops of key geological sediment layers. The accompanying geotechnical model involves the gathering of geotechnical information (sediment properties and water table levels) from boring logs, and modeling liquefaction potential of the shallow sediments. Seismological data gathering includes making new measurements of sediment velocity with depth in the study area. The final step is to integrate the geological, geotechnical, and seismological data into a county wide hazard model and maps that included the effects of local geology (sediments).

Geological Model

Introduction

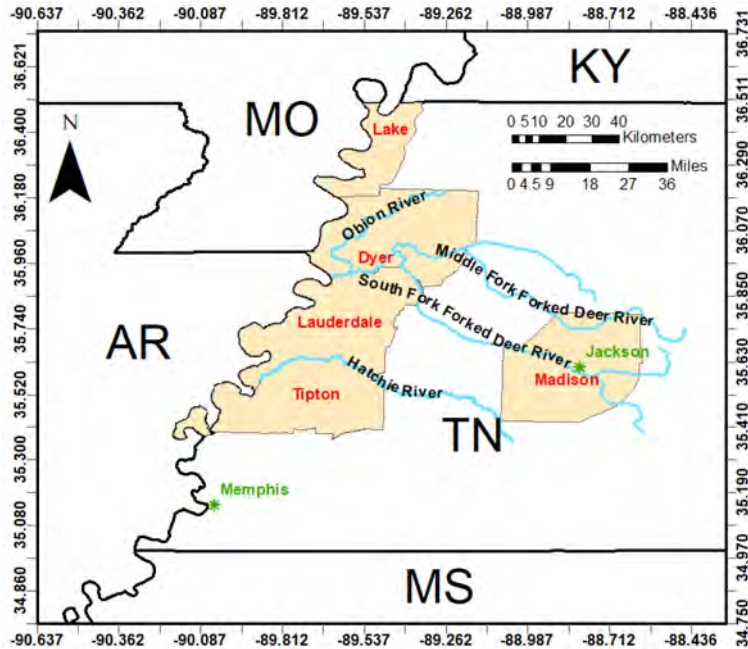
Madison County in western Tennessee was mapped as part of a five-county earthquake hazard mapping program (Figure 2) (Cramer et al., 2018b). Located 100 km southeast of the New Madrid seismic zone, Madison County may be vulnerable to both earthquake ground shaking and liquefaction in the event of future large New Madrid earthquakes (Chiu et al., 1992; Cramer, 2006; Csontos and Van Arsdale, 2008; Cramer and Boyd, 2014; Cramer et al., 2018a and b).

The topography of Madison County consists of lowland floodplains of the South Fork of Forked Deer, Middle Fork of Forked Deer, and Hatchie rivers, terraces of these rivers, and areas of Paleogene and Late Cretaceous strata (Figure 2) (Brown, 1968a, 1968b; Parks, 1968a-f; Saucier, 1987; Jewel, 2006; Antonacci, V., and Hoyal, M., 2011, 2012a, 2012b, 2014a, 2014b). Thin Pleistocene loess (wind-blown silt) overlies the terraces, Paleogene, and Cretaceous sediments. Beneath the floodplain and terrace deposits are Eocene (~34 Ma) sediments that overlie older Paleogene, Late Cretaceous, and Paleozoic strata (Figures 3 and 4). No faults have been mapped in Madison County (Figure 3A). The surface and subsurface geology of a region influences how the landscape will react during a large proximal earthquake. In this study we present geologic maps and a three-dimensional geologic model of Madison County that provide important information for companion seismologic and liquefaction hazard modeling studies (e. g. Cramer et al., 2020a).

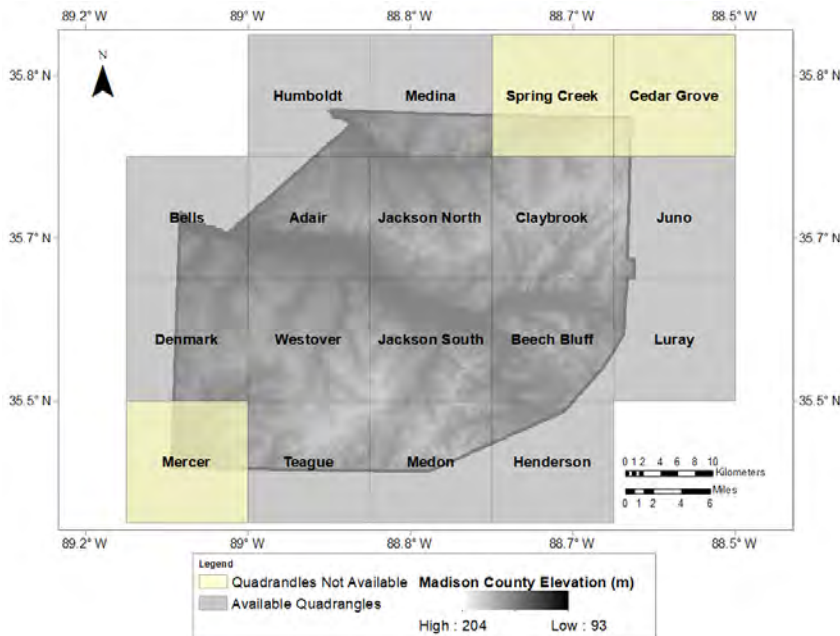
Methods

The surface geology of Madison County, except for the Mercer, Cedar Grove, and Spring Creek 7.5 minute topographic quadrangles, has been mapped at a scale of 1:24,000 (Figure 2A) (Brown, 1968a, 1968b; Parks, 1968a-f; Jewel, 2006; Antonacci and Hoyal, 2011, 2012a, 2012b, 2014a, 2014b). For the purposes of this seismic hazard investigation, Madison County was divided into three surface geologic units: Holocene river floodplain alluvium, Pliocene and or Pleistocene river terrace alluvium, and semi-consolidated sediments of Paleogene and Cretaceous age (Figures 4 and 5). Bedrock beneath Madison County is Paleozoic limestone and dolomite (Figure 2B) (Jewel, 2006). To complete the surface geology of Madison County, 1 m lidar digital elevation models (DEM) of the Mercer, Cedar Grove, and Spring Creek 7.5-minute quadrangles (Figure 1B) were interpreted based on the adjacent 7.5-minute published geologic quadrangle maps and local elevation. Most of the Mercer Quadrangle in Madison County was mapped by Saucier (1987) as Hatchie River terrace and so Saucier's mapping is herein included. The remaining area within the Mercer Quadrangle was mapped by extending alluvium from streams in the surrounding quadrangles through the Hatchie River terrace. To complete the mapping of Madison County, Spring Creek, and Cedar Grove quadrangles were subdivided into sections (27 polygons) (Figure 4). The polygons adjacent to the published surface geology were split into the three classifications of Holocene floodplain alluvium, Pliocene/Pleistocene terrace alluvium, and Paleogene/Cretaceous sediments based on surface elevation. These polygons

were then reclassified until the pattern at the perimeter of the DEM matched the pattern of the known adjacent published surface geology (Figure 2A). This process was then repeated for each polygon. The resulting rasters were then merged into a mosaic to represent the interpreted surface geology of the three quadrangles and then merged with the geology classification of Figure 5 to produce Figure 6.

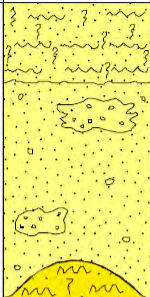
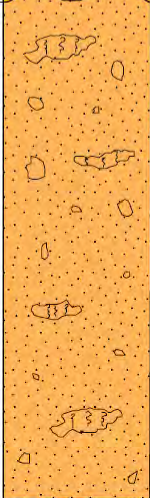


A



B

Figure 2: A) Location of Madison County, Tennessee. B) Mapped 7.5' geologic quadrangle maps of Madison County. The Mercer, Spring Creek, and Cedar Grove quadrangles have not been geologically mapped and published.

SYSTEM AND SERIES		GROUP, FORMATION AND MEMBER		LITHOLOGY	THICKNESS IN FEET	LEGEND
Quaternary	Pleistocene and Holocene	Surficial Deposits			Up to 45'	<p>Qal</p> <p>Alluvium</p> <p>Quartz sand, silt and clay. Alluvial materials are medium gray, olive gray light-olive gray, moderate yellowish-brown, pale yellowish-brown, and light gray. Bedding is normally indistinct or poor. The alluvial rocks are, for the most part, locally derived. Contains occasional and scattered pebbles of quartz and quartzite. The lower part is generally composed of fine-to-coarse grained sand with local lenses of gravel. The upper part, generally, is made up of fine-grained sand, silt, and clay. Thickest concentrations are found in the flood plains of the South Fork and the Middle Fork of the Forked Deer River.</p>
Tertiary(?) and Quaternary	Pliocene(?) and Pleistocene	Fluvial Deposits			Up to 100'	<p>Qf</p> <p>Fluvial Deposits</p> <p>Quartz sand, silty and clayey in part, fine-to-very coarse-grained, normally poorly sorted, poorly stratified to locally cross-bedded. Weathers light-brown to dark reddish-brown. Badly weathered outcrops often display a mottled appearance. Locally contains scattered granules and pebbles of quartz, quartzite, and small pieces of ferruginous sandstone. The basal sand is commonly cemented to form thin layers of ferruginous sandstone. Clay is rarely present. Generally, the lower part of these alluvial deposits consist of chiefly sand and gravel with minor interbeds of clay and the upper part is predominantly composed of silt. The fluvial deposits are remnants of ancient flood-plain alluvium of an earlier drainage system or present streams. These deposits are thickest on the north side of the city of Jackson.</p>
Tertiary	Middle Eocene	Claiborne Formation			Maximum of 40'	<p>Tc</p> <p>Claiborne Formation</p> <p>Quartz sand, pale orange to yellowish-gray (weathers reddish-orange to reddish-brown), fine-to very coarse-grained, poorly sorted to well-sorted, poorly to distinctly cross-bedded. The coarser fraction often contains pebbles of quartz and quartzite. In the western part of the investigated area, a clay stratum is often observed at the contact between the overlying fluvial deposits and the underlying Claiborne Formation. On the whole, however, clay normally occurs as irregular lenses within the predominating sand bodies. The base of the Claiborne Formation was not observed in the quadrangle. The maximum thickness of the formation can only be speculated, but subsurface data in the southwestern part of the quadrangle indicates a total thickness of approximately 220 feet.</p>

C

Figure 3: A) Mapped 7.5' quadrangles of Madison County (from Antonacci, V., and Hoyal, M., 2011, 2012a, 2012b, 2014a, 2014b; Brown, 1968a, 1968b; Jewel, 2006; Parks, 1968a-f). Quadrangles labeled in Figure 2. A-A' line in Jackson North quadrangle indicates location of B cross section. B) West-east geologic cross section of the Jackson North 7.5' geologic quadrangle map (from Jewel, 2006). C) Geologic column of Jackson North 7.5' geologic quadrangle map with 4X vertical exaggeration (from Jewel, 2006).

Subsurface stratigraphic interpretations based on oil and gas and hydrologic test wells.

Tertiary:	Wilcox Group	(Tw)
	Porters Creek Clay	(Tp)
	Clayton Fm.	(Tcl)
Cretaceous:	Owl Creek Fm.	(Ko)
	McNairy Sand	(Km)
	Demopolis Fm.	(Kd)
	Coffee Sand	(Kc)
Paleozoics:		(Pal)

Figure 4: A) Stratigraphy of the subsurface geology of the Jackson North 7.5 Minute Quadrangle map in northcentral Madison County (Figure 2) (from Jewel, 2006). This stratigraphy is appropriate for all of Madison County.

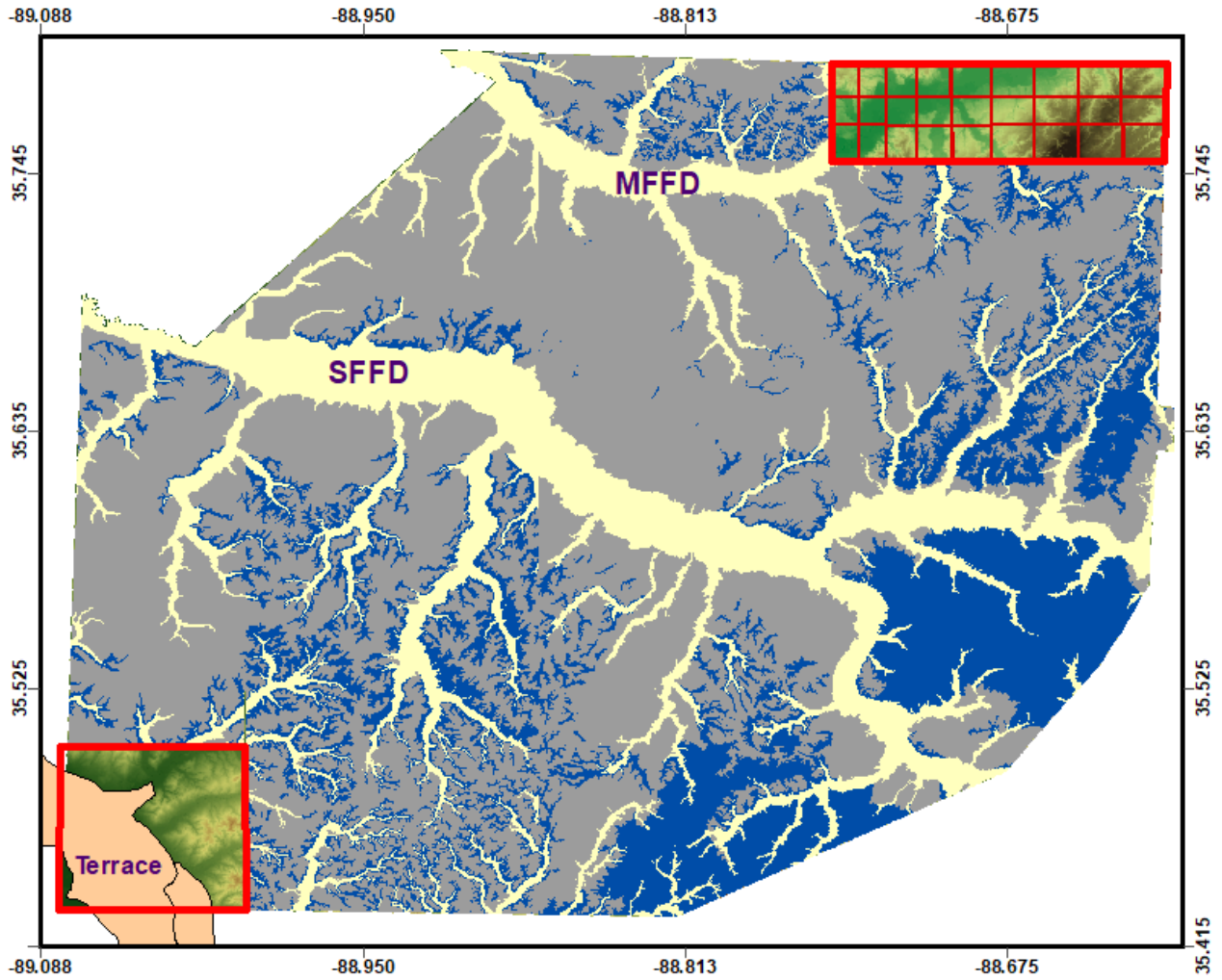


Figure 5: Interpreted portions of Mercer, Spring Creek, and Cedar Grove 7.5-minute quadrangles.

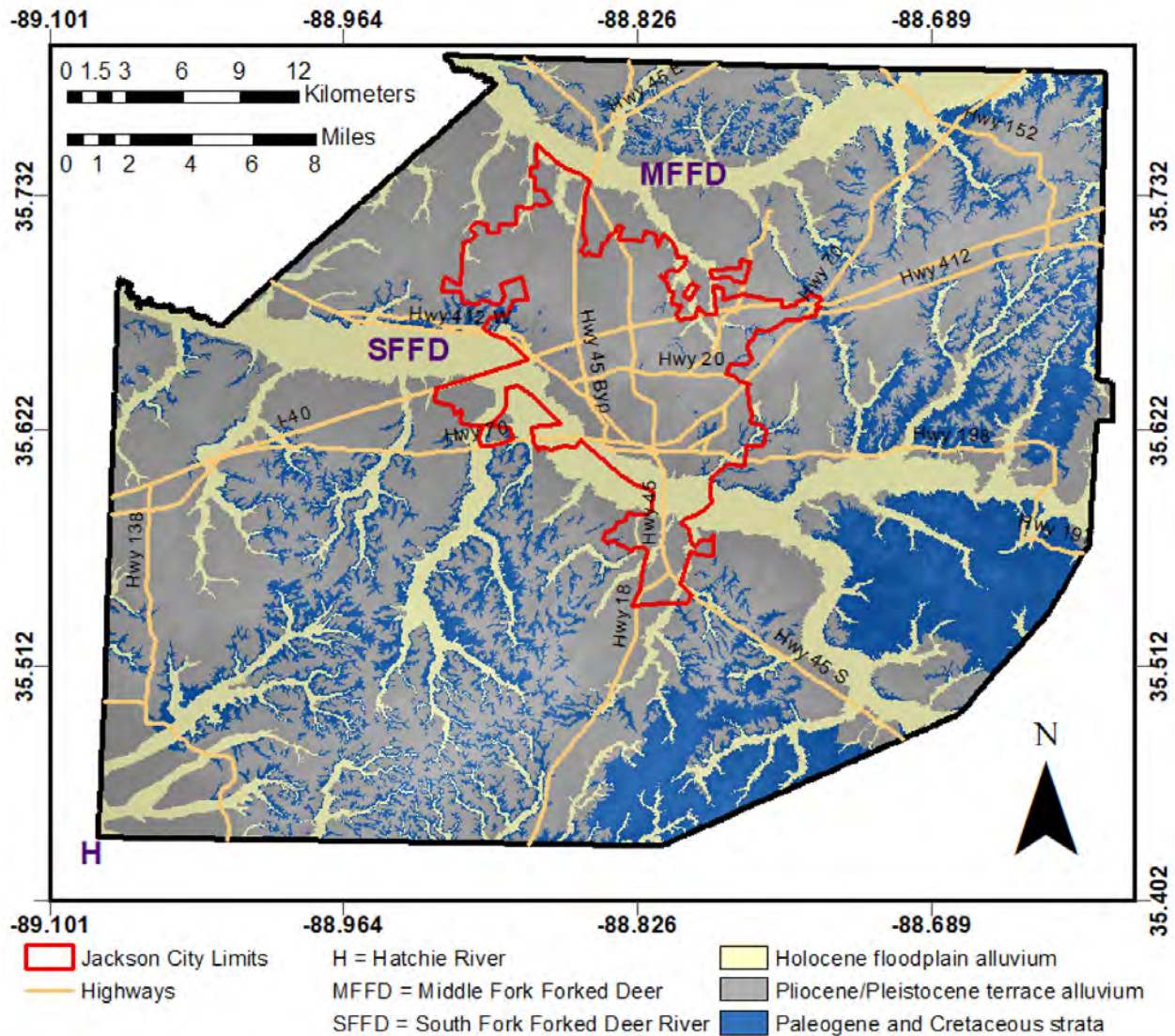


Figure 6: Simplified geologic map of Madison County for this seismic ground motion and liquefaction investigation. MFFD-Middle Fork of Forked Deer River, SFFD-South Fork of Forked Deer River, H-Hatchie River just off map to west.

Subsurface lithologic boring logs were acquired from petroleum exploration wells (http://environment-online.tn.gov:8080/pls/enf_reports/f?p=9034:34300:0:), Tennessee Department of Environmental Control, and the State of Tennessee Department of Environment and Conservation Division of Geology. Deep bedrock mapping was conducted down to the top of the Paleozoic strata, which is at a depth of ~ 410 m below the Jackson North geologic quadrangle near the middle of Madison County (Figures 2B and 3B).

The subsurface geology of Madison County is generalized in the cross section that accompanies the 7.5-minute Jackson North Geologic Quadrangle map (Figure 3B) (Jewel, 2006). The basal portion of the Paleocene Clayton Formation is difficult to differentiate from the underlying

Cretaceous sediment in some published quadrangles (e.g. Figure 3B) and therefore these units are combined in those maps. Since the lithologies are apparently indistinguishable they should have the same seismic velocities. Thus, we use the term top of Cretaceous even where a thin section of Paleocene Clayton Formation is included. The elevations of the tops of the Wilcox Group, Porters Creek Clay, and Cretaceous were determined by picking surface contact elevations from published 7.5-minute geologic quadrangle maps in Madison and adjacent counties (Figure 3A) and from well data. All tops of Paleozoic picks in Madison County are from well data.

Structure contour maps were made of the elevations of the tops of the Claiborne Formation, Cretaceous strata, and the top of the Paleozoic strata (Figures 3, 7, 10, and 11). These maps were made using the Natural Neighbor contouring algorithm. Planar trend surfaces of the tops of the Wilcox Group, and Porters Creek Clay were also made (Figures 8 and 9). The planar trend surfaces were used to extrapolate the tops of the Wilcox Group and Porters Creek Clay under most of Madison County. Control for the top of the Cretaceous was obtained from outcrop data in eastern Madison County and adjacent counties and from petroleum exploration wells (Figure 10). The top of Paleozoic structure contour map was constructed from oil well exploration data (Figure 11). Strikes and dips of the mapped units were determined from the structure contour lines in Figures 7-11.

Isopach (thickness) maps were made of the Lowland Holocene alluvium, Pliocene/Pleistocene terrace alluvium, Claiborne Formation, Wilcox Group, Porters Creek Clay, and Cretaceous section (Figures 12-18). Lowland Quaternary alluvium thicknesses were locally determined from published 7.5' minute geologic quadrangle maps that had cross sections across river floodplains (Figure 7B). In addition, road bridge crossings of the middle and south forks of the Forked Deer River in Madison County (Figure 12A) were visited and the height from the bridge deck to the bottom of the deepest part of the river flowing beneath the bridge was measured by dropping a weighted measuring tape to the riverbed. Immediately adjacent to the bridge crossings, 1 m lidar DEM data were used to make topographic profiles across the floodplain (Figure 12B). Bridge deck elevation, floodplain surface elevation derived from the 1 m lidar data, and the height of the bridge deck to the bottom of the channel were used to estimate the floodplain thickness at the bridge crossings.

$$\begin{aligned} &\text{Bridge deck height above channel bottom} - \text{bridge deck height above floodplain} \\ &= \text{channel depth} = \text{approximate floodplain alluvium thickness} \end{aligned}$$

The calculated elevations of the base of the floodplains were used to approximate planar trend surfaces of the base of the alluvium beneath the south and central Forked Deer River floodplains. Isopachs of the south and central Forked Deer River floodplains were made by subtracting the elevations of the floodplain base planar trend surface from the floodplain surface elevations (Figure 13). The isopach of the Pliocene/Pleistocene terrace alluvium was determined by subtracting the elevations of the base of the terrace alluvium from the ground surface elevations (Figure 14). The Claiborne Formation isopach was made by subtracting the elevation of the top of the Wilcox formation from the surface elevation where the Claiborne is

exposed and from the elevation of the top of the Claiborne where covered by Holocene flood plain alluvium or Pliocene/Pleistocene terrace alluvium. Isopach maps of the Wilcox Group, Porters Creek Clay, and Cretaceous section were made by subtracting the elevations from the basal structure contour map from the overlying structure contour map of each mapping unit (e.g. Porters Creek Clay top elevation – Cretaceous top elevation = thickness of Porters Creek Clay) (Figures 15-18).

All data used in this study are in Appendix A. The surface geology of Figure 5 and structure contour maps were compiled into a three-dimensional model and animation of the geology of Madison County (Figure 19 and Appendix B).

Results

Surface Geologic Map

The surface geology of Madison County was geologically differentiated into three mapping units for seismic hazard analyses: Holocene river floodplain alluvium, Pliocene/Pleistocene river terrace alluvium, and semi-consolidated sediments of Paleogene and Cretaceous age (Figure 6). The Figure 3B cross section from the Jackson North 7.5' geologic quadrangle is representative of the geology that underlies most of Madison County.

Holocene river floodplain alluvium thickness measurements along the Forked Deer rivers range from 1 to 9 m (Figures 12 and 13). The Pliocene/Pleistocene river terraces are topographically higher than the Holocene floodplains and we suspect, like the Holocene alluvium, consist of surface silt and clay that overlies sand and gravel sediment. A thin layer of Pleistocene loess (wind-blown silt) overlies the river terrace alluvium. There are at least two terrace levels apparent in 1 m lidar DEM data, but the different terrace levels are not differentiated in this report. Paleogene and Cretaceous strata are exposed in eastern Madison County and underlie all of Madison County (Figures 3 and 6). In some areas the Paleogene strata are covered with a thin veneer of Pleistocene loess.

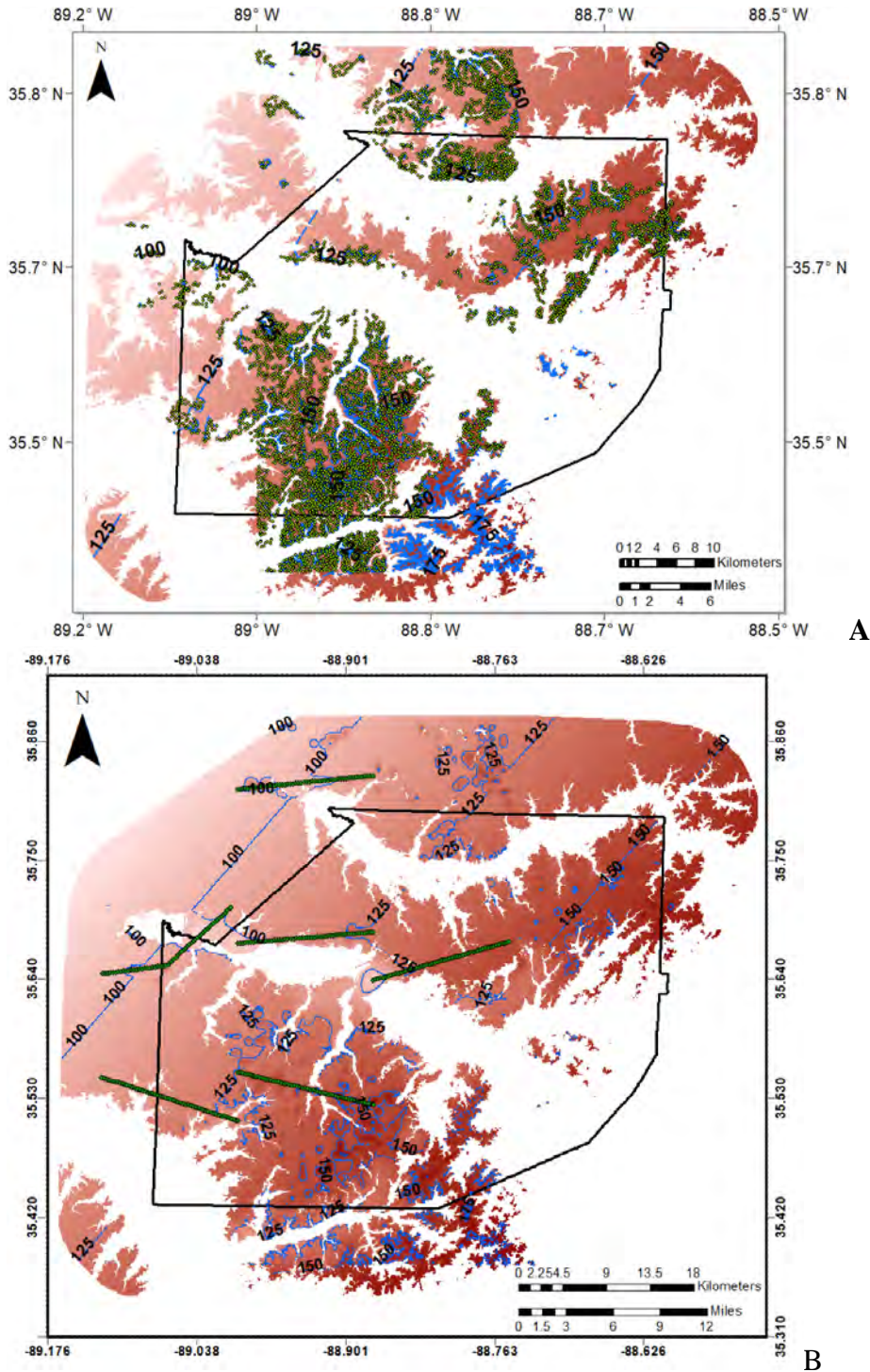


Figure 7: A) Data used to make structure contour map in “B” of the top of partially exposed Claiborne Formation in Madison County with surface data points in green. The Claiborne Formation strikes N37°E and dips 0.06° NW. Contours are in meters with respect to sea level.

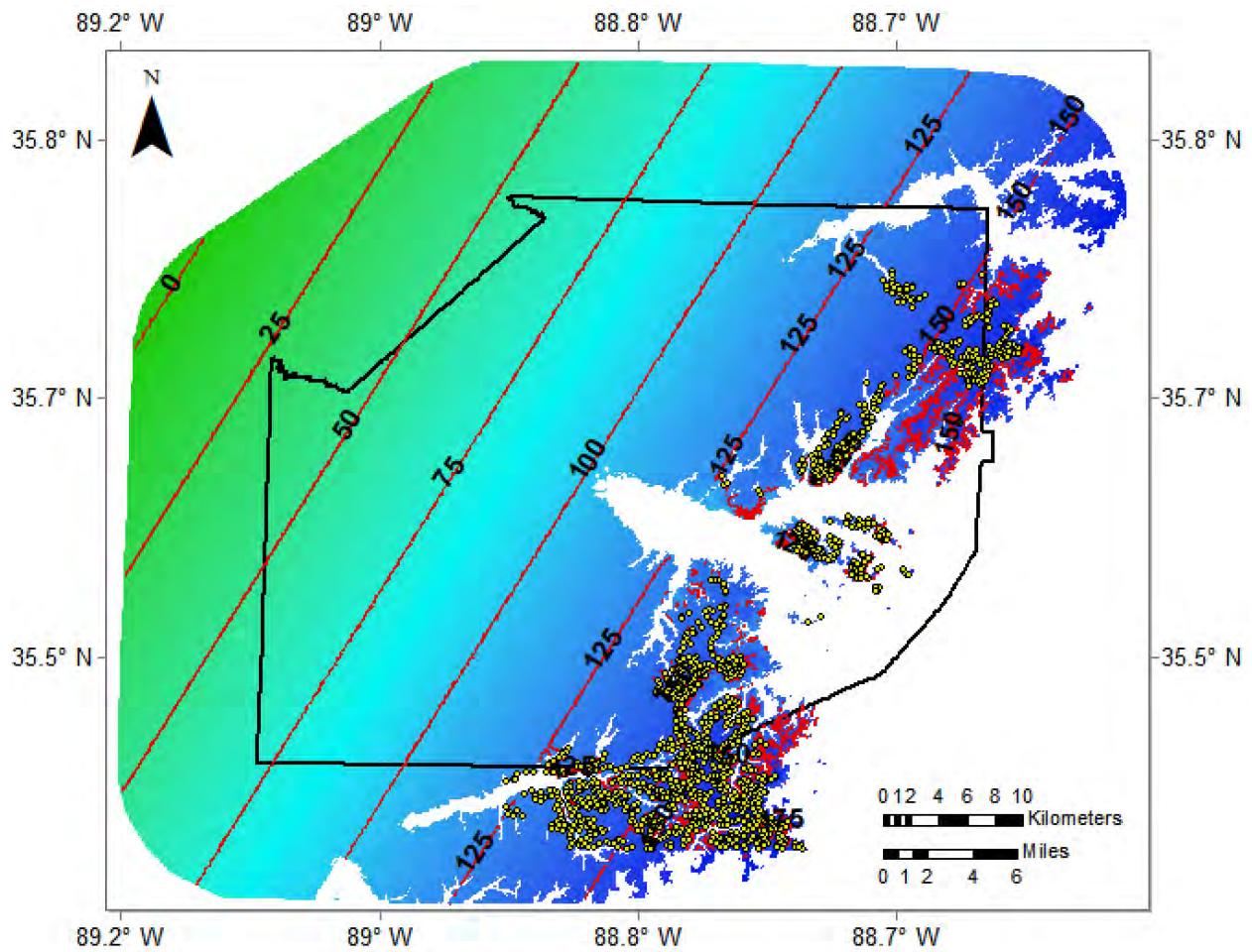


Figure 8: Planar structure contour map of the top of the Wilcox Group in Madison County. The planar trend surface is extrapolated west beneath Madison County based on the formation's strike (N28°E) and dip (0.21° NW) calculated from the outcrop data points (yellow dots) and shown in the contour lines. Contours are in meters with respect to sea level.

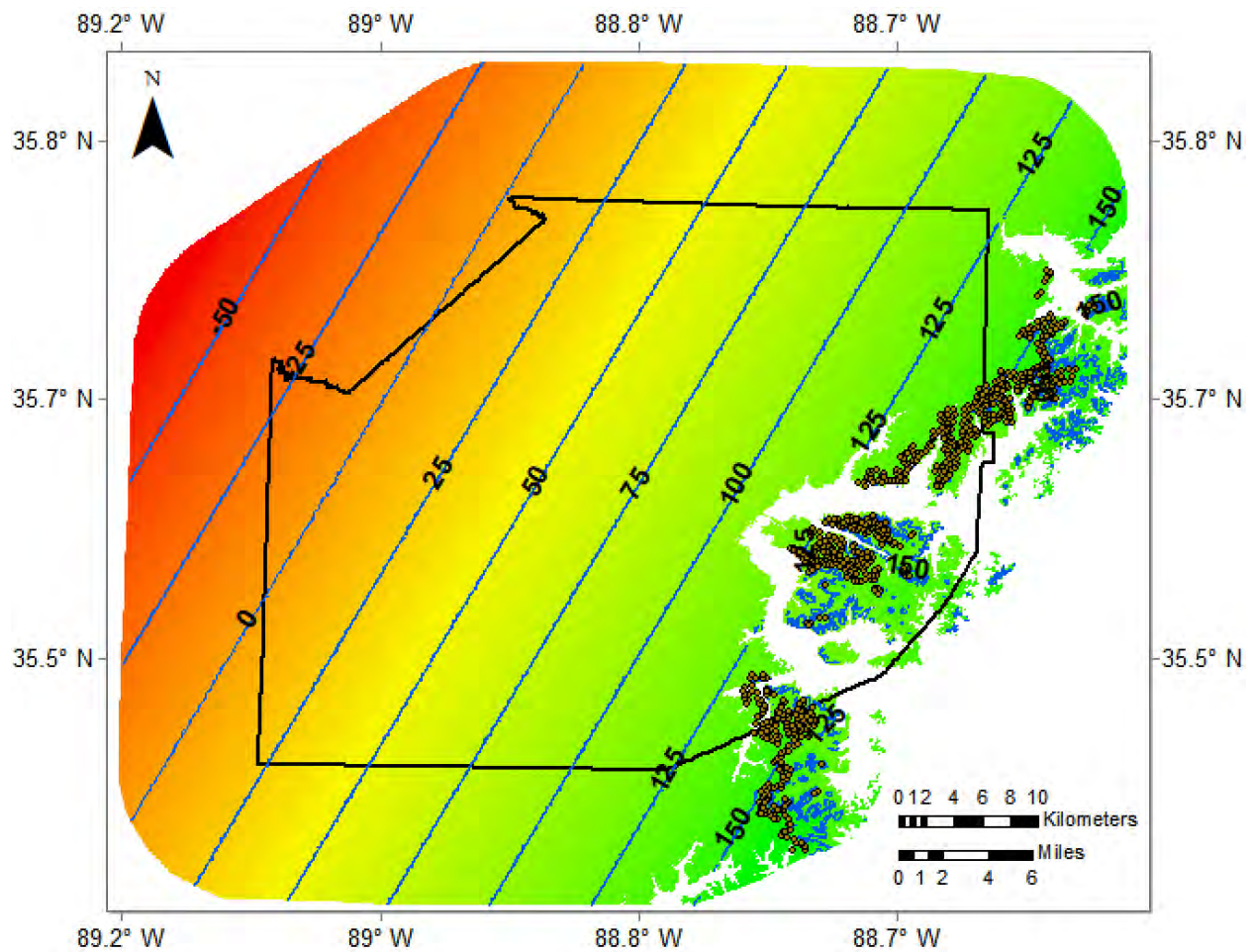


Figure 9: Planar structure contour map of the top of the Porters Creek Clay in Madison County. The planar trend surface is extrapolated west beneath Madison County based on the formation's strike (N27°E) and dip (0.27°NW) calculated from the outcrop data points (blue dots) and shown in the contour lines. Contours are in meters with respect to sea level.

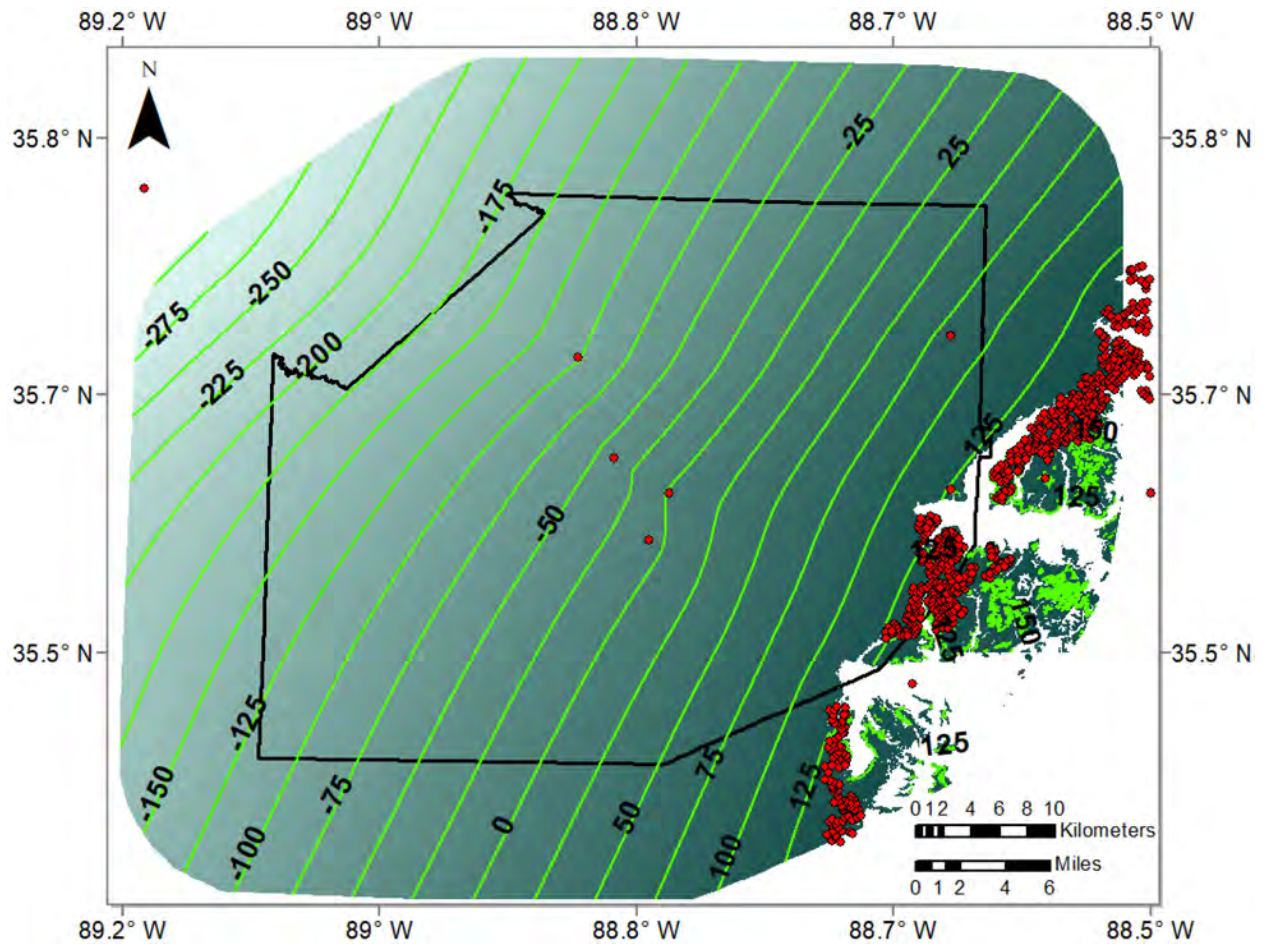


Figure 10: Structure contour map of the top of the Cretaceous strata in Madison County determined from surface exposures and well data (red dots). The strike (N28°E) and dip (0.48° NW) of the top of the Cretaceous are approximated beneath Madison County from the structure contour lines on this map. Contours are in meters with respect to sea level.

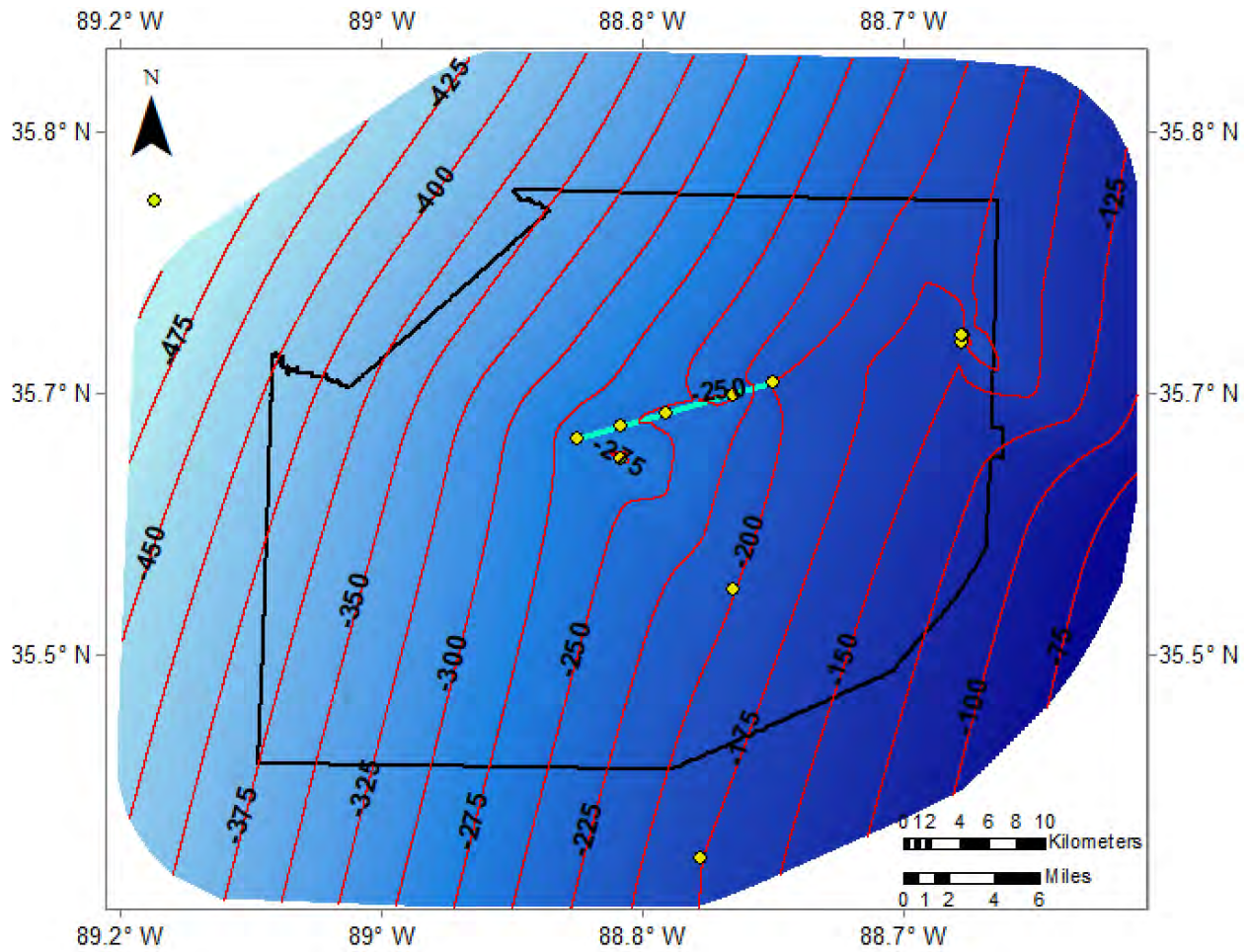
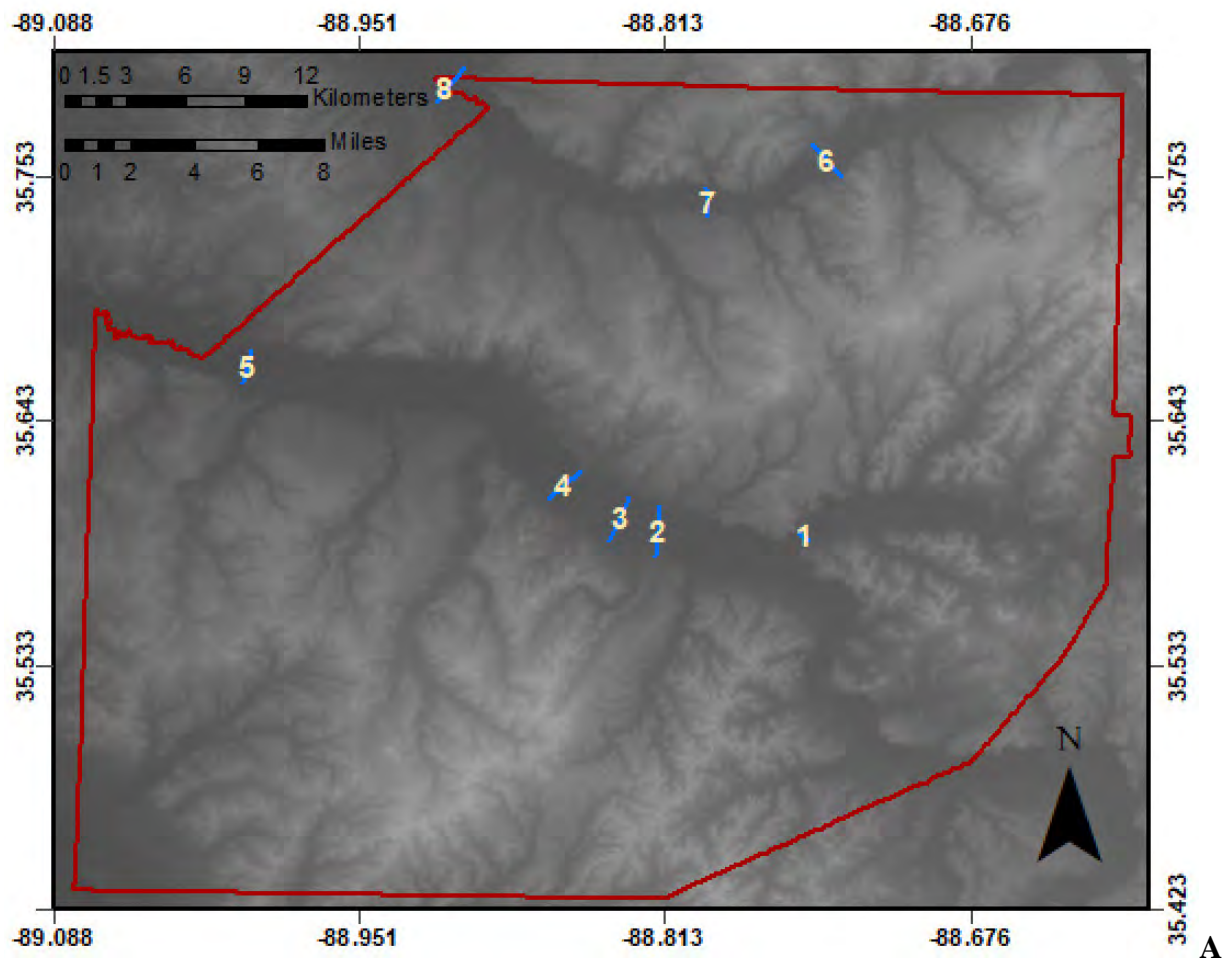
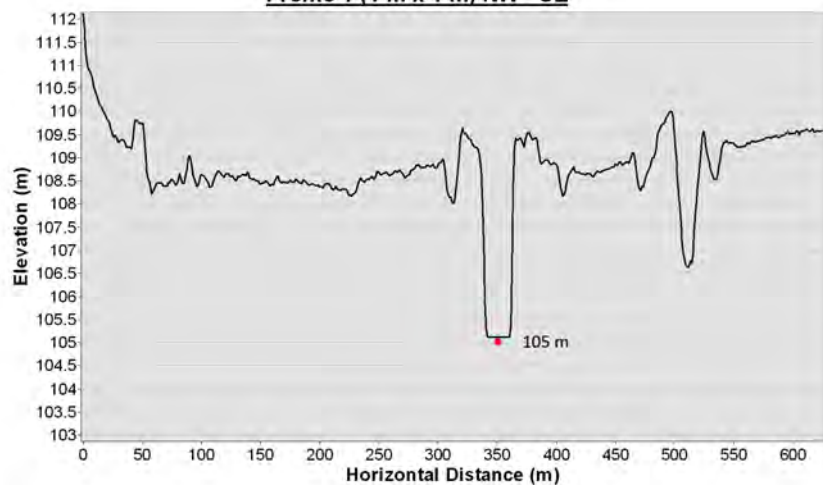


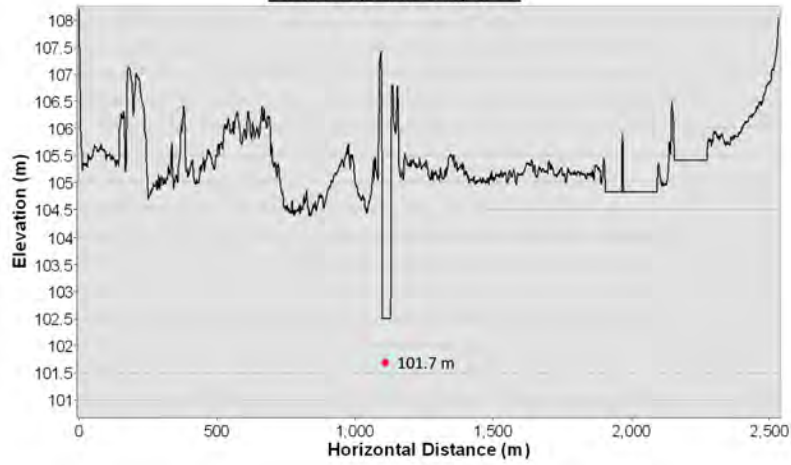
Figure 11: Structure contour map of the top of the Paleozoic beneath Madison County based on well data and Jackson North 7.5' geologic cross section (yellow dots). The strike (N21°E) and dip (0.44° NW) of the top of the Paleozoic is approximated beneath Madison County from the structure contour lines on this map. Contours are in meters with respect to sea level.



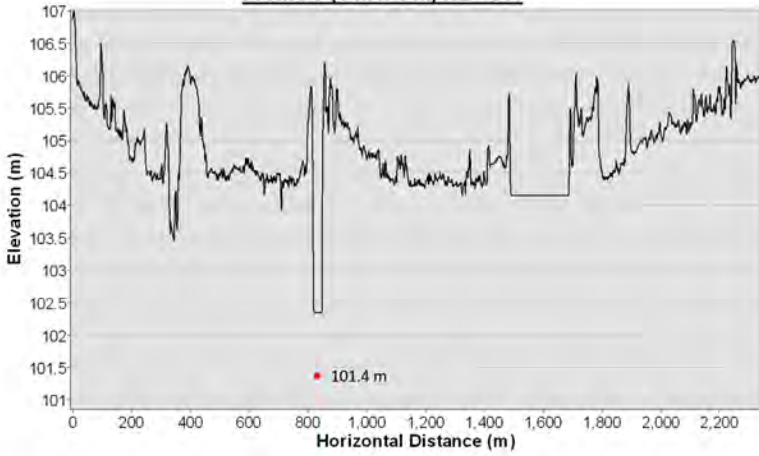
Profile 1 (1 m x 1 m) NW - SE



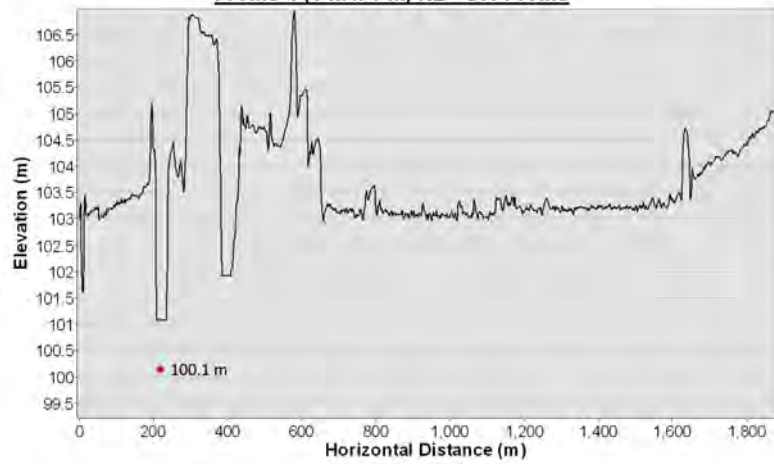
Profile 2 (1 m x 1 m) N - S



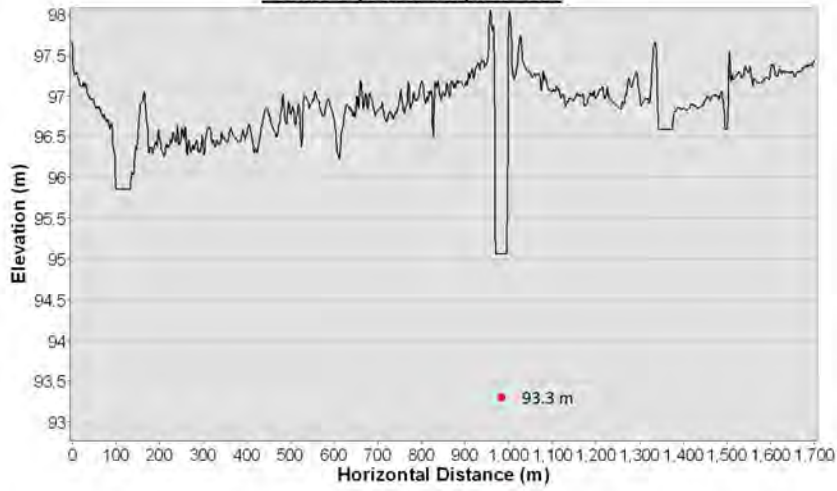
Profile 3 (1 m x 1 m) NE - SW



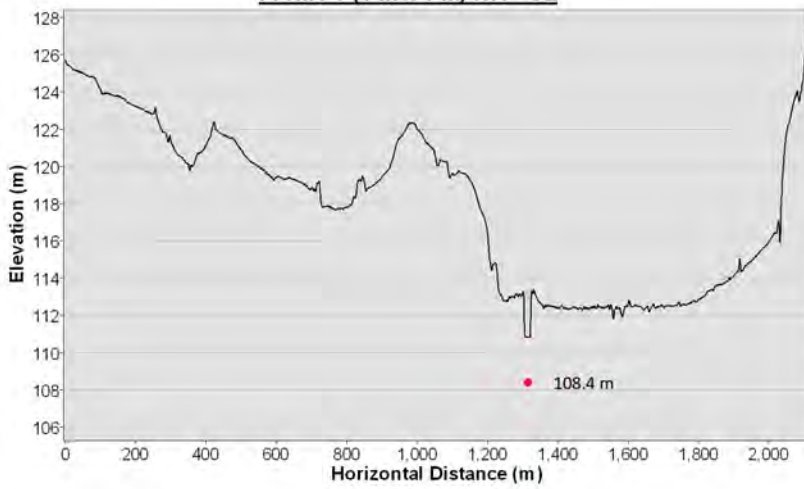
Profile 4 (1 m x 1 m) NE - SW Profile



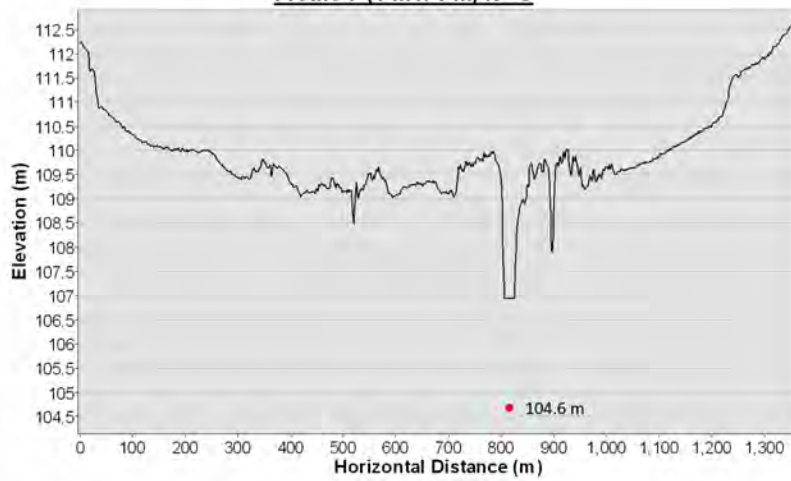
Profile 5 (1 m x 1 m) NE - SW

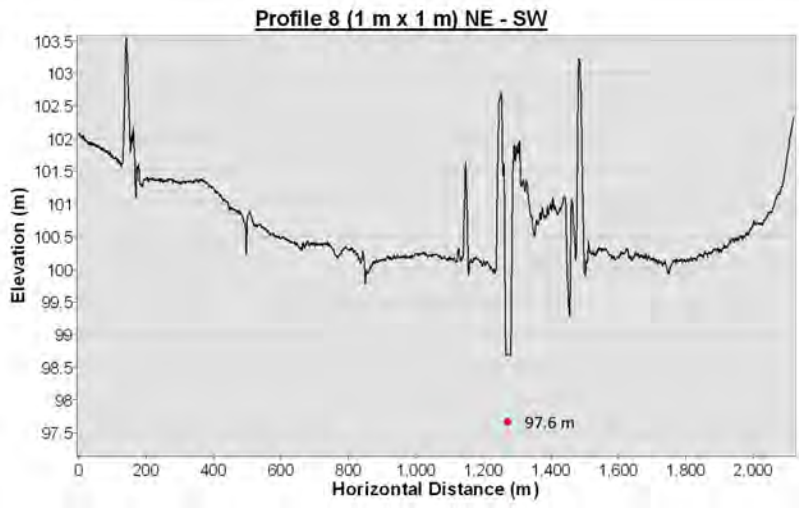


Profile 6 (1 m x 1 m) NW - SE



Profile 7 (1 m x 1 m) N - S





B

Figure 12: Quaternary Lowland alluvium thickness. A) Numbered locations of floodplain topographic 1 m LiDAR profiles and corresponding bridge measurements. B) The 1-8 floodplain surface profiles and floodplain thickness measurements. Red dot is bottom of channel measured at bridge locations.

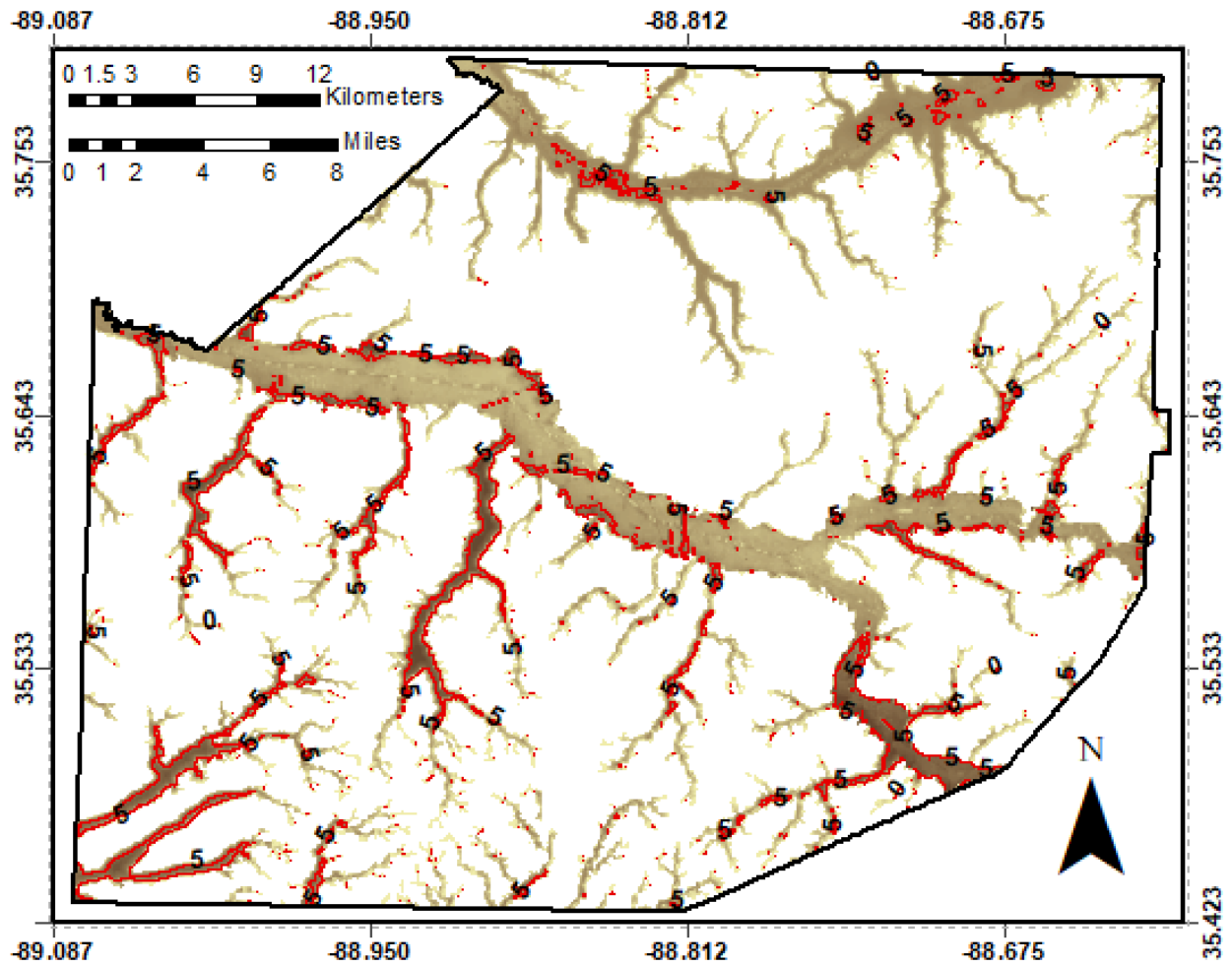


Figure 13: Isopach (thickness) of the Lowland Holocene floodplain alluvium in Madison County. Contours are in meters.

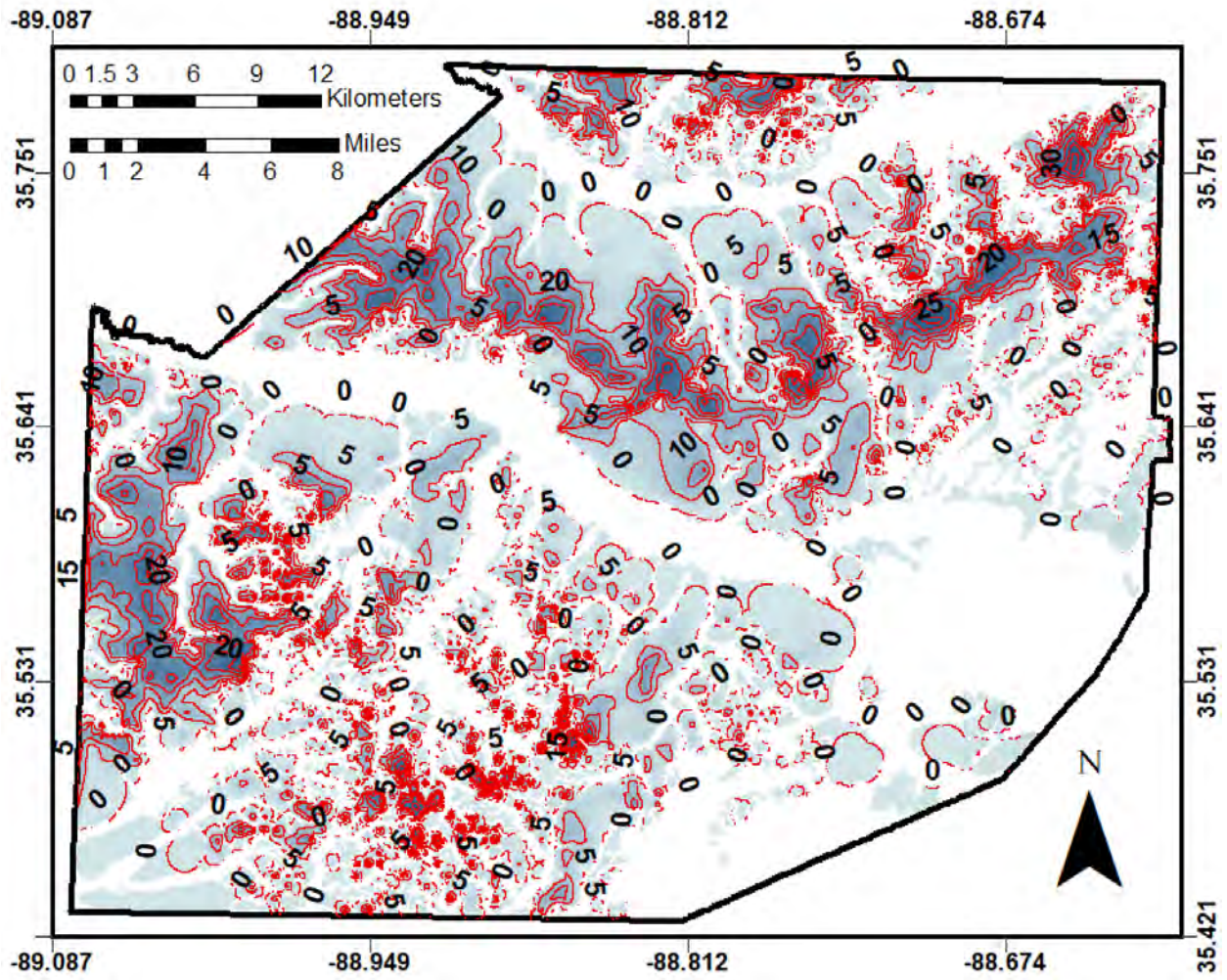


Figure 14: Isopach (thickness) of the Pliocene/Pleistocene terrace alluvium in Madison County. Contours are in meters.

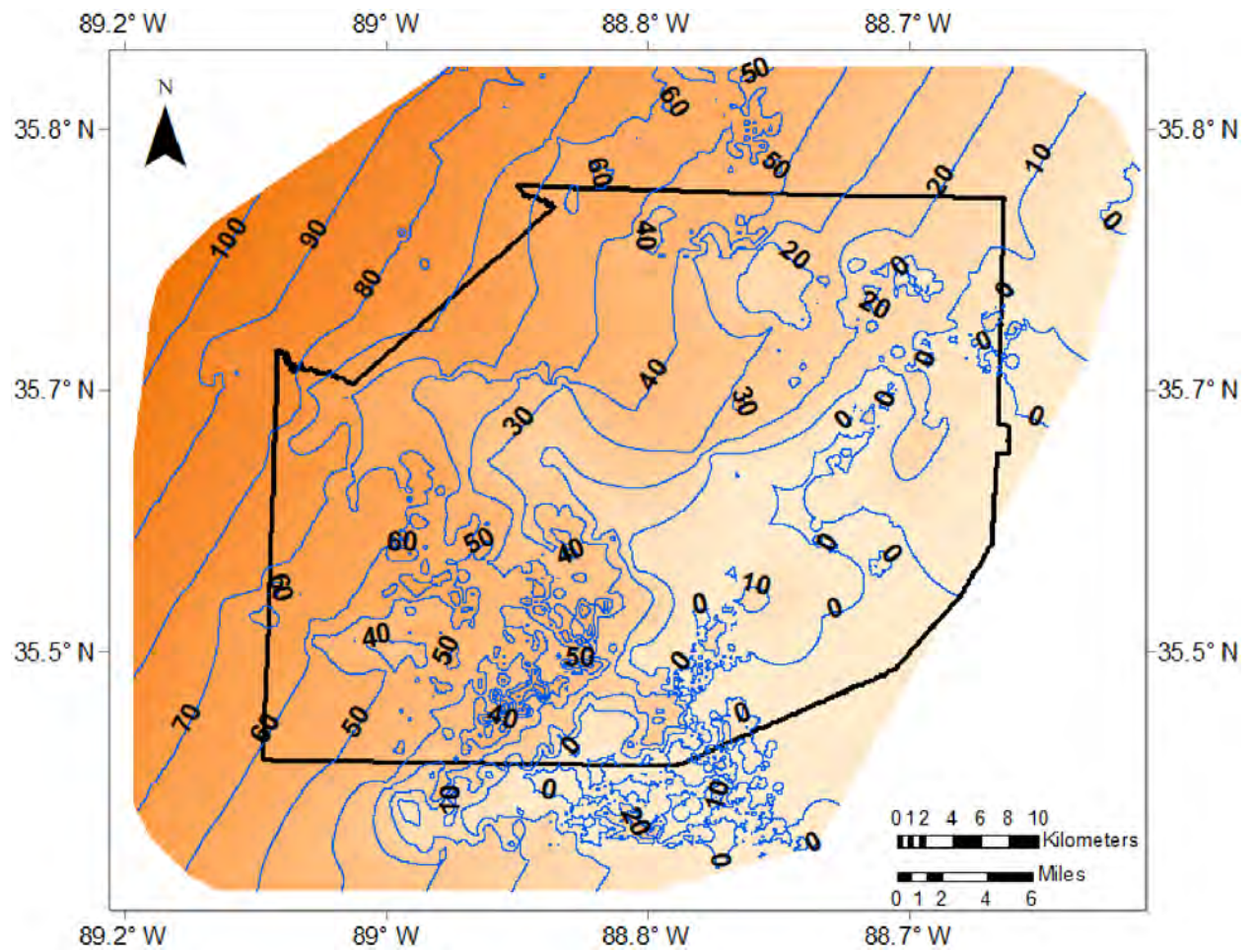


Figure 15: Isopach map of the Claiborne Formation in Madison County. Contours are in meters.

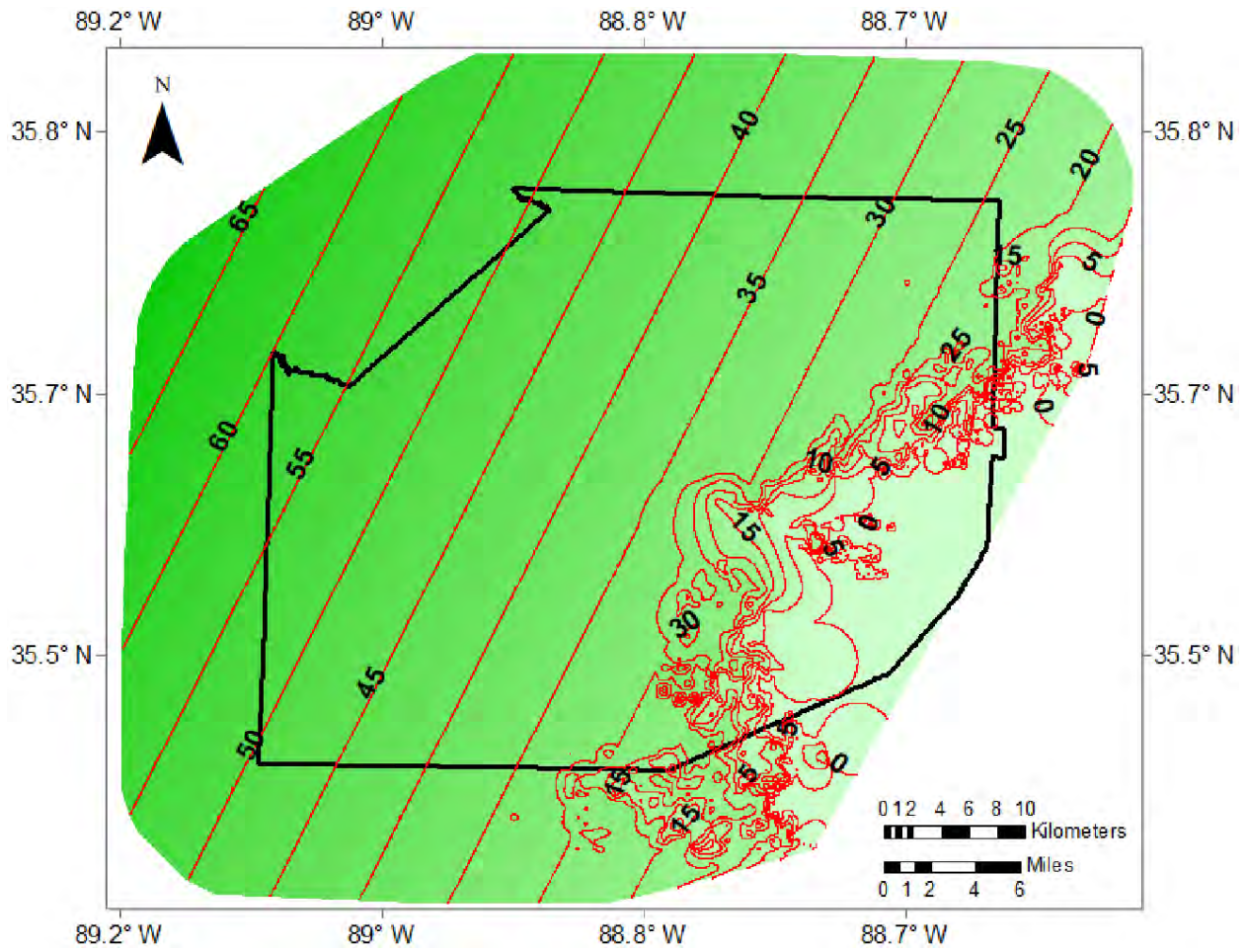


Figure 16: Isopach map of the Wilcox Group in Madison County. Contours are in meters.

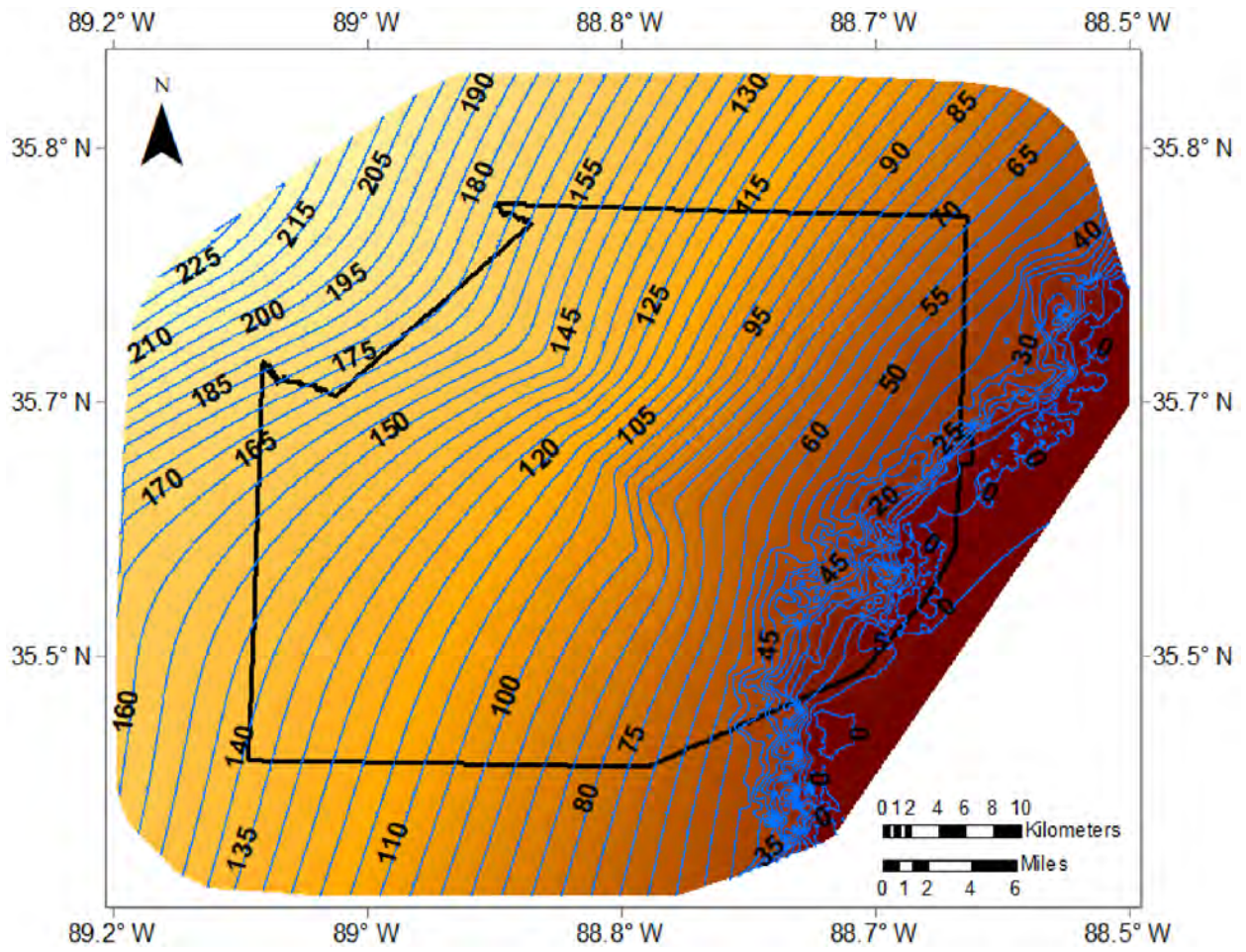


Figure 17: Isopach map of the Porters Creek Clay in Madison County. Contours are in meters.

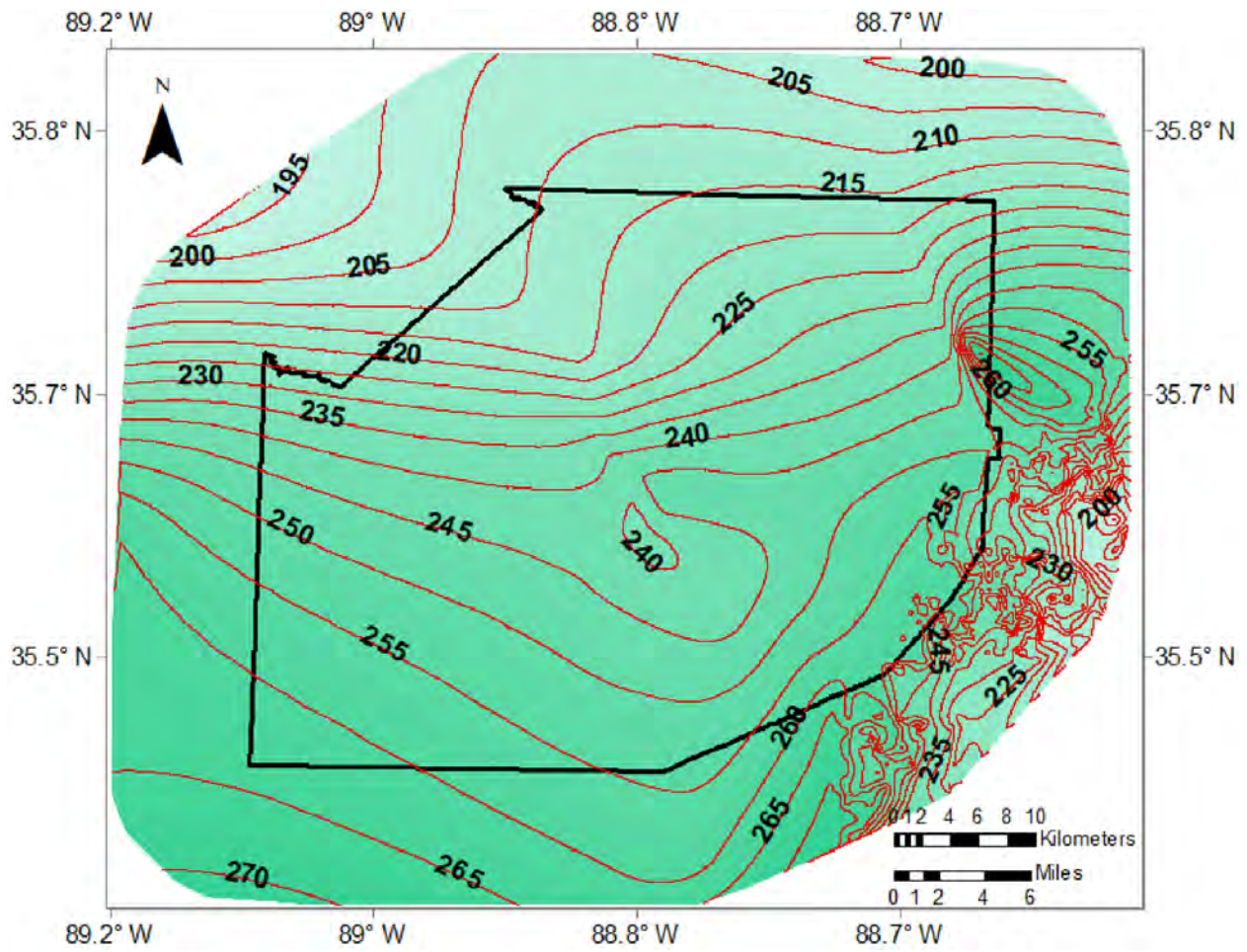


Figure 18: Isopach map of the Cretaceous strata in Madison County. Contours are in meters.

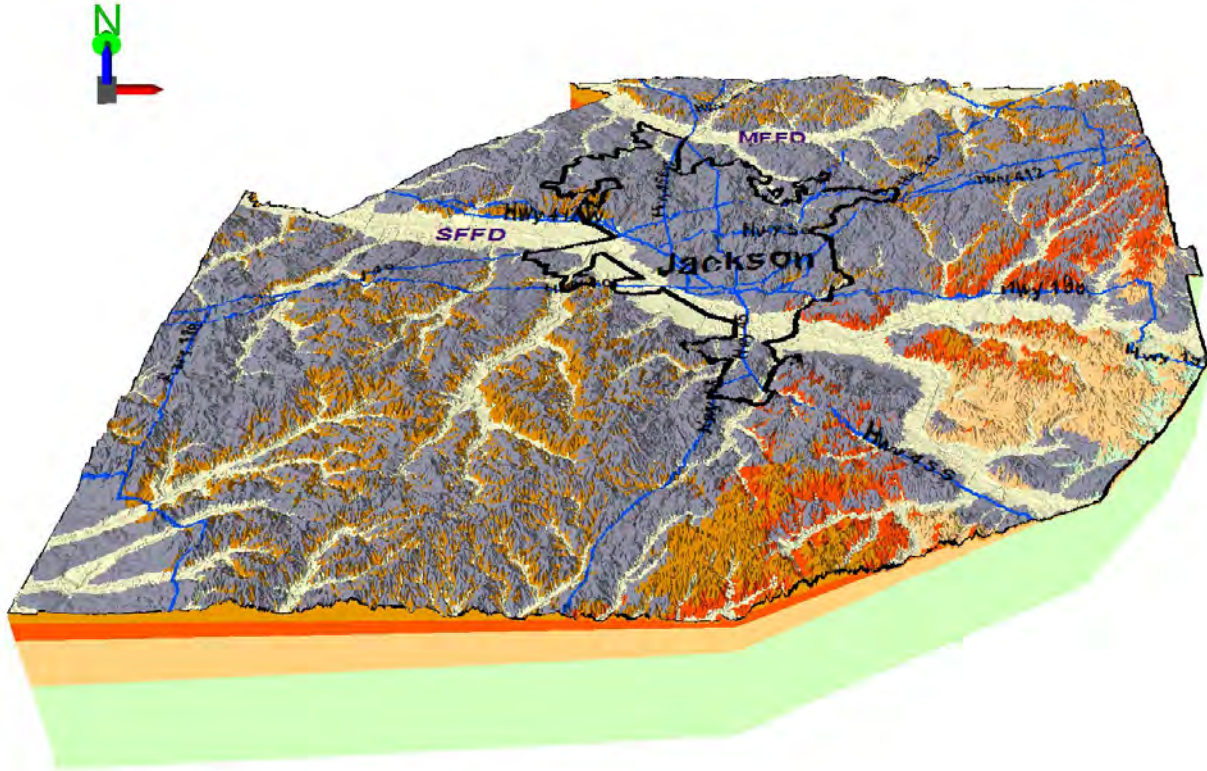


Figure 19: Three-dimensional oblique model of the surface and subsurface geology of Madison County. Colors correspond to colors used in Figure 3A. Vertical exaggeration is 50X.

Structure Contour Maps

The top of the Paleogene and Cretaceous strata are exposed in easternmost Madison County. Over much of the county 1 to 25 m of Pliocene/Pleistocene terrace alluvium and 1 to 9 m of Holocene river alluvium overlie Paleogene and Cretaceous strata (Figure 6).

Structure contour maps were made from surface data of the tops of the Claiborne Formation, Wilcox Group, Porters Creek Clay, and Cretaceous strata mapped in the published 7.5' geologic quadrangle maps of Figure 3 (Figures. 7-11) (Antonacci, V., and Hoyal, M., 2011, 2012a, 2012b, 2014a, 2014b; Brown, 1968a, 1968b; Jewel, 2006; Parks, 1968a-f). Planar trend surfaces were fit to the elevations of the tops of the Wilcox Group and Porters Creek Clay to make planar trend surface structure contour maps (Figures 8 and 9). Fitting planes to these data formation tops is justified because no faulting or folding has been mapped in Madison County (Figure 3A). Strike and dip of the geologic formations were determined from the contour lines in their planar trend surfaces (Figures 8 and 9). All these formation tops slope westerly at less than one degree: Wilcox Group is N28°E, 0.21° NW, and Porters Creek Clay is N27°E, 0.27° NW. The strikes and dips of the tops of the Cretaceous (N28°E, 0.48°NW) and Paleozoic (N21°E, 0.44° NW) in Madison County were determined from the contour lines on their structure contour maps (Figs. 10 and 11). It is apparent that in Madison County the entire stratigraphic section

from the top of the Paleogene to the top of the Paleozoic slopes westerly at $< 1^\circ$ and thus is essentially flat.

Isopach Maps

The Holocene floodplain alluvium thickness along the Forked Deer rivers varies from 1 to 9 m based on the published cross sections and bridge measurements. Our floodplain alluvium thickness, as determined from the bridge measurements (Figures 12 and 13), is an estimate because floodplain alluvium could underlie the channel base, or the channel base could be incised into Paleogene strata. We also do not know the composition of the floodplain because we do not have borings in the floodplain. However, we suspect a surface silt and clay overbank layer overlies point bar sand that may contain gravel.

Pliocene/Pleistocene terrace alluvium thickness is variable with values ranging from 1 to 25 m (Figure 14). In general, terrace alluvium is thickest along drainage divides and thins towards modern streams.

The Claiborne Formation thickens northwesterly (Figure 15), but thickness is irregular because its upper surface has been eroded to various elevations by the Pleistocene rivers that have flowed and Holocene rivers that continue to flow across Madison County (Figure 3A). The Wilcox Group (Figure 16) and Porters Creek Clay (Figure 17) thicken to the northwest and the Cretaceous section thickens southerly (Figure 18). The Claiborne Formation averages 33 m thick, Wilcox Group 37 m, Porters Creek Clay 107 m, and the Cretaceous strata averages 237 m thick in Madison County.

Conclusions

Approximately 3.6 Ma (Odum et al., 2020) the ancestral Mississippi river system flowed across a vast area in the central United States and deposited floodplain sediments now discontinuously preserved as a high level terrace called the Upland Complex (Van Arsdale et al., 2007; Cupples and Van Arsdale, 2014; Cox et al., 2014; Lumsden et al., 2016). Remnants of the 3.6 Ma terrace have been mapped in Obion, Dyer, Lauderdale, Tipton, and Shelby counties in westernmost Tennessee (Figure 2A) (Van Arsdale et al., 2007). Incision through the Upland Complex throughout the lower Mississippi/Ohio river system began in the early Pleistocene with growth of continental ice sheets and resultant lower sea levels (Saucier, 1994; Van Arsdale et al., 2007). During the Pleistocene, the Humboldt, Hatchie, and Finley terraces formed along the Obion, Forked Deer, and Hatchie rivers (Saucier, 1987; Rodbell, 1996) and up to four loess layers were deposited in western Tennessee (Markewich et al., 1998). In Dyer County (Figure 2A), Rodbell (1996) identified Peoria loess (< 20 ka) and underlying Roxanna silt (> 65 ka loess) on top of Humboldt and Hatchie River terrace alluvium (Cramer et al., 2020a). Based on the Dyer and Lauderdale County geologic histories we believe the ancestral Mississippi/Ohio river system and its tributaries entrenched > 65 ka in westernmost Tennessee because the Humboldt terrace alluvium is overlain by the > 65 ka loess. Subsequently, the Mississippi/Ohio river system and its tributaries further entrenched to form the Hatchie (also > 65 ka) and then Finley (~ 22 ka)

terrace levels. The final entrenchment of the Mississippi and its tributary rivers in westernmost Tennessee occurred within the last 22,000 years resulting in most of the modern floodplain alluvium being < 12 ka.

Holocene alluvium, with estimated thicknesses ranging between 1 and 6 m, underlies Forked Deer floodplains in Madison County. The surface geology of Madison County also consists of more than one extensive Pliocene/Pleistocene floodplain (terrace) that have been incised by Holocene rivers. We speculate that the terraces of Madison County are remnant headwater floodplains of the ancestral Mississippi/Ohio river. We do not have radiometric dates for the Madison County terraces but think it reasonable that the terraces may be equivalent to those mapped in westernmost Tennessee (Saucier, 1987; Van Arsdale et al., 2007; Lumsden et al., 2016; Odum et al., 2020). Specifically, the highest Madison County terrace may be equivalent to the 3.6 Ma Upland Complex and sequentially lower terraces equivalent to the Humboldt and Hatchie terraces preserved in the downstream reaches of the Forked Deer River in Dyer and Lauderdale counties and the Hatchie River in Lauderdale and Tipton counties (Fig. 2A) (Cramer et al., 2020b, 2021). This terrace interpretation is consistent with the regional terrace mapping by Saucier (1987) wherein he mapped Humboldt and Hatchie terraces along the Hatchie River in southwestern Madison County.

Surface and subsurface geologic mapping has provided insight into the three-dimensional geology (Figure 19) and the Pliocene-Quaternary geologic history of Madison County. Of importance to the county's earthquake hazards are the seismic velocity structure of the underlying geologic strata, strata thicknesses, the recurrence intervals of Reelfoot rift faults (Tuttle et al., 2002; 2019; Cox et al., 2001; 2006; 2013), and the liquefaction potential of the Holocene floodplain sediments of the Forked Deer rivers.

Geotechnical Model

Introduction

A summary of geotechnical analyses performed to generate liquefaction probability curves (LPCs) based on different approaches for Madison County, Tennessee is provided in this section of the report. Background information on the subsurface data collection procedures followed by the methodologies of developing LPCs is presented in this section.

Data Collection

To develop LPCs of Madison County, the liquefaction potential of the county had to be analyzed based on subsurface data. The subsurface data that was collected within Madison County consisted of Standard Penetration Test (SPT) resistance, and groundwater level data. A summary of the procedures used to collect these data is presented next.

SPT Data

For the liquefaction potential analysis of Madison County, like Lake, Dyer, Lauderdale, and Tipton Counties the main analyses were performed based on available SPT data within the area of study. For Madison County, SPT data were provided from three organizations of U.S Army Corps of Engineers (USACE), Tennessee Department of Transportation, and Construction Material Laboratory, Inc. Like Dyer, Lauderdale, and Tipton Counties, the TDOT boring logs did not provide a coordinate location of where the boring was obtained. We were only provided with a project location map (without scale) or a general project location description. Using Google Earth and Google Map, we estimated the location of the projects and used the project location for all soil borings of a project to find the geologic unit of the borings and to interpolate the GWL of each boring using the GWL contour map described later in this report. A total of 233 SPT soil boring logs data were received from the three organizations. The total number of soil boring logs that were obtained from each organization is provided in Table 1.

Table 1. Summary of the total number of borings.

Organization	Boring Log
USACE	10
Construction material lab	209
TDOT	14

Like the other four counties of Lake, Dyer, Lauderdale, and Tipton, to use the soil boring logs in liquefaction analysis they must meet some criteria. The soil boring selection screening criteria can be summarized as:

- Borings must be at least 20 m (66 ft) deep.
- Borings must include N-values and USCS classifications to a depth of 20 m (66 ft).
- The boring locations must have latitude and longitude coordinates.

To include additional boring data in the development of LPCs, the screening criteria was revised to accept boring logs with most N-values included to a depth of 15 m (50 ft) instead of 20 m (66 ft) based on the following procedure:

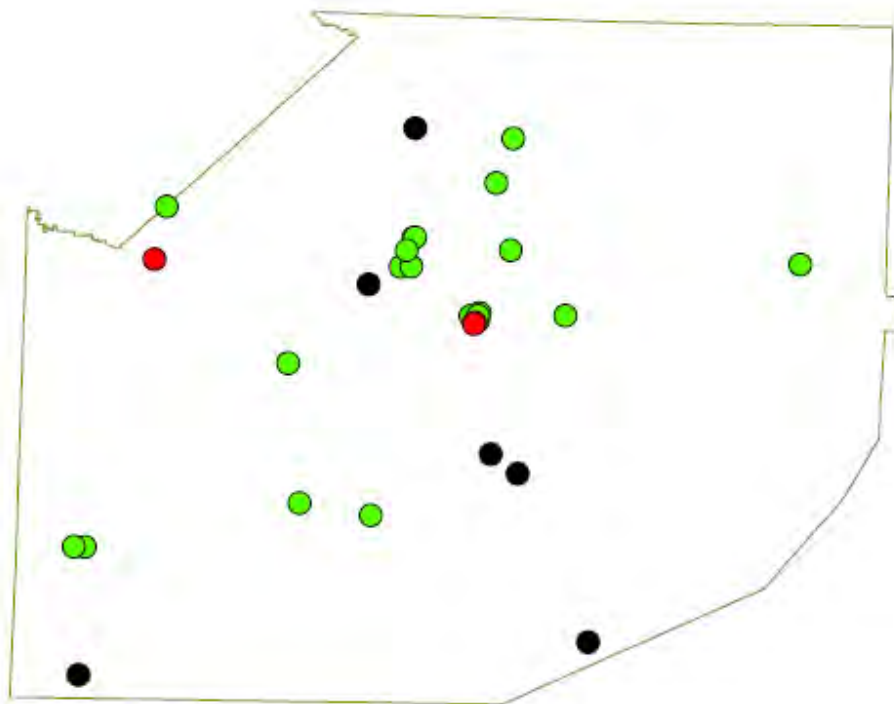
- Missing N-values for any depth at a given boring location were estimated by using the same N-value for a given N-value above or below the depth of the missing N-value if the overlying and underlying soil had the same soil classification.
- If the soil layers above and below the layer of missing N-value did not have the same classification or did not have N-value in a given boring, the N-value was extracted from closest boring for the same classification and the same depth as classification and depth of the missing N-value.

Unfortunately, a majority of the obtained boring logs did not meet the above criteria and only a total of 69 soil boring logs were selected to be utilized in liquefaction analyses. Table 2 provides

the total number of selected boring logs, and Figure 20 shows the distribution of selected soil borings within Madison County.

Table 2. Total number of selected borings.

Organization	Boring Log
USACE	3
Construction material lab	52
TDOT	14 from 6 projects
TOTAL	69



Legend

- TDOT Projects
- USACE Borings
- construction material lab projects
- Madison_Outline

Figure 20: Location of selected soil borings for use in developing LPCs.

Geology Classification of selected SPT boring logs

To develop the liquefaction hazard maps for the entire Madison County, the LPCs must be developed for each surface geologic unit of the county, separately. Thus, the SPT soil borings had to be classified based on the surface geology map of Madison County. As described in the “Geology Model” section, the surface geology of Madison County for hazard analysis of the county were divided into three geologic units of Holocene river floodplain alluvium, Pliocene/Pleistocene river terrace alluvium, and semi-consolidated sediments of Paleogene and Cretaceous age. According to the geology analysis of Madison County, topographically, the Holocene river floodplain alluvium has a lower elevation than Pliocene/Pleistocene river terraces

and Paleogene/Cretaceous strata which mostly are consisted of silt and clay; therefore, the most susceptible geologic unit to liquefaction is floodplain alluvium. To develop LPCs for each primary surficial geology unit separately, the boring logs had to be classified for each surface geologic unit.

The distribution of selected borings on the surface geology map of Madison County is illustrated in Figure 21. Among the total of 69 boring logs selected from USACE, TDOT, and Construction Material Lab, Inc. 25 are in the floodplain alluvium, 44 are in the Pliocene/Pleistocene river terraces, and zero are in the Paleogene/Cretaceous strata of Madison County.

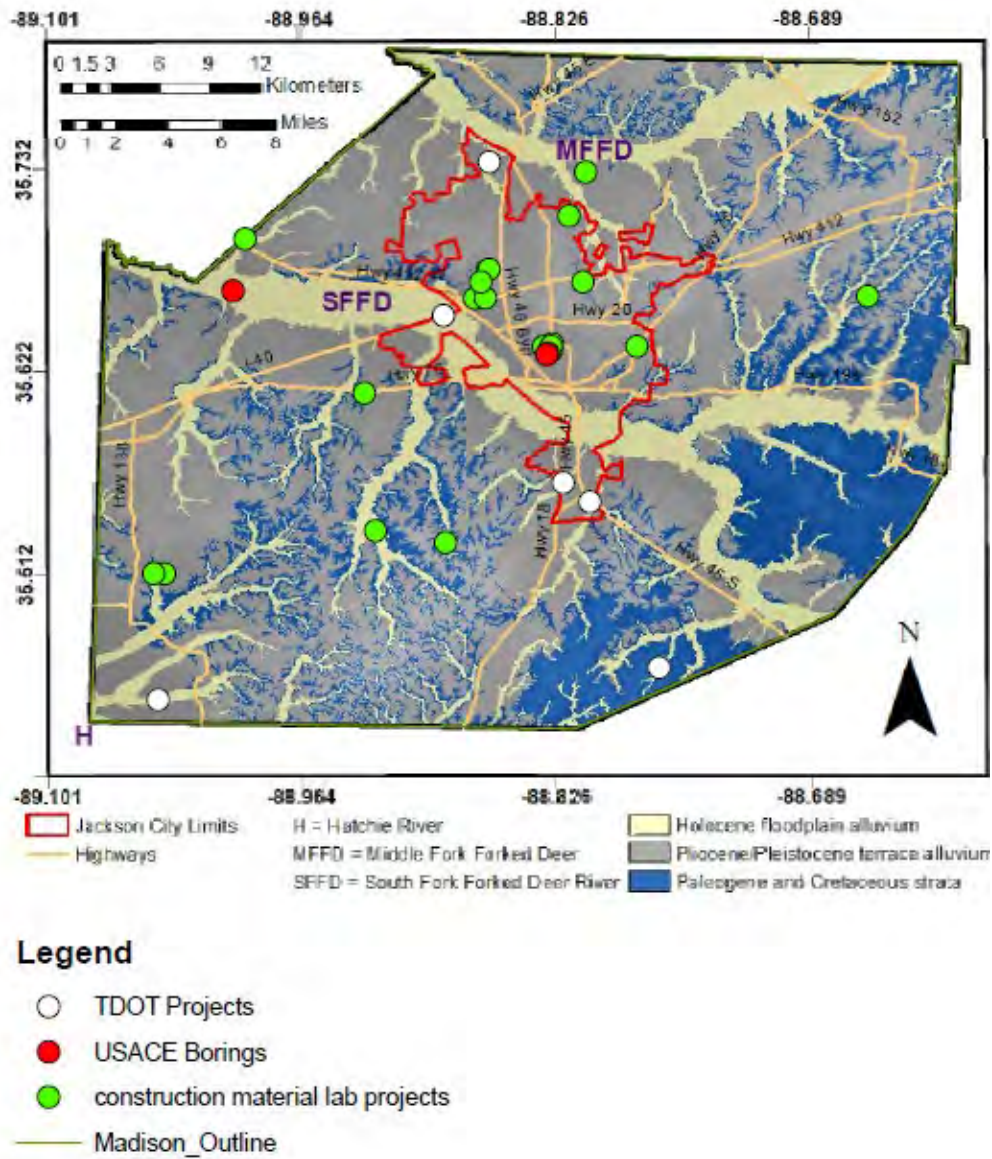


Figure 11: Soil boring locations on the surface geology map of Madison County.

Groundwater data

To perform the liquefaction analysis of Madison County, the groundwater level at each soil boring/project location was required. To estimate the GWL at each soil boring's location within Madison County, we utilized the same procedure that was used for Lake, Dyer, Lauderdale, and Tipton Counties (Cramer et al., 2019, 2020a, b, 2021). We established a GWL contour map for Madison County based on the groundwater level contour map within the surface alluvial aquifer of Mississippi Embayment developed by Schrader (2008) and published by USGS shown in Figure 22.

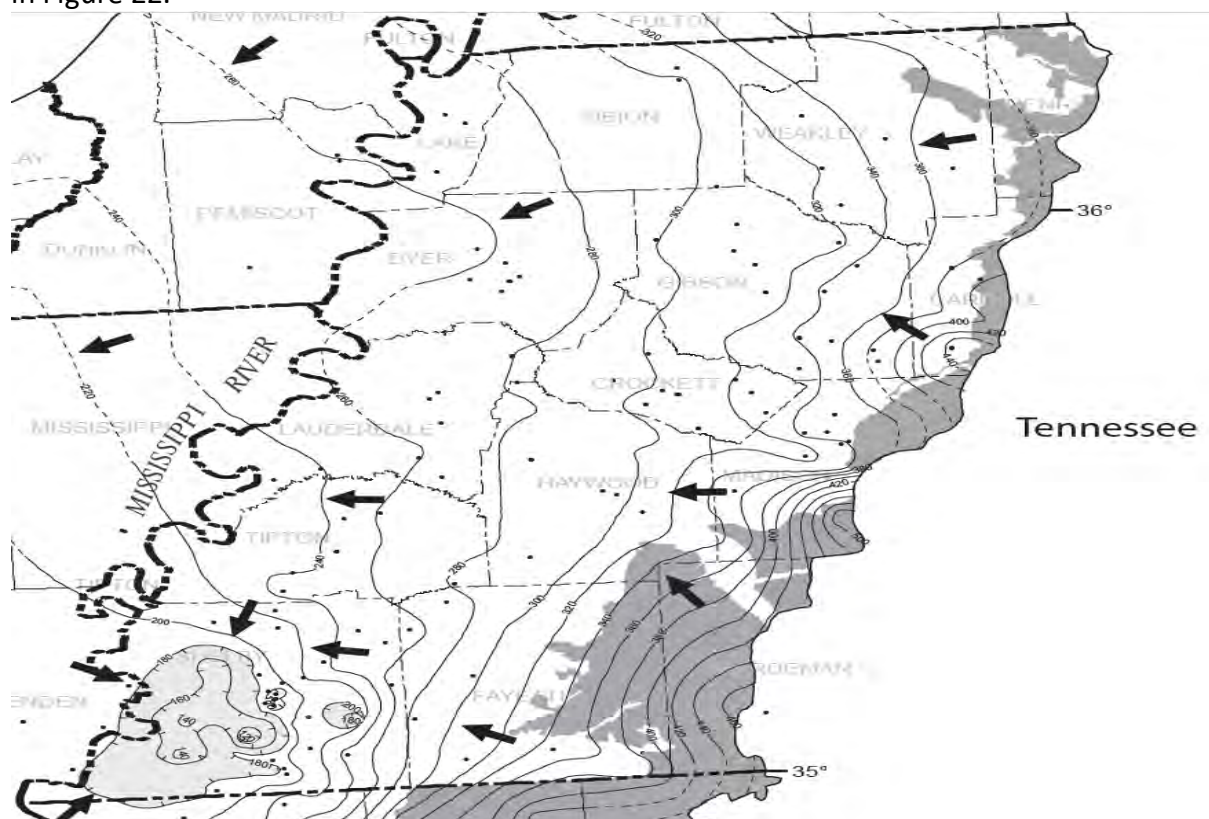


Figure 22.: USGS groundwater level contour map (Schrader 2008).

To establish the GWL contour map that covers the entire area of Madison County, initially, the contour lines which cover the entire county were extrapolated for longitude and longitude from Schrader's map, and then they were digitized on the 2D Madison County boundary shapefile in ArcMap. There are various tools to generate a contour map in ArcMap, however, to be consistent with Lake, Dyer, Lauderdale, and Tipton Counties, the Inverse Distance Weighting (IDW) tool was used to create the GWL contour map of Madison County. Figure 23 indicates the generated GWL contour map of Madison County in the format of a raster file (contours are in the format of ft.-NGVD 1929).

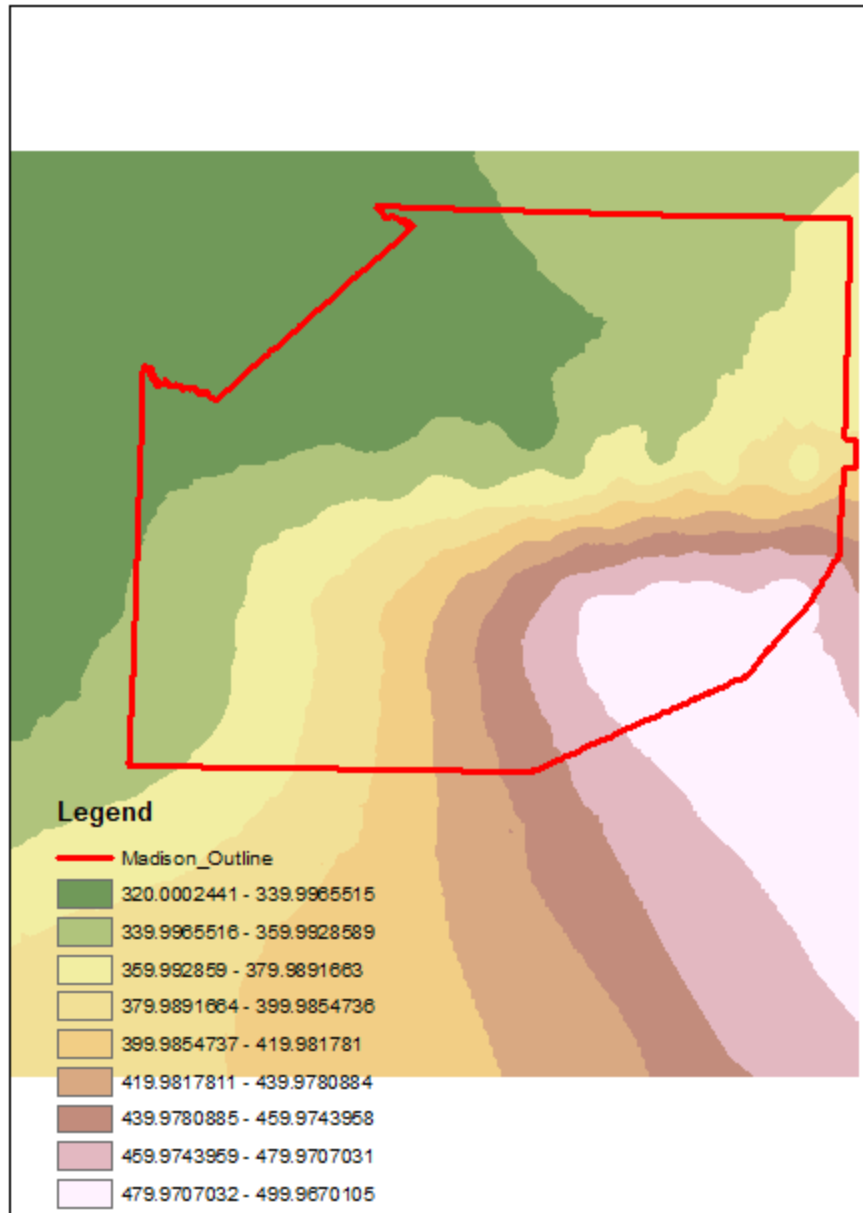


Figure 23: Groundwater level contour map of Madison County.

In contrast with the other four counties of Lake, Dyer, Lauderdale, and Tipton that additional groundwater data of water wells within the area of study were obtained from the United States Geological Survey (USGS) groundwater data website (<https://maps.waterdata.usgs.gov>) to verify the accuracy of the GWL contour map, at the time, for Madison County there was no water well data available from USGS database. Therefore, to verify the accuracy of the GWL contour map, we coordinated with Dr. John Smith of Jackson Energy Authority (JEA) to obtain supplemental groundwater level data within Madison County. JEA provided the groundwater

level data of 23 wells in Madison County that most of which are in Jackson city. Figure 24 shows the distribution of wells within Madison County.

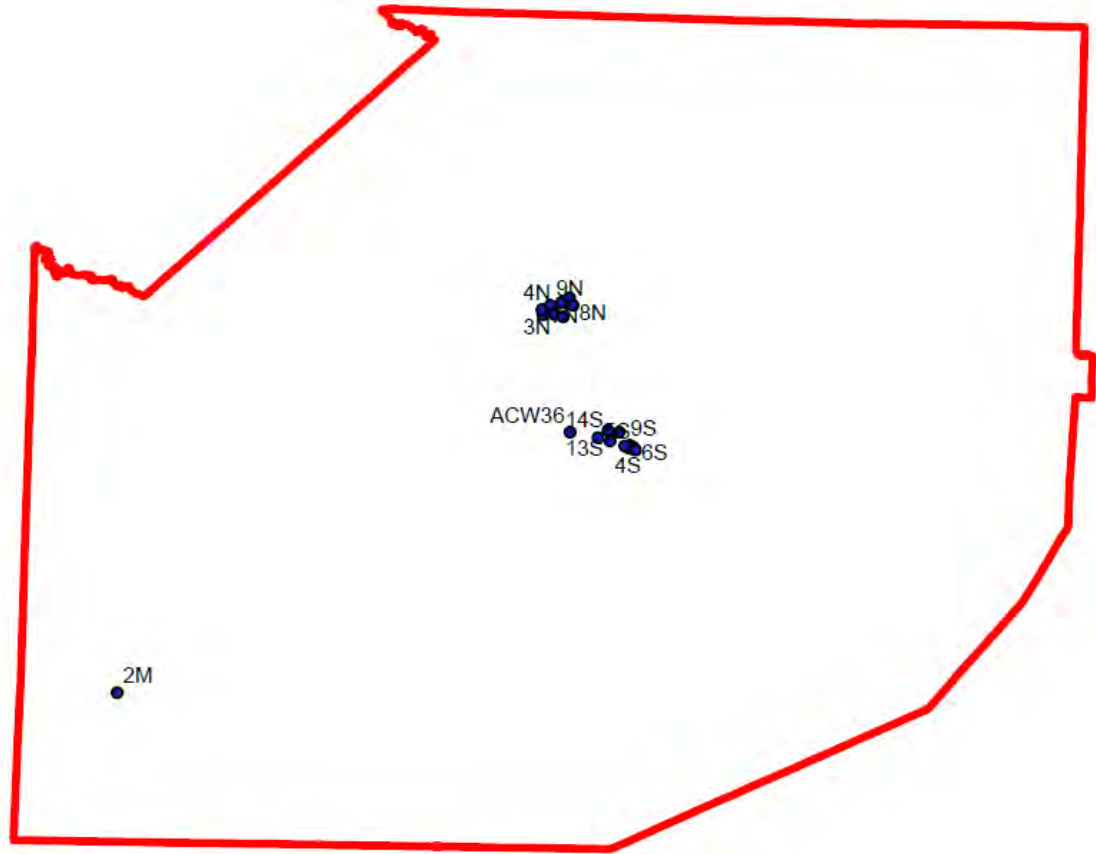


Figure 24: Distribution of groundwater wells of JEA within Madison County.

The groundwater level data of 23 wells were recorded for 15 years from 2006 to 2020 that during the monitoring water level of wells in 15 years, the change in water level was minor. Additionally, according to the information obtained from JEA, they have not encountered any sudden rise in water levels near rivers.

In the next step, we placed the water wells of JEA on the GWL contour map of Figure 23 and interpolated the GWL of each well from the contour map. By comparing the obtained GWL of JEA wells from the contour map with the latest measurements of GWL of wells by JEA, it was observed that the difference is negligible as Table 3 provides. Thus, the GWL contour map shown in Figure 23, will be utilized to obtain the GWL at each SPT soil borings of Madison County to perform liquefaction analysis.

Table 3. Comparison of obtained GWL of JEA wells from contour map with the latest measurement of GWL of wells by JEA.

Well No.	GWL Contour map (ft. NGVD 1929)	Measured GWL (ft. NGVD 1929)
1N	330	328.82
2N	339	339
3N	337	337
4N	340	340.5
5N	343	343.6
6N	349	349
7N	349	349
8N	338	338.13
9N	341	340
10N	342	342
11N	344	344
2S	351	351.3
3S	352	352.27
4S	353	353.1
5S	318	318.55
6S	345	345.02
9S	348	348.75
10S	354	354.31
11S	346	346.77
12S	340	340.26
13S	346	346.39
14S	341	341.1

Methodologies Used to Develop Liquefaction Probability Curves

Using the same general procedure of developing LPCs used for Lake, Dyer, Lauderdale, and Tipton Counties (Cramer et al., 2019, 2020a, b, 2021), we generated the LPCs of Madison County. To develop the LPCs of Madison County, the following three general main steps were taken:

1. Calculating the factor of safety (FS) against liquefaction at a given depth in the soil profile of each soil boring using the simplified procedure (Seed and Idriss, 1971).
2. Calculating the liquefaction potential index (LPI and LPI_{ISH}) of each soil boring location using:
 - o Iwasaki et al. (1978, 1982) method or,
 - o Maurer’s (2015) framework denoted as the LPI_{ISH} method herein.
3. Developing LPCs for the probability of exceeding LPI of 5 and 15 and LPI_{ISH} of 5 for each primary surficial geologic unit.

Like Tipton County, for Madison County, LPCs have been developed based only on SPT field test data. The procedure of developing LPCs based on SPT data for each geologic unit is described in the subsequent section.

Liquefaction Probability Curves Based on the Standard Penetration Test (SPT)

For Madison County, the SPT data were employed into two different approaches of LPI- and LPI_{ISH} -based to develop LPCs. In both methods, the LPCs were developed for the same 10 Peak Ground Accelerations (PGA) of 0.1, 0.2, 0.3, 0.4, 0.5, 0.6, 0.7, 0.8, 0.9, and 1.0 and seven Magnitude (M_w) of 5, 5.5, 6, 6.5, 7, 7.5, and 8 that we used in Dyer, Lauderdale, and Tipton County studies (Cramer et al., 2020a, b, 2021). Thus, we determined the distribution of LPI and LPI_{ISH} for each of the 70 possible combinations of PGA and M_w using the same methodologies and equations that we utilized for Dyer, Lauderdale, and Tipton County studies (Cramer et al., 2020a, b, 2021).

Furthermore, using the same procedure as Lake County, Dyer County, Lauderdale County, and Tipton County studies (Cramer et al., 2019, 2020a, b, 2021), we computed the probability of exceeding liquefaction potential indices (LPI and LPI_{ISH}) threshold values that will be discussed later in this report.

LPI-Based LPCs

Initially, the LPCs were developed based on the LPI approach in which it is assumed that all liquefiable layers equally contribute to the surficial manifestation of liquefaction without considering the impact of the non-liquefiable cap on liquefiable layers. LPI-based LPCs were generated for two surface geology units of floodplain alluvium and non-floodplain alluvium which is consisted of terrace alluvium and Paleogene/Cretaceous strata; however, for non-floodplain alluvium, all borings are within terrace alluvium and there is no boring is within the Paleogene/Cretaceous which has the highest elevation; consequently, the lowest GWL and the lowest probability of liquefaction. For the floodplain alluvium part of Madison County, LPCs were developed based on SPT data of 25 soil borings while for the non-floodplain alluvium the number of utilized soil borings data was 44. Figures 25 and 26 show the LPCs for floodplain alluvium and non-floodplain alluvium for the probability of exceeding LPI of 5 and 15 denoted as $P[LPI>5]$ and $P[LPI>15]$ versus the ratio of PGA over magnitude scaling factor (MSF).

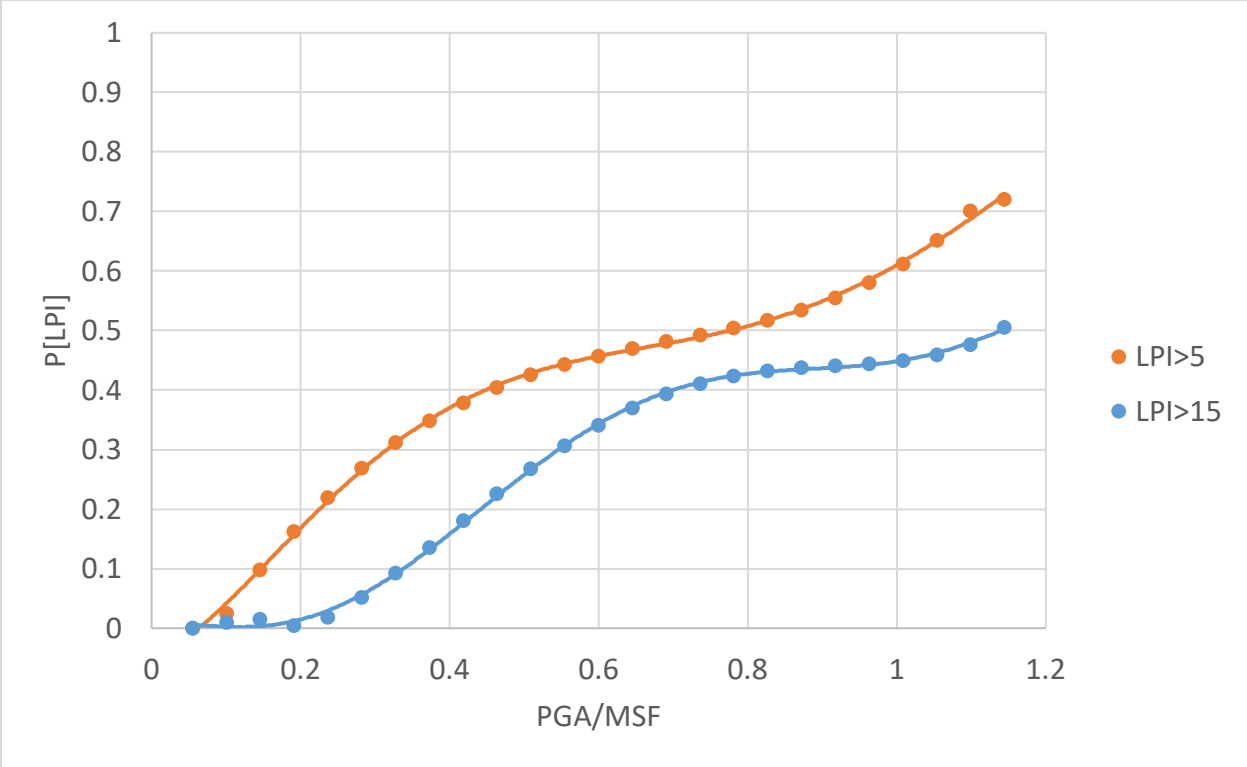


Figure 25: LPI-based LPCs of floodplains from SPT data.

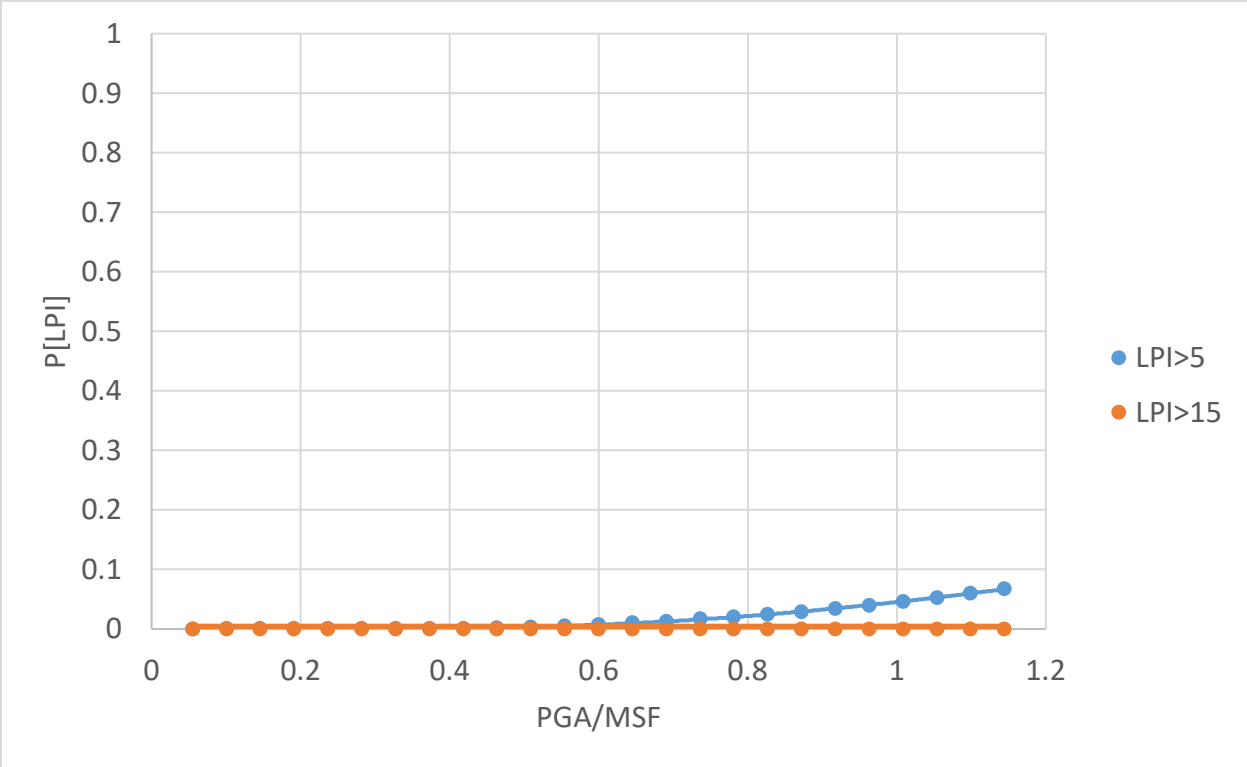


Figure 26: LPI-based LPCs of non-floodplains from SPT data.

As was expected, the floodplain alluvium LPCs are significantly higher than the non-floodplain alluvium LPCs for both $P[LPI>5]$ and $P[LPI>15]$. Table 4 provides the maximum probability of exceeding $LPI>5$ and $LPI>15$ for each geologic unit that was observed from the LPCs at the highest ratio of PGA/MSF.

Table 4. The maximum probability of exceeding $LPI>5$ and $LPI>15$ at each geologic unit.

The maximum probability of exceeding	Floodplain alluvium	Non-floodplain alluvium
$P[LPI>5]$	0.72 (72%)	0.07 (7%)
$P[LPI>15]$	0.50 (50%)	0.0 (0%)

According to the above table, for the floodplain alluvium the probability of moderate to severe liquefaction ($P[LPI>5]$), reaches 70% while for non-floodplain alluvium this probability is a small percent of 7%. On the other hand, the maximum probability of severe liquefaction occurrence ($P[LPI>15]$) in the floodplain is a significant value of 50% and in non-floodplain alluvium is completely 0%.

LPI_{ISH}-Based LPCs

In addition to the LPI-based method of developing LPCs, Maurer’s (2015) framework which employs the LPI_{ISH} index has been utilized to develop LPCs by considering the influence of non-liquefiable layers thickness on the surface manifestation of liquefaction. The detail of Maurer’s framework is provided in Seismic and Liquefaction Hazard Mapping of Dyer County report (Cramer et al., 2020a). However, the $P[LPI_{ISH}>15]$ was not determined for Madison County because Maurer’s framework (Maurer, 2015) is based on only $P[LPI_{ISH}>5]$.

Using Maurer’s framework based on LPI_{ISH} , we generated new LPCs for both floodplain alluvium and non-floodplain alluvium parts of Madison County. Also, later in this section, we will compare the LPCs obtained based on LPI and LPI_{ISH} .

Figures 27 and 28 illustrate the LPCs obtained based on SPT boring data for floodplain alluvium and non-floodplain alluvium parts of Madison County, respectively.

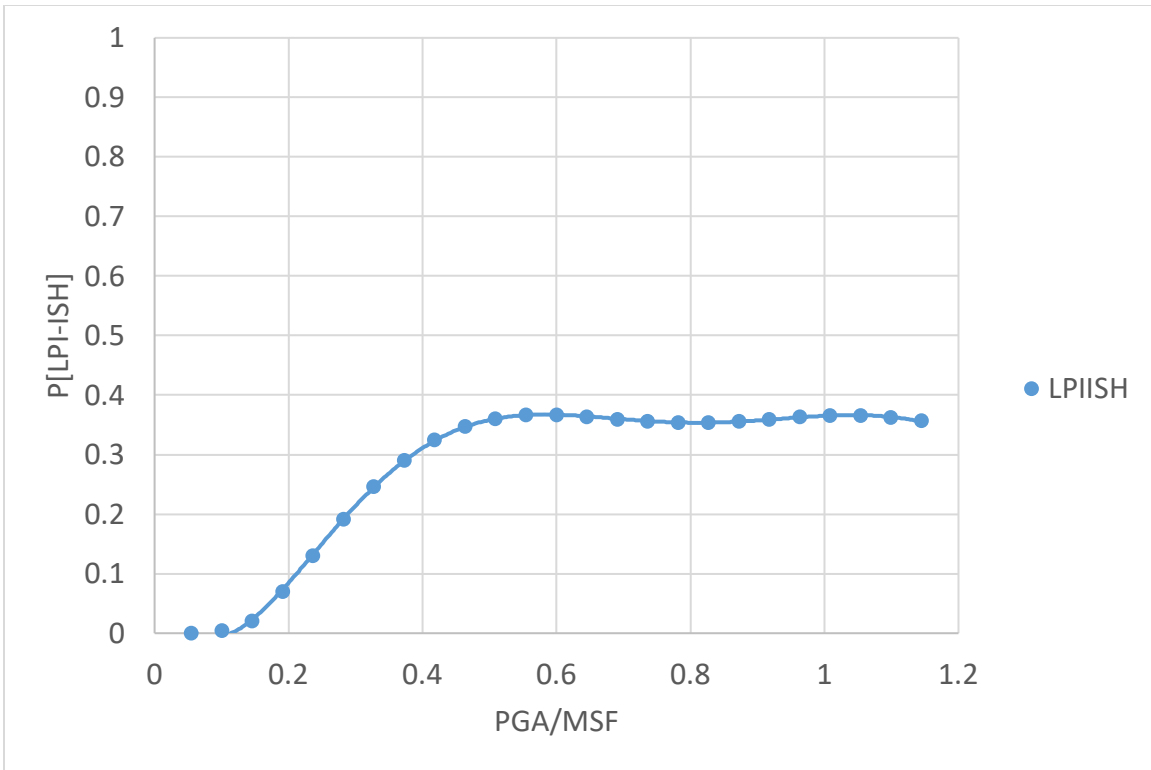


Figure 27: LPI_{ISH} based LPCs of the floodplain from SPT data.

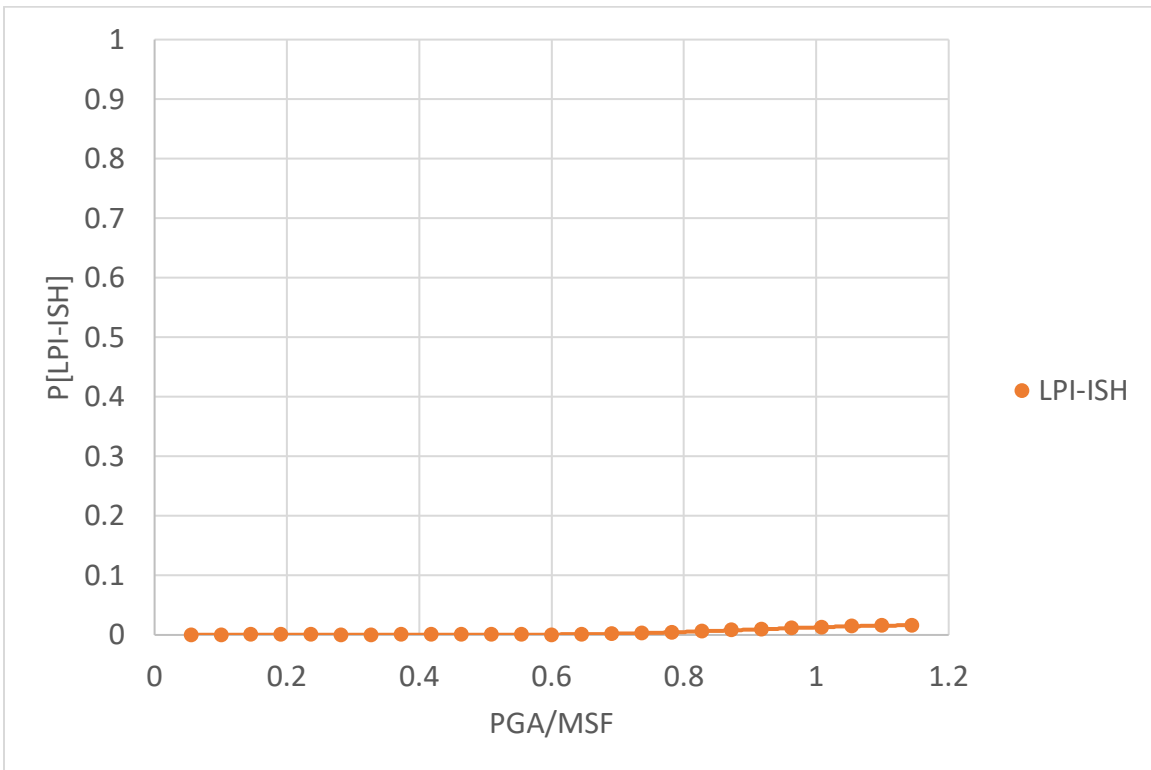


Figure 28: LPI_{ISH} based LPCs of non-floodplain from SPT data.

For the floodplain, the LPI_{ISH} based LPC shows a maximum liquefaction probability of ~36% for the most intense earthquake scenario. On the other hand, for the non-floodplain areas of Madison County, LPI_{ISH} based LPC barely reaches a maximum of 2% probability of liquefaction occurrence.

The results of the LPI- and LPI_{ISH} - based methods are compared and discussed in the next section.

Comparison of LPI- and LPI_{ISH} -based LPCs

Figure 29 provides a comparison of LPCs for floodplain areas of Madison County for $P[LPI > 5]$. According to Iwasaki's method, $LPI > 5$ represents the range of moderate to severe liquefaction, and based on Maurer's framework, LPI_{ISH} of 5 is the threshold value of liquefaction occurrence that above 5, liquefaction occurs and below 5 there is no liquefaction. Figure 29 indicates that the probability of liquefaction provided by the LPC based on the LPI_{ISH} framework is significantly lower than the probability of liquefaction provided by the LPC based on the LPI framework especially at higher ratios of PGA/MSF in which the maximum difference is about 37% for $P[LPI/LPI_{ISH} > 5]$.

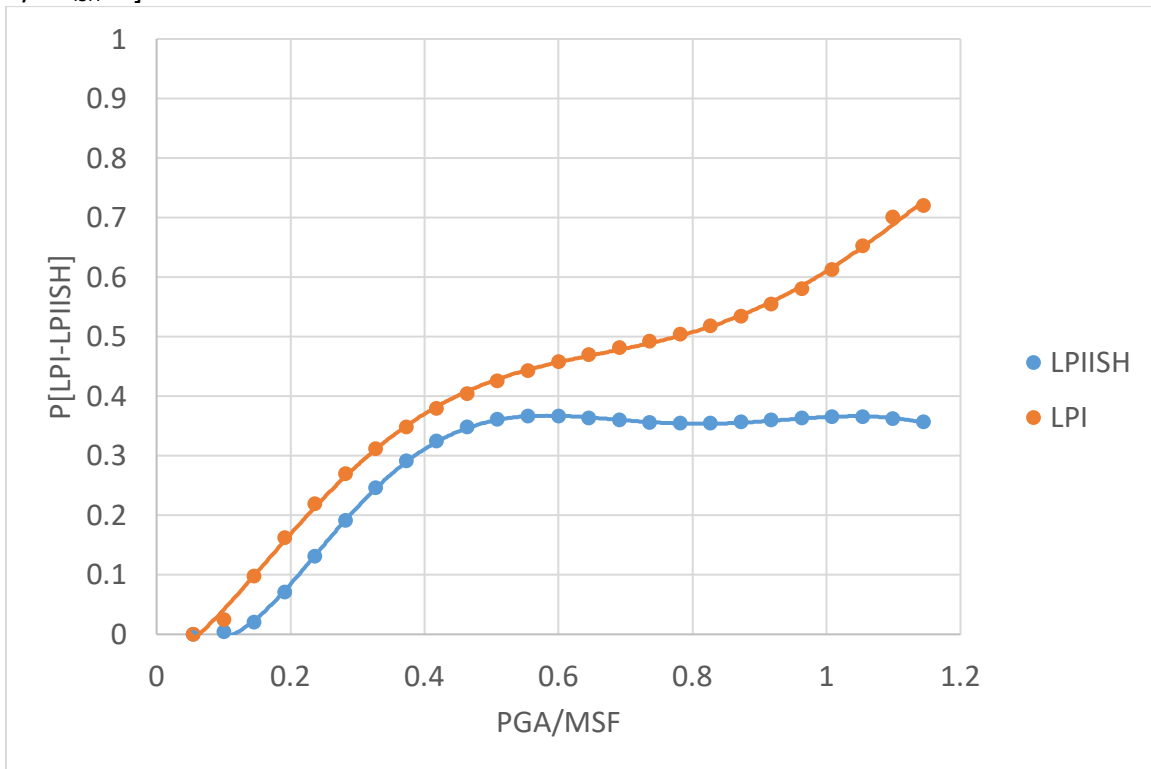


Figure 29: LPI- and LPI_{ISH} -based floodplain LPCs for $P[LPI/LPI_{ISH} > 5]$.

For the non-floodplain parts of the county, the comparison between LPI and LPI_{ISH} based LPCs is shown in Figure 30. Similar to the results of the floodplain areas, for the non-floodplain areas the LPI_{ISH} based LPC show lower probabilities than LPC from the LPI method. However, the

amount of difference between the LPCs of the two frameworks is less for the non-floodplain than the floodplain.

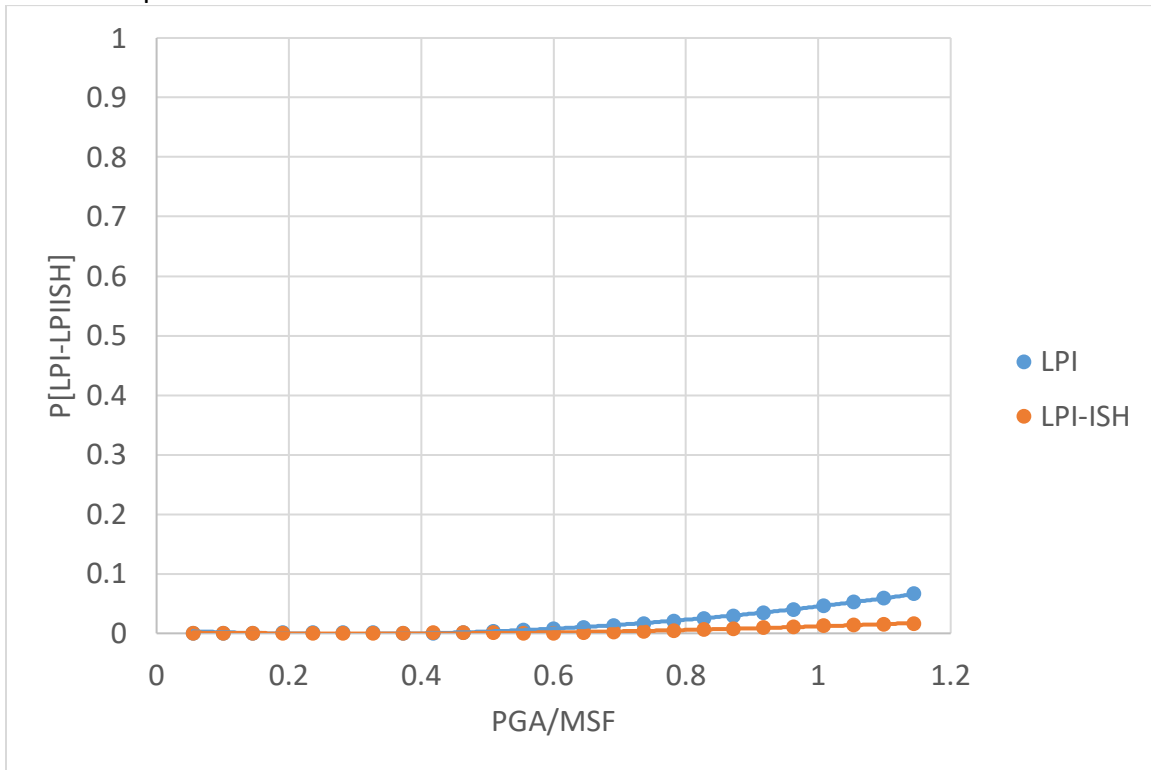


Figure 30: LPI- and LPI_{ISH}-based non-floodplain LPCs for P[LPI/LPI_{ISH}>5].

Figure 30 depicts that both LPCs are showing the same probability in the range of 0 to 0.4 PGA/MSF while for PGA/MSF higher than 0.4, LPI-based LPC reaches ~7% probability for PGA/MSF of 1.2 for which the LPI_{ISH} LPC is showing a probability of ~1.6%.

LPCs for liquefaction hazard maps of Madison County

This section discusses the recommended LPCs for floodplain and non-floodplain parts of Madison County that are utilized to generate liquefaction hazard maps. For Madison County, because there was not enough Vs profile data available the LPCs were developed only based on the SPT borings data of USACE, TDOT, and Construction Material Lab, Inc.

Floodplain LPCs Recommendation for Liquefaction Hazard Maps of Madison County

For the floodplain near-surface geology part of Madison County, the LPCs were developed using SPT data of 25 borings based on Iwasaki’s LPI method for P[LPI>5] and P[LPI>15], and LPI_{ISH} of Maurer’s framework for P[LPI_{ISH}>5]. As shown in the Comparison of LPI- and LPI_{ISH} -based LPCs section of this report, because Maurer’s framework considers the impact of non-liquefiable layers thickness on the surficial manifestation of liquefaction, Maurer’s framework-based LPCs show a significantly lower probability of liquefaction than LPI-based LPCs. Thus, to consider the influence of non-liquefiable layer thicknesses on liquefaction hazard maps, it is suggested that

the liquefaction hazard maps of the floodplain part of Madison County be based on the LPCs of both frameworks of Iwasaki and Maurer as presented in Figures 25 and 27, respectively.

Non-Floodplain LPCs Recommendation for Liquefaction Hazard Maps of Madison County

Similar to the floodplain part of the county, for the non-floodplain parts (Pliocene/Pleistocene river terraces and Paleogene/Cretaceous strata), the LPCs were also developed based on both approaches of Iwasaki and Maurer's LPI_{ISH} using SPT data from 44 borings. Although all 44 SPT soil borings are within Pliocene/Pleistocene river terraces, it is recommended the developed LPCs based on these 44 SPT soil borings be utilized for the Paleogene/Cretaceous strata too.

As noted in the Comparison of LPI- and LPI_{ISH} -based LPCs section of this report, the LPI-based LPCs show a higher trend than Maurer's based LPCs due to the impact of non-liquefiable layers thickness on liquefaction surface manifestation of liquefiable layers. For the non-floodplain areas of Madison County, it is suggested that the liquefaction hazard maps be developed based on both frameworks of Iwasaki and Maurer as presented in Figures 26 and 28, respectively.

Geotechnical Summary

We used the same general procedure to develop LPCs that we utilized to develop the Dyer, Lauderdale, and Tipton Counties LPCs (Cramer et al., 2020a, 2020b, 2021). However, unlike Dyer County where the LPCs were developed based on SPT-N as well as V_s profile data, in Madison County due to the COVID-19 situation the procedure of conducting V_s tests could not be done and the LPCs were developed based only on the SPT-N data.

The surficial geology of Madison County consists of three primary units of floodplain alluvium, Pliocene/Pleistocene river terraces, and Paleogene/Cretaceous strata. The primary LPCs of Madison County were developed based on Iwasaki's LPI methodology that was utilized to develop the LPCs of Shelby County (Cramer et al., 2015; Cramer et al., 2018a) as well as Lake County (Cramer et al., 2019), Dyer County (Cramer et al., 2020a), Lauderdale County (Cramer et al., 2020b), and Tipton County (Cramer et al., 2021). The LPI-based LPCs of floodplain and non-floodplain (Pliocene/Pleistocene river terraces and Paleogene/Cretaceous strata) parts of the county are provided in Figures 25 and 26, respectively. For each geologic unit, the LPCs are shown for $P[LPI > 5]$ and $P[LPI > 15]$ which represent the "moderate to severe" and "severe" probability of liquefaction, respectively. For Madison County, because there was no SPT-N boring available within the Paleogene/Cretaceous strata, therefore the developed LPCs based 44 SPT borings of Pliocene/Pleistocene river terraces are utilized for entire non-floodplain areas of the county.

Additionally, the LPCs of Madison County were developed based on Maurer's (2015) framework based on LPI_{ISH} to contribute the impact of non-liquefiable layer thickness on the surficial manifestation of liquefaction that was utilized in Dyer County (Cramer et al., 2020a) and referred herein as LPI_{ISH} method. Figures 27 and 28 illustrate the LPCs obtained using the LPI_{ISH} method and based on the SPT boring data for the floodplain and non-floodplain areas,

respectively. For both the floodplain and non-floodplain areas of Madison County, the probability of liquefaction provided by the LPCs based on the LPI_{ISH} framework are lower than the LPCs based on the LPI framework especially at higher ratios of PGA/MSF.

For the floodplain parts of Madison County, it is suggested that the liquefaction hazard maps be based on both LPI- and LPI_{ISH}-based LPCs developed from SPT data of 25 soil borings. For the floodplain parts of Madison County, the LPI- and LPI_{ISH}-based LPCs are presented in Figures 25 and 27, respectively. For the non-floodplain, it is recommended that the LPCs of LPI and LPI_{ISH} based approaches were developed based on the SPT data of 44 boring logs within the Pliocene/Pleistocene river terraces parts of the county be used to develop liquefaction hazard maps. The non-floodplain LPI- and LPI_{ISH}-based LPCs are provided in Figures 26 and 28, respectively.

Seismic Measurements

Introduction

Multichannel Analysis of Surface Waves (MASW) is a geophysical exploration technique that measures shear-wave velocity of underground layers using the dispersion of surface waves along an array of geophones. The MASW seismic survey obtains velocity structure of the layers using surface waves.

The seismic refraction method is sensitive to low velocity layers. If low velocity layers are not detected, the results of seismic refraction may be compromised, while seismic reflection can detect geological features not seen in refraction tests. Geophysical exploration at shallow depths (less than 50 meters) can be a challenge. Invasive procedures such as downhole and crosshole seismic surveys can be expensive. Non-invasive procedures such as MASW can be advantageous and economical and can be a viable alternative.

In the MASW method, an array of geophones captures the surface waves that are generated by an energy source such as a sledgehammer or a heavier source (Figure 31). The changes in amplitude and arrival times are measured using a post-processing software at different frequencies (e.g., SurfSeis, developed by Kansas Geological Survey, KGS). These “changes” are associated with the dispersion of surface waves. Complicated propagation of surface waves has unique characteristics that can relate the amplitude of surface waves with shear-wave velocity, depth, and frequency. In a few words, amplitude (and consequently, velocity) of a certain frequency of surface waves (phase velocity) is affected by the shear-velocity structure of the ground down to certain depths. This combination provides us with valuable information called dispersion curves, which is a plot of phase velocity versus frequency. Figure 32 shows the amplitude variation of surface waves with respect to wavelength, which is the normalized depth on the vertical axis and normalized motion (amplitude at depth z over amplitude at surface) on the abscissa. As shown in Figure 33, longer wavelength (or lower frequencies) can sample larger depths.

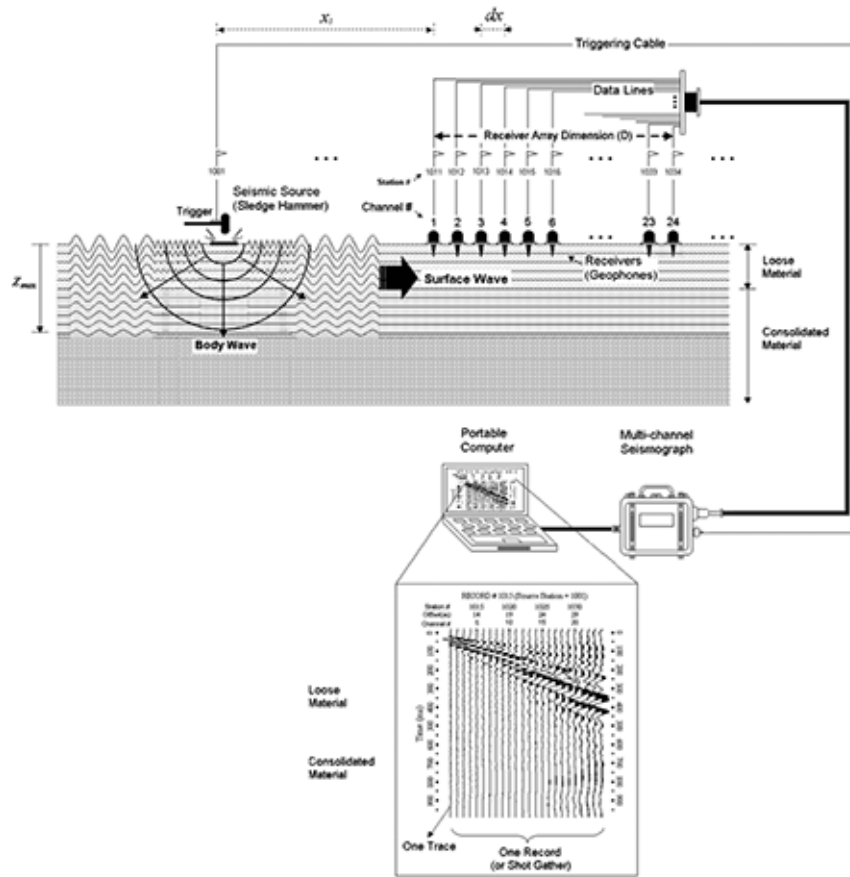


Figure 31: Active MASW test setup. (from KGS.ku.edu).

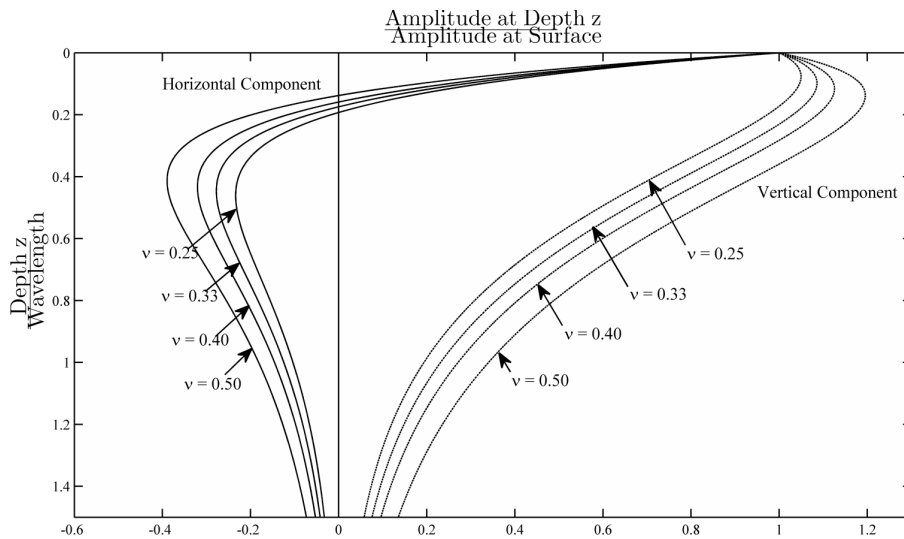


Figure 32: Variation of horizontal and vertical normalized components of displacements induced by Rayleigh waves with normalized depth in a homogeneous isotropic, elastic half-space.

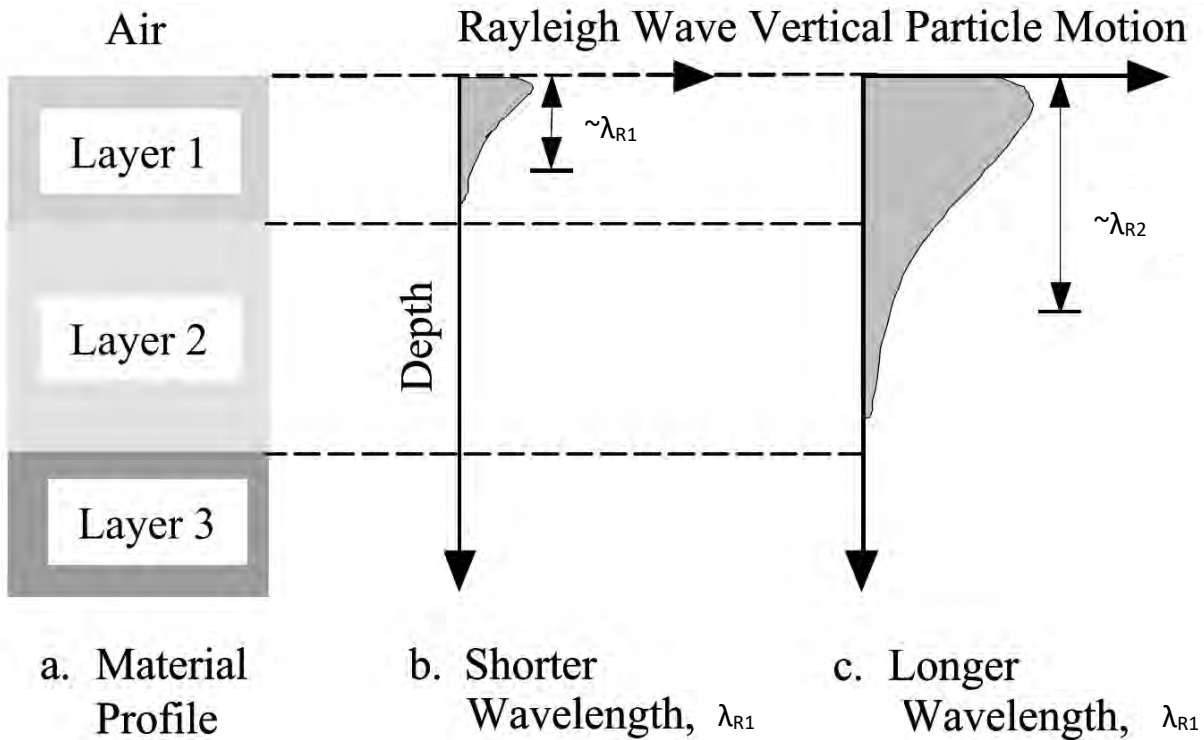


Figure 33: Depth sampled by Rayleigh waves with different wavelengths (Stokoe II and Santamarina, 2000).

Finally, through an iterative inversion process using the SurfSeis software, the best matching velocity profile is obtained. It is important to mention that the inversion process may produce several shear-wave velocity profiles with similar dispersion curves matching the experimental dispersion curve which is referred to as the non-uniqueness of the inversion process. There are some provisions embedded in the software that can remove irrelevant velocity profiles. Also, geological studies and prior expert knowledge can help mitigating the non-uniqueness issue.

MASW Equipment and Testing procedure

In all the sites that we performed MASW survey in 2020 (7 in Madison County), we used a 96 m linear array of 48 4.5 Hz geophones with 2 meters of spacing between geophones. Our active energy source was a large sledgehammer. The energy produced by striking the sledgehammer on a plate on the ground's surface was experimentally considered enough for the entire length of the array plus a 8m offset from the first geophone.

We started shooting at an 8 m offset from the first geophone and advanced every 4 meters through the middle of the spread. Each location was shot three times. Several shots per location can help reduce the effects of noise by stacking the records. Stacking will average out the noise and enhance the main signal, to reach a higher signal to noise ratio.

To obtain deeper velocity structures (e.g., lower frequency range) we recorded ambient noise using the Refraction Microtremor (ReMi) seismic survey. An array of 24 geophones with 10 ft spacing was placed at the same location and several 32s second records of data was acquired multiple times. The dispersion curve obtained using the MASW seismic survey was augmented with the dispersion curve points obtained by the ReMi procedure to better estimate the shear-wave velocity of deeper layers of the soil structure. We used the SeisOpt ReMi software to process data collected using the ReMi seismic survey.

Data Processing

Data processing is performed using the SurfSeis software. The recordings were analyzed to obtain the “Overtone Images” (Figure 34). In Figure 34 and 35, the vertical axis is the phase velocity in m/sec and the horizontal axis is the frequency. The dispersion curves were automatically picked, and visually checked. Furthermore, the dispersion curve obtained using the ReMi procedure were combined with the MASW dispersion curve as shown in Figure 35. In some cases, dispersion curves from MASW were augmented with ReMi at low frequencies to obtain information at greater depths. Then, the dispersion curves were inverted to obtain the shear-wave velocity profile associated with the site. In Figure 35, the orange curve is the high energy (the middle of the overtone image from ReMi analysis) and the gray curve is the lower energy curve (the lower margin of the overtone image). The lower limit of the apparent phase velocities can be recognized as the true phase velocities (Louie, 2001).

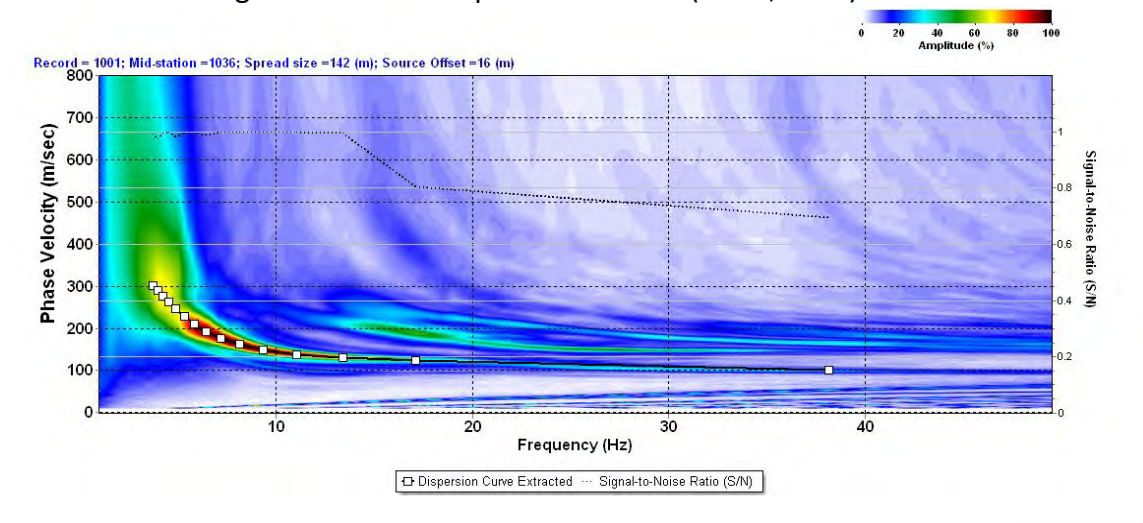


Figure 34: A sample of the dispersion curve obtained by the Surfseis Software.

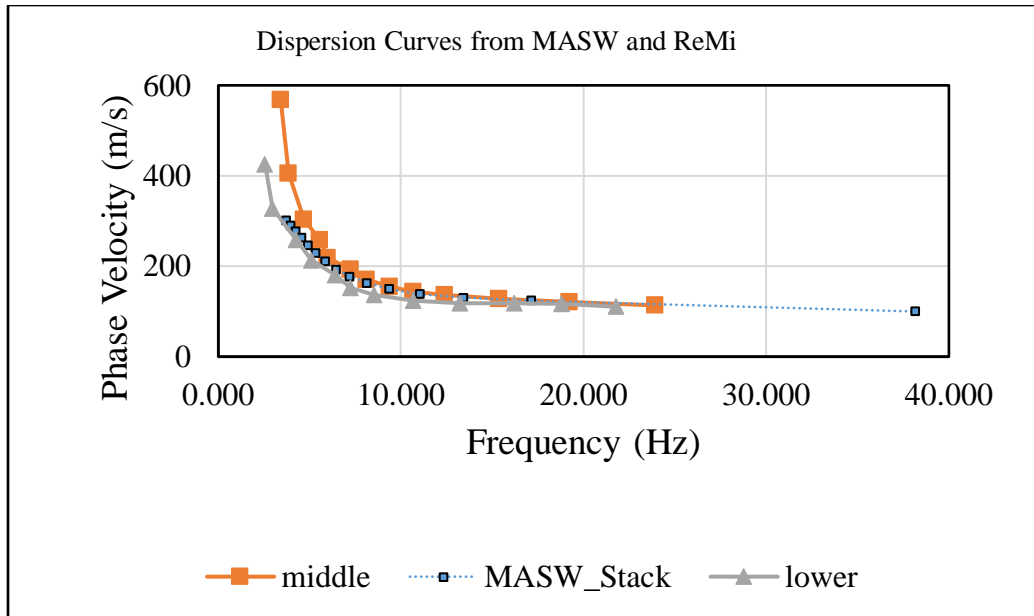


Figure 35: Comparison of dispersion curves obtained with MASW and ReMi.

Depth of investigation is proportional to the largest wavelength captured by the instruments (Schuler, 2008).

$$\text{Depth of Investigation} = 0.4 \times \text{Wavelength} = 0.4 \times \text{Velocity} / \text{frequency}$$

Depth of investigation depends on a few parameters.

- Corner frequency of the geophones, which was 4.5Hz in our case that is a widely and practically used device for surface exploration methods.
- Energy source. The energy source should be strong and capable of generating enough low frequencies.
- Velocity of subsurface soil. The faster the velocities, the greater depth we can measure.
- Noise in the area. A noisy location can obscure wave motion at long distances, where the wave has attenuated.

Results

The final results of the 7 MASW and ReMi 2020 seismic surveys (Figure 36) in Madison County are summarized in this section (Figure 37). We were able to obtain shear-wave velocity profiles to depths of about 30m. We compared these results with the Pezeshk et al. (1998) Jackson TDOT downhole Vs profile to a depth of 50m. Our studies in Lake (Cramer et al., 2019), Dyer (Cramer et al., 2020a), and Lauderdale (Cramer et al., 2020b) Counties confirms that the MASW

procedure can estimate down to 50m depth with acceptable accuracy. In Madison County data quantity does not support the reliability and accuracy at depths higher than 20-30m. In general, uncertainty increases with depth. In some cases, we included higher modes into our inversion process to enhance the resolution of the velocity profiles. Although, the estimated depth of the velocity profile is only dependent on the wavelength (frequency) of the modes, meaning that including higher modes does not increase the depth of conversion. Yet, the benefit of recognizing higher modes is to increase the resolution of the profile and decreasing the uncertainty of the inversion process.

Figure 38 presents the mean and standard deviation of the velocity profiles with depth. There is not a lot of sampling of the three soil types (river alluvium, terrace, and Claiborne). In Figure 38 it is clear that these three soil types are only distinct above 10 m depths. At depth, all the profiles merge to the Claiborne soil profile. The Claiborne soils are found below the river alluvium and terrace deposits in Madison County. The Jackson TDOT profile penetrates well into the Claiborne deposits at depth and indicates similar Vs values as the Claiborne MASW profiles at the surface.

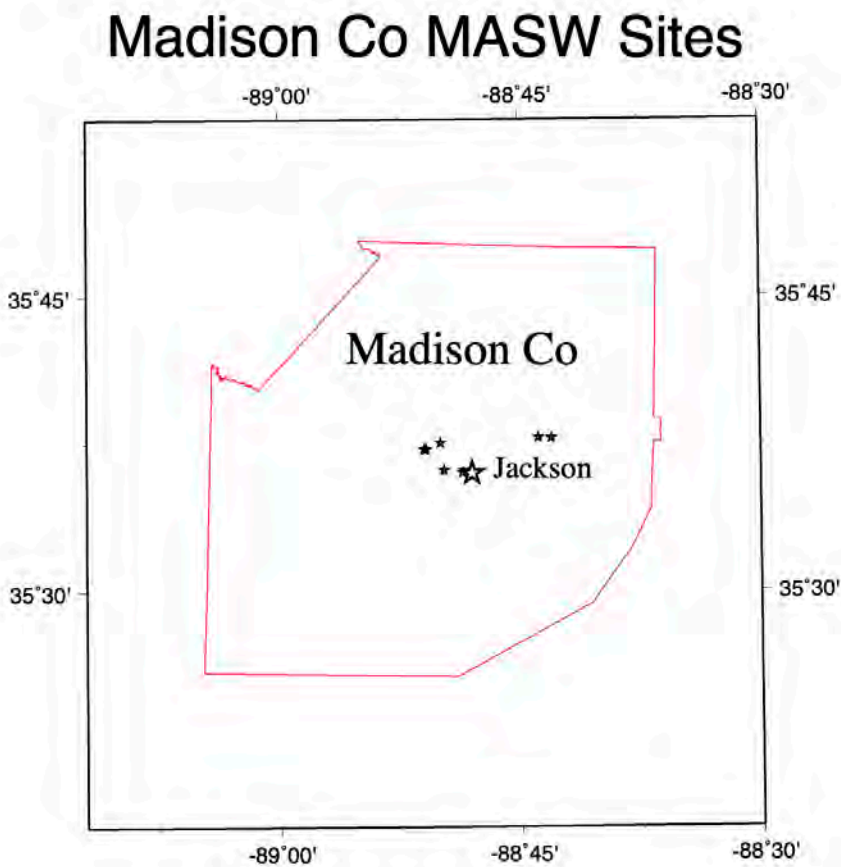


Figure 36: Location of MASW measurements (filled stars) in Madison County (red outline).

Madison Co Vs Profiles

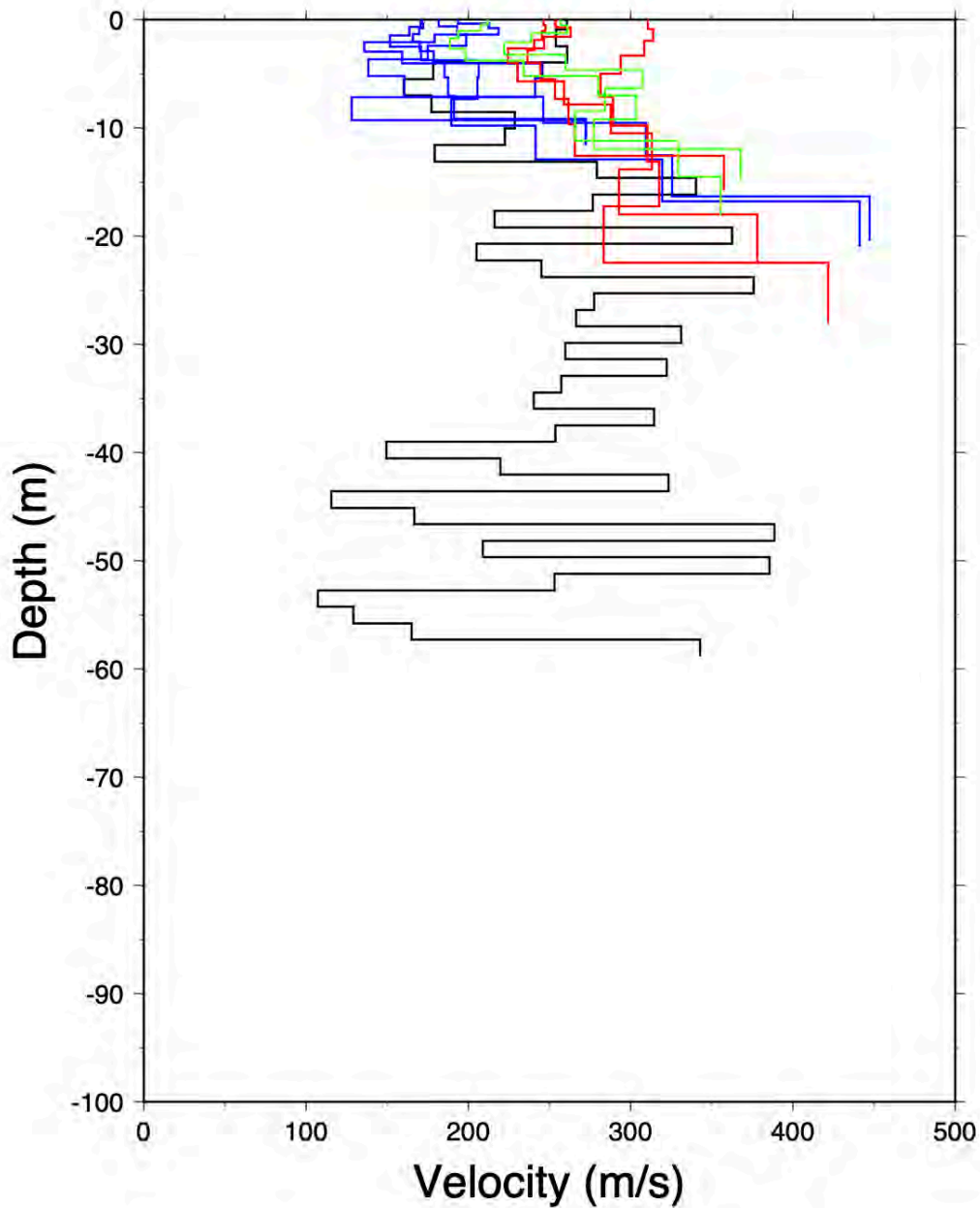


Figure 37: Comparing the velocity profiles obtained via testing at 7 Madison County sites and the Jackson TDOT site (black). Blue is for river alluvial sites, green is for terrace sites, and red is for Claiborne sites.

Madison Co Vs Profiles

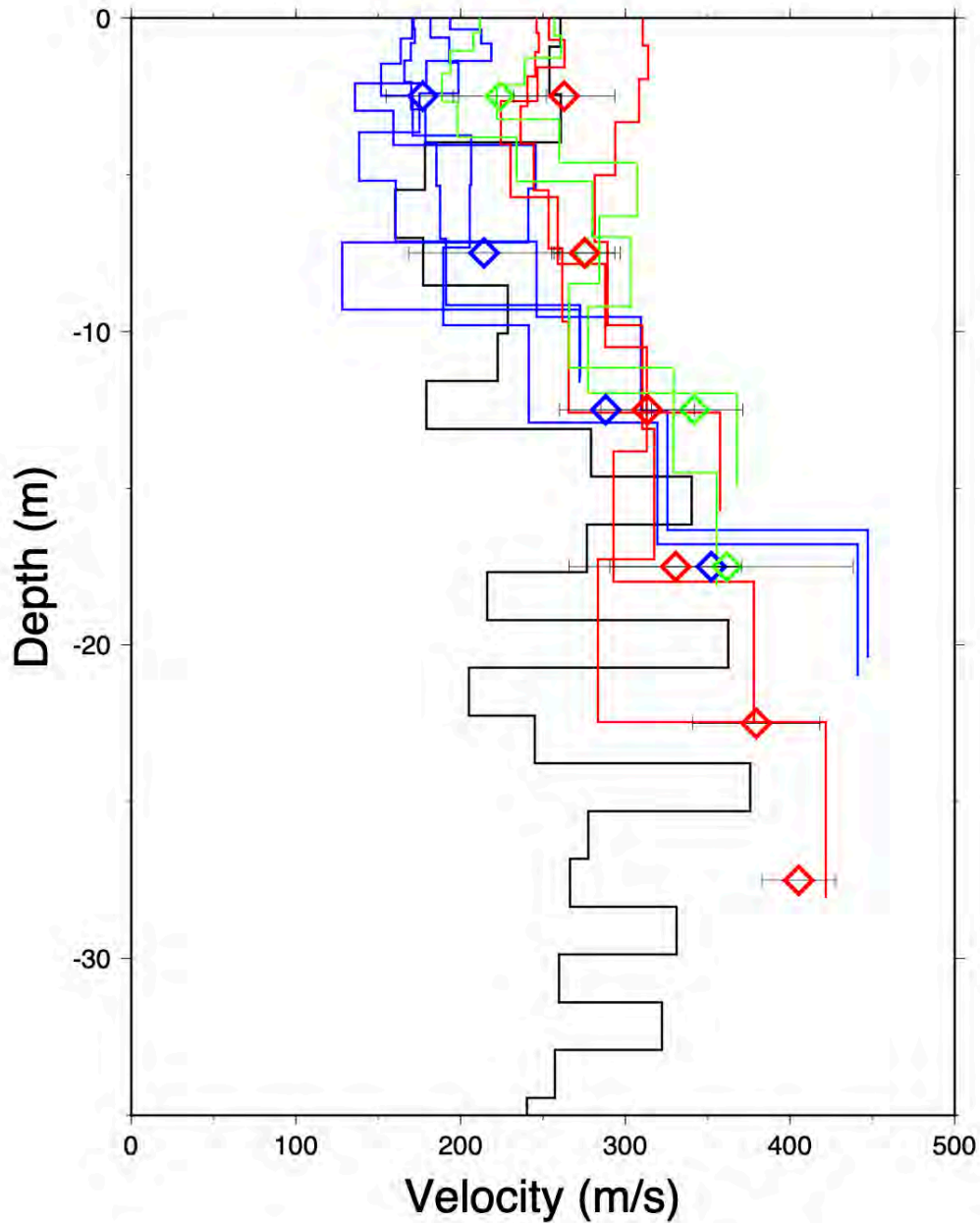


Figure 38: Mean and standard deviation (diamonds with error bars) of river alluvial (blue), terrace (green), and Claiborne (red) velocity profiles in Madison County. Also shown is the Jackson TDOT profile (black) on river alluvium at the surface.

Hazard Maps Development

Methodology

A standard methodology for including the effects of local geology in seismic and liquefaction hazard estimates was used in this study. We followed the approach of Cramer et al. (2006, 2008, 2014, 2017, and 2018a) of developing site amplification distributions on a grid, applying those distributions to modify hard rock hazard curves to geology-specific hazard curves and develop seismic hazard maps, and then applying geology-specific liquefaction probability curves to develop liquefaction hazard maps. The site amplification distributions are based on the 3D geological, geotechnical, and seismological models developed above for Madison County. The 2014 U.S. Geological Survey (USGS) National Seismic Hazard Project's seismic hazard model (seismic sources and ground motion attenuation model of Petersen et al., 2014) for hard rock was modified using our Madison County site amplification distributions. Probabilistic seismic hazard maps were generated from the USGS probabilistic model and scenario (deterministic) seismic hazard maps were generated using selected scenario fault ruptures (earthquakes) and the USGS ground motion attenuation model. The resulting peak ground acceleration (PGA) seismic hazard maps were then modified using appropriate Madison County liquefaction probability curves (discussed above) to generate liquefaction hazard maps (both probabilistic and scenario).

Madison County Shear-wave Velocity Model

Seismic hazard maps with the effects of local geology depend on developing site amplification distributions on a grid for the 3D geology of the study area. The 3D geology is converted to geologic (sediment) profiles on a uniform grid. The geology layers are converted to shear-wave velocity (V_s) profiles at each grid point and input to a geotechnical soil response program (SHAKE91), along with appropriate geotechnical properties, to develop site response distributions at each grid point using the University of Memphis High Performance Computing (HPC) facility. The site amplification distributions model frequency and amplitude dependent amplification/deamplification at the surface of hard rock ground motions input at the bottom of the sediment profile.

The Madison County representative velocity models used were developed from published and measured V_s profiles in and near the county. The MASW results suggest that average V_s for river alluvial deposits (Qal) is 180 m/s, for the terrace deposits (QTf) is 225 m/s, and for the Claiborne deposits is 300 m/s, within measurement uncertainties. No measurement of V_s are available for the deeper deposits of the Wilcox Group, Porter's Creek Clay, and Cretaceous geological layers of the Madison 3D geology model. We assigned values of 500, 700, and 900 m/s, respectively, to these geologic deposits based on observations in Shelby County (Cramer et al., 2004; Cramer, 2006) reduced for the shallower depths of burial in Madison County. A fairly large uncertainty was assigned to these V_s values (Table 5).

Table 5: Geotechnical profile used in 3D geology hazard model. Uncertainties are one std. deviation.

Formation	DepthToTop(m)	Damping	Density(g/cc)	Velocity(m/s)
Alluvium	0.	0.05	2.00	180±13
Terrace	5.0±1.00	0.05	2.00	225±13
Claiborne	10.0±1.00	0.03	2.00	300±25
Wilcox Group	20±2.5	0.02	2.00	500±50
Porter's Creek Clay	40±2.5	0.02	2.00	700±25
Cretaceous	150±13	0.01	2.50	900±50
Paleozoic	400±25	0.001	2.80	2800

Grids

There is one grid size used in our Madison County study. The 3D geology for the depth to the top of the Alluvium, Terrace, Claiborne, Wilcox, Porter’s Creek, Cretaceous, and Paleozoic layers were provided on a 0.005-degree grid (~500 m). These geology inputs were combined using the Vs models discussed above for site amplification distribution and seismic hazard calculations. The final seismic and liquefaction hazard maps use this 0.005-degree grid spacing.

Time History Database

The site amplification distribution calculations use a suite of input time histories (seismograms) at the bedrock/sediment interface to estimate sediment response. Time histories are required by soil response computer programs to estimate site response. The time histories used are listed in Table 6 and have been used by Cramer et al. (2006, 2017, and 2018a) in similar seismic hazard analyses. At each grid point, the time history used is randomly selected for each iteration in the soil profile randomization to properly include uncertainty in the site amplification distribution calculations.

Table 6: Strong motion time series on rock used in the analysis (Cramer, 2006).

Earthquake	Station	Components
1989 M 6.9 Loma Prieta, California	G01	E, N
1992 M 7.1 Cape Mendocino, California	CPM	E, N
1992 M 7.3 Landers, California	JOS	E, N
1995 M 6.9 Kobe, Japan	KJM	E, N
1999 M 7.4 Kocaeli, Turkey	GBZ	W
	IZT	S
1999 M 7.6 Chi-Chi, Taiwan	TCU	N, W
1999 M 7.1 Duzce, Turkey	1060	E, N
Atkinson and Beresnev (2002)	M 7.5 and M 8.0 at Memphis, Tennessee	

Hazard Maps

Seismic and liquefaction hazard maps have been developed for both probabilistic and scenario cases. Probabilistic hazard maps have been generated for 10%, 5%, and 2% probability of exceedance in 50 years. The 2%-in-50-year maps correspond to current building code standards and represent up to the 80 percentile New Madrid seismic ground motions. 5%-in-50-year maps are similar to median scenario ground motion maps for the **M**7 earthquakes in the New Madrid seismic zone and represent up to 60 percentile ground motions. The 10%-in-50-year maps correspond to an older design standard and only represent up to 35 percentile ground motions from the New Madrid seismic zone (NMSZ) sources. The 10%-in-50-year maps do not adequately represent expected median ground motions from New Madrid 1811-1812

earthquakes, are no longer recommended for design purposes by regulatory agencies, and are not presented here.

Median ground motion scenario (deterministic) hazard maps have been generated for seven scenario earthquakes (Table 7 and Figure 39) and represent median expected ground motions from those earthquakes. The scenarios are for the largest earthquakes from the 1811-1812 New Madrid sequence, a **M6** earthquake in 1843, and for a hypothetical **M5.8** earthquake in Madison County near Jackson. Because of its distance from Madison County and low expected ground motions, the historical **M6** in 1895 earthquake is not included in our collection of scenarios for Madison County. The **M5.8** scenario represents the effects of recent **M5.5-6.0** Central and Eastern North American earthquakes if a similar size earthquake were to occur in Madison County.

The ground motion periods represented in the Madison County seismic hazard maps are peak ground acceleration (PGA), 0.2 s, and 1.0 s. 0.3 s maps have also been generated for compatibility with HAZUS, a risk and loss assessment package commonly used in loss analysis. The 0.2 and 0.3 s hazard maps are similar so the 0.3 s hazard maps are not shown in this report.

Table 7: Scenario earthquakes used in Madison County study.

- M 7.7** on the Reelfoot Thrust (central segment)
- M 7.5** on the Cottonwood Grove Fault (SW segment)
- M 7.3** on the New Madrid North Fault (NE segment)
- M 6.9** “Dawn” Aftershock (2 alternatives)
- M 6.2** near Marked Tree, Arkansas (1843 earthquake)
- Hypothetical **M 5.8** earthquake near Jackson (recent CEUS earthquakes)

Madison Co Scenario Eqqs

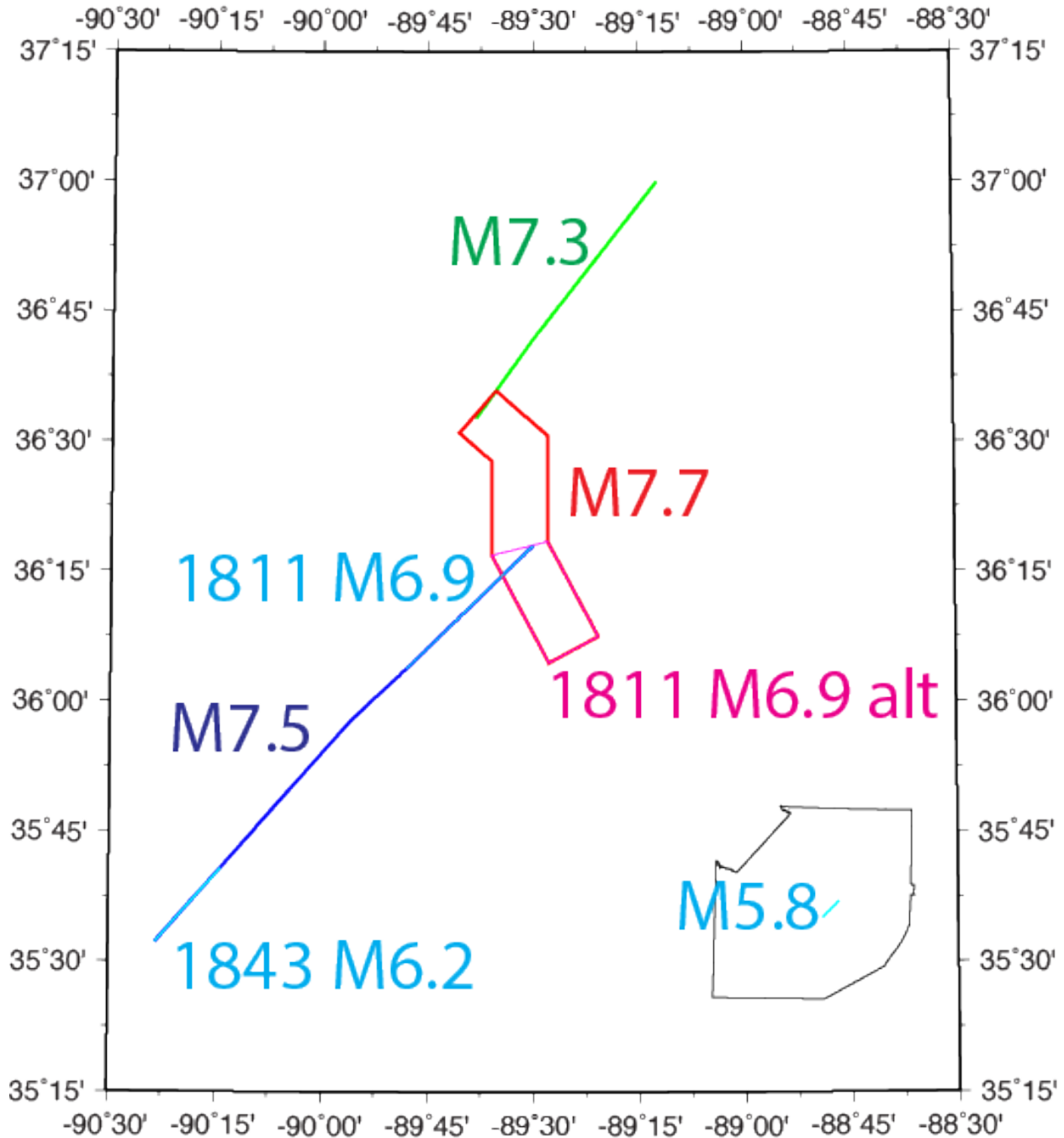
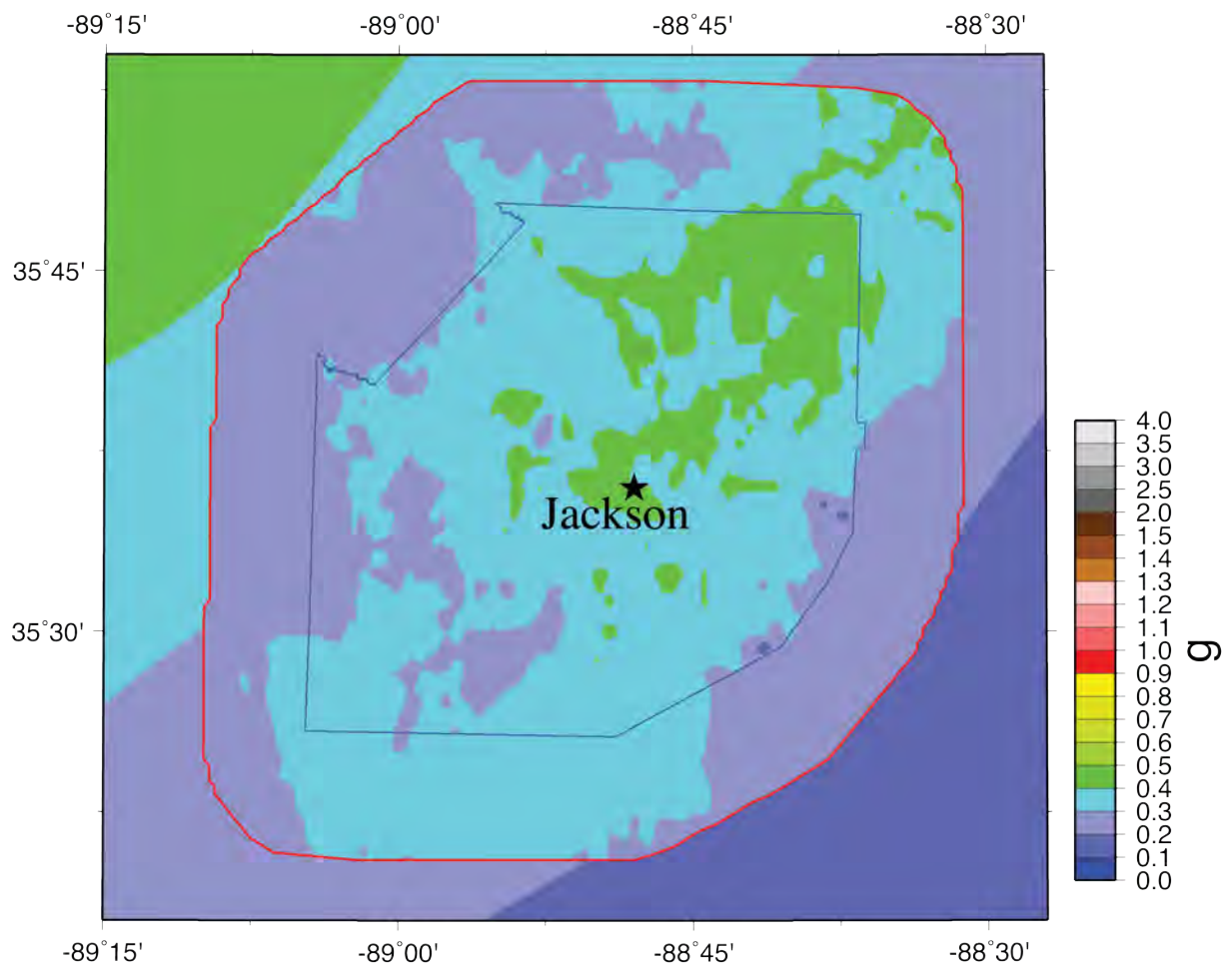


Figure 39: Potential scenario ruptures for Madison County. 1811–1812 **M7** ruptures indicated by **M7.5**, **M7.3**, and **M7.7**. 1811 **M6.9**s indicate two alternative “Dawn” aftershock ruptures. 1843 **M6.2** indicate historic south end of seismic zone rupture. The **M5.8** is a hypothetical earthquake in Madison County near Jackson.

Seismic Hazard Maps

Figures 40 - 42 show the 5%-in-50-year probabilistic seismic hazard maps for Madison County for PGA, 0.2 s, and 1.0 s. The background maps are the equivalent 2014 USGS national seismic hazard maps for B/C boundary conditions ($V_{s30} = 760$ m/s). At short periods (PGA and 0.2 s) the Madison County range of values is 0.3 – 0.6 g (g is the acceleration of gravity at the earth's surface – 9.80665 m/s). At long periods (1.0 s) the range is 0.2 – 0.4 g. Short period seismic hazard is for 1-2 story buildings, while long period hazard is for ~10 story buildings.

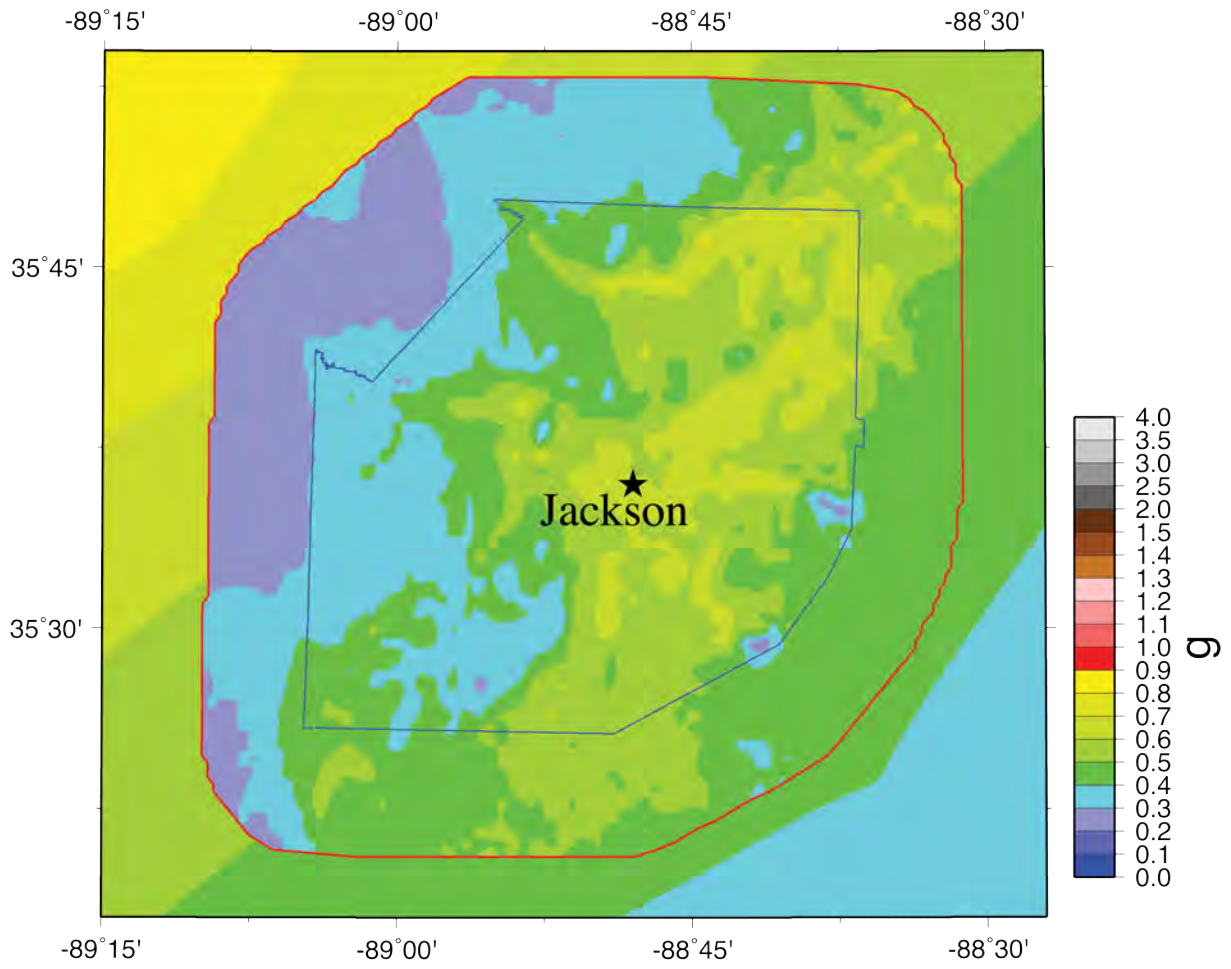
Madison Co PGA Hazard



5% in 50 year, September 2021

Figure 40: 5%-in-50-year PGA hazard map for Madison County with the effects of local geology inset on the U.S. Geological Survey's national seismic hazard map for BC boundary conditions.

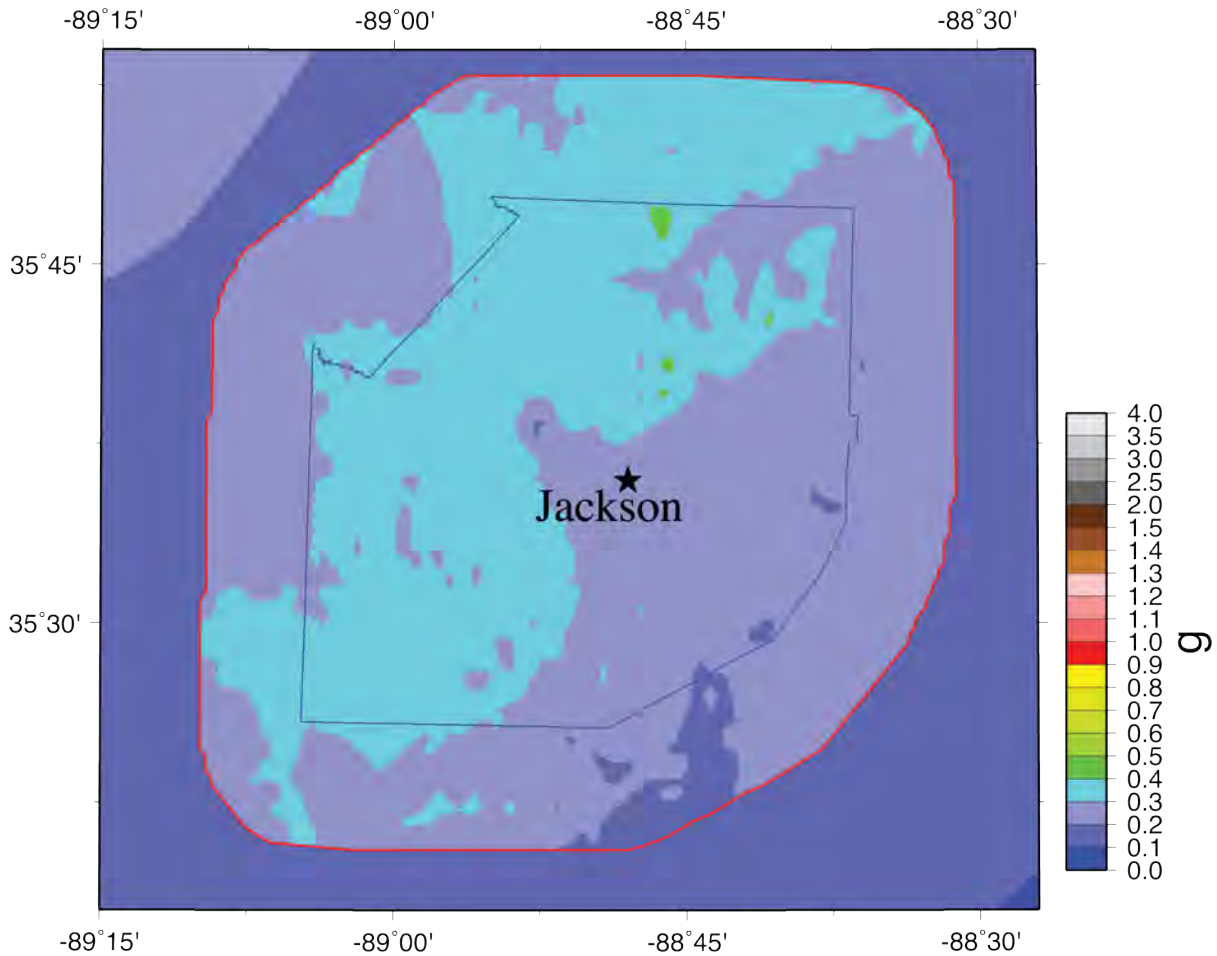
Madison Co 0.2s Hazard



5% in 50 year, September 2021

Figure 41: 5%-in-50-year 0.2 s hazard map for Madison County with the effects of local geology inset on the U.S. Geological Survey's national seismic hazard map for BC boundary conditions.

Madison Co 1.0s Hazard



5% in 50 year, September 2021

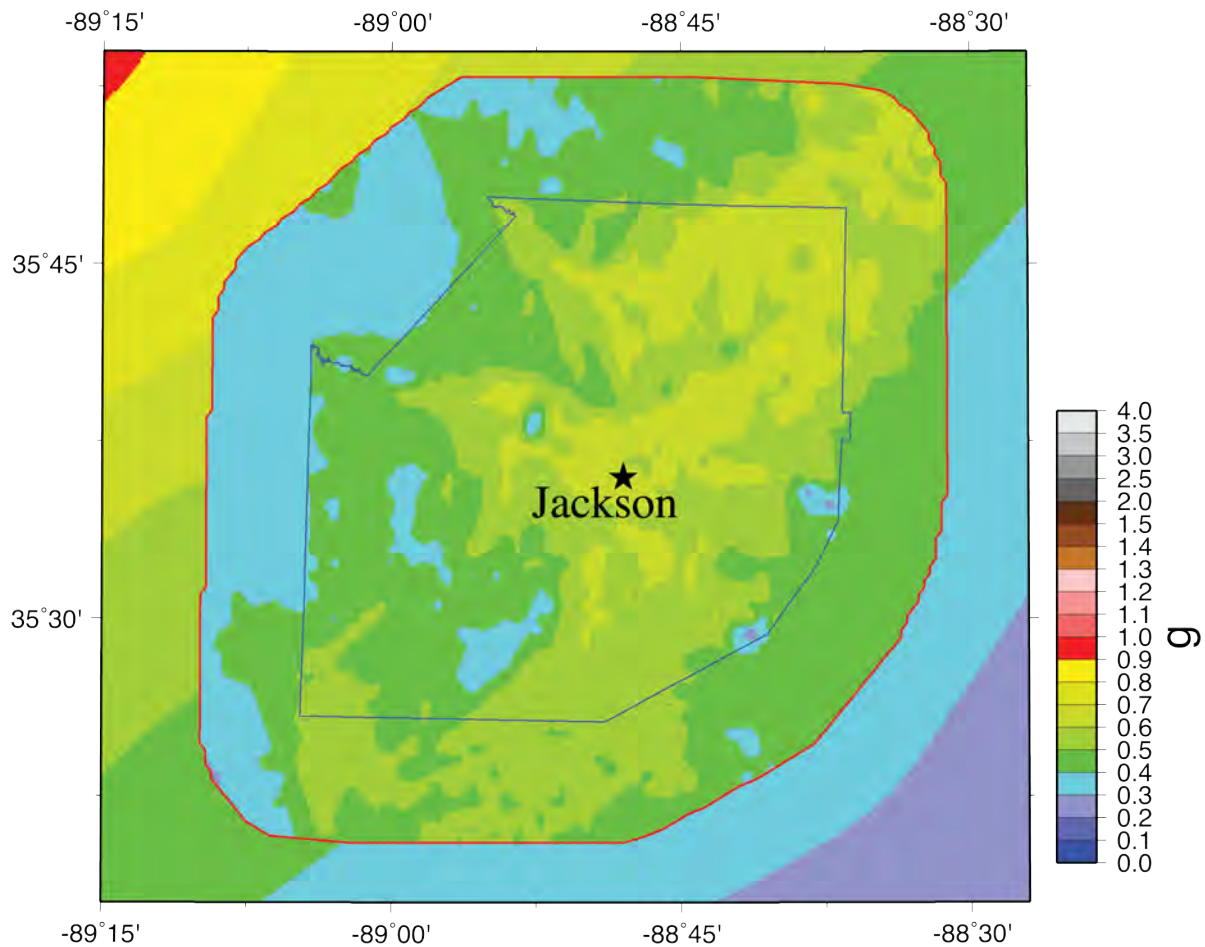
Figure 42: 5%-in-50-year 1.0 s hazard map for Madison County with the effects of local geology inset on the U.S. Geological Survey's national seismic hazard map for BC boundary conditions.

Figures 43 - 45 show the 2%-in-50-year probabilistic seismic hazard maps for Madison County. The hazard range is higher than the 5%-in-50-year maps: 0.3 – 0.7 g for PGA, 0.4 – 1.0 g for 0.2 s, and 0.3 – 0.6 g for 1.0 s.

The probabilistic seismic hazard maps with the effect of local geology show a short period reduction of 50% to an amplification of 100%, and at long periods there is an amplification of 0% to 100% relative to the 2014 USGS national seismic hazard maps at the same periods. The short period reduction is due to estimated ground motion nonlinear soil effects strongly reducing the high ground motions expected closer to the earthquake sources. Further from the sources (to the SE) the ground motions are less and the nonlinear effects are much reduced so there is amplification at short periods. Also the geology changes in the eastern portion of Madison County to stiffer, higher Vs soils, which also reduces the nonlinear soil effects at short

periods. The long period amplification is due to the reduced nonlinear effects and increase dominance of soil column resonant effects amplifying ground motions. As we progress further from the earthquake sources the ground motion level decreases, the nonlinear effects decrease, and the dominance of resonance effects increases. In Shelby County, about 50 km from the New Madrid earthquake sources, Cramer et al. (2018a) show Shelby County seismic hazard maps with 40 – 60% decreases at short period and 50 – 100 % increases at long period over the USGS national seismic hazard maps.

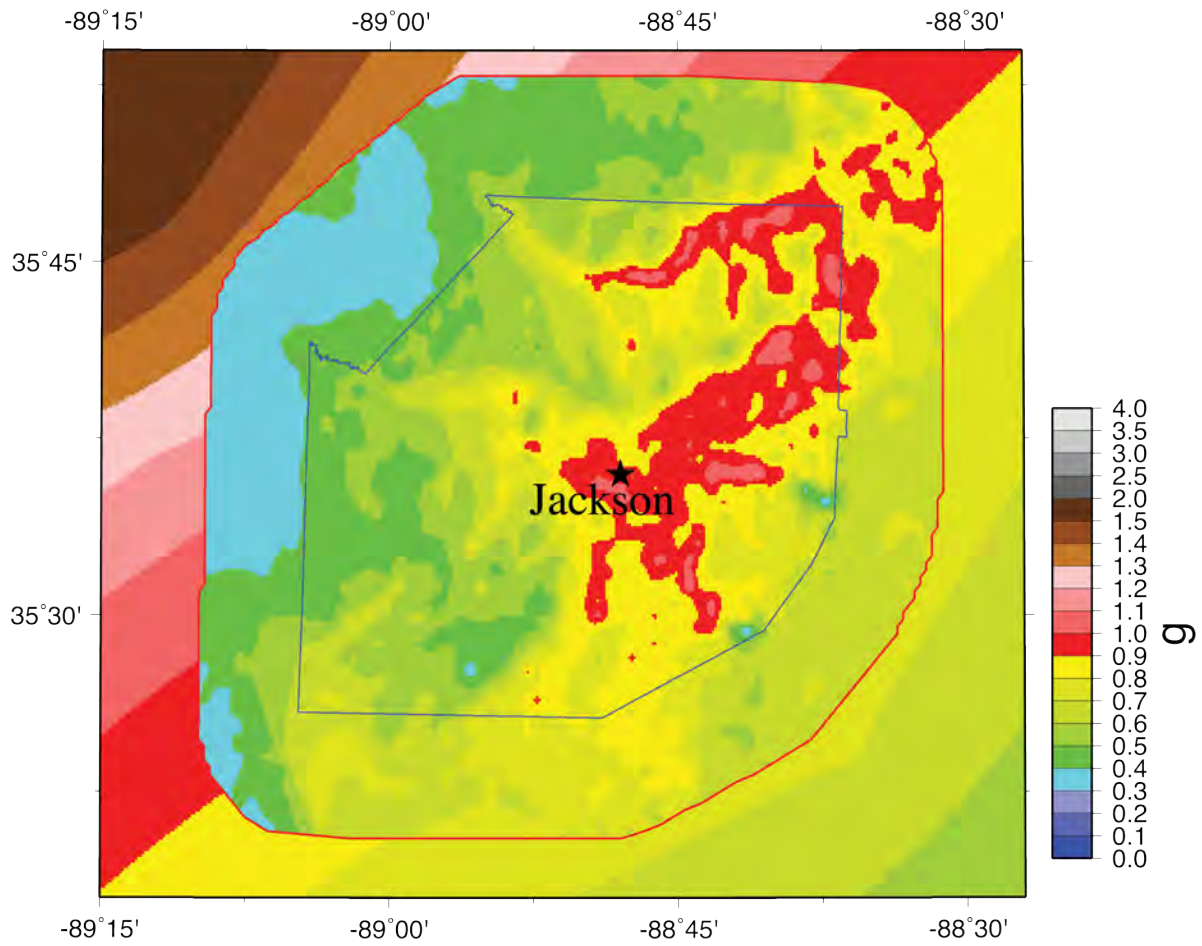
Madison Co PGA Hazard



2% in 50 year, September 2021

Figure 43: 2%-in-50-year PGA hazard map for Madison County with the effects of local geology inset on the U.S. Geological Survey's national seismic hazard map for BC boundary conditions.

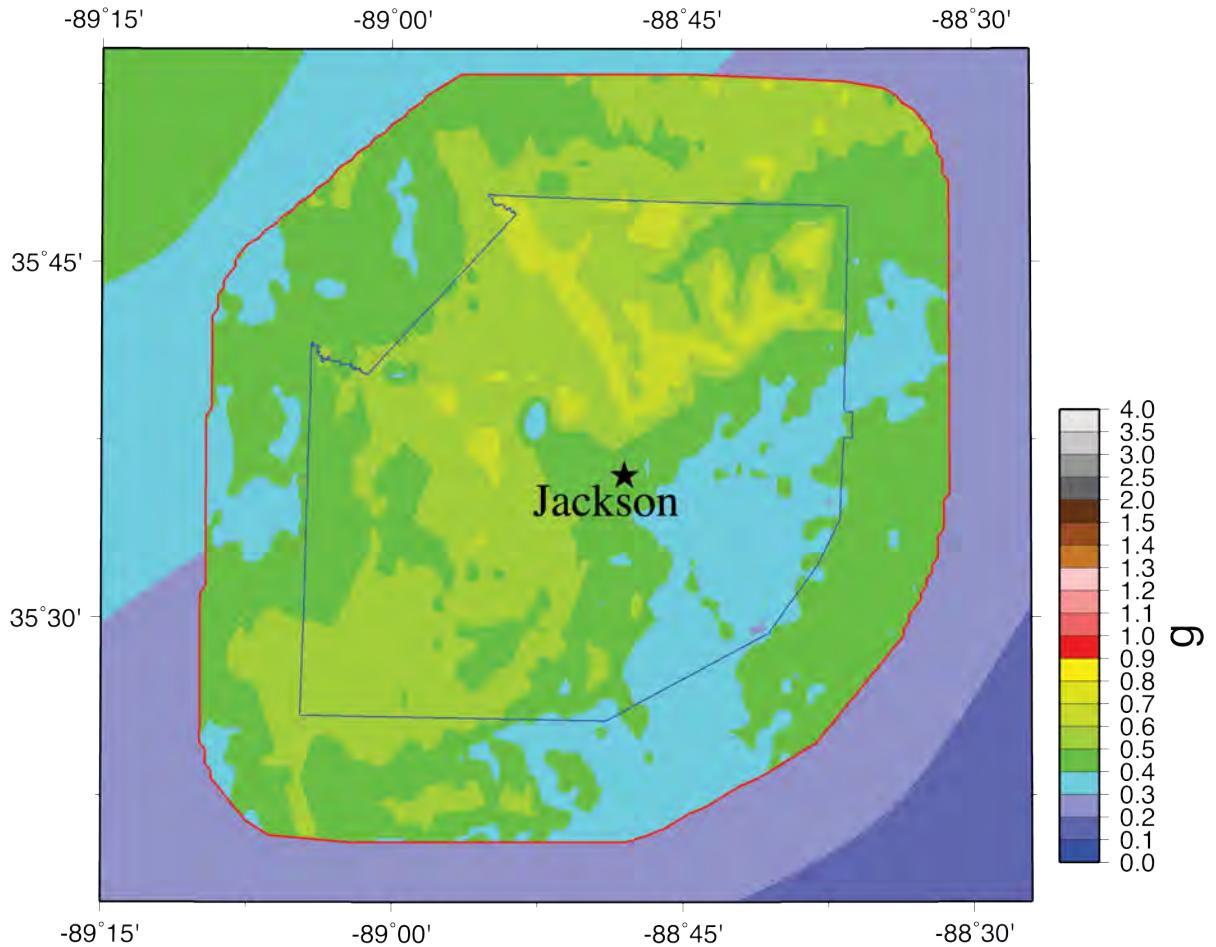
Madison Co 0.2s Hazard



2% in 50 year, September 2021

Figure 44: 2%-in-50-year 0.2 s hazard map for Madison County with the effects of local geology inset on the U.S. Geological Survey's national seismic hazard map for BC boundary conditions.

Madison Co 1.0s Hazard

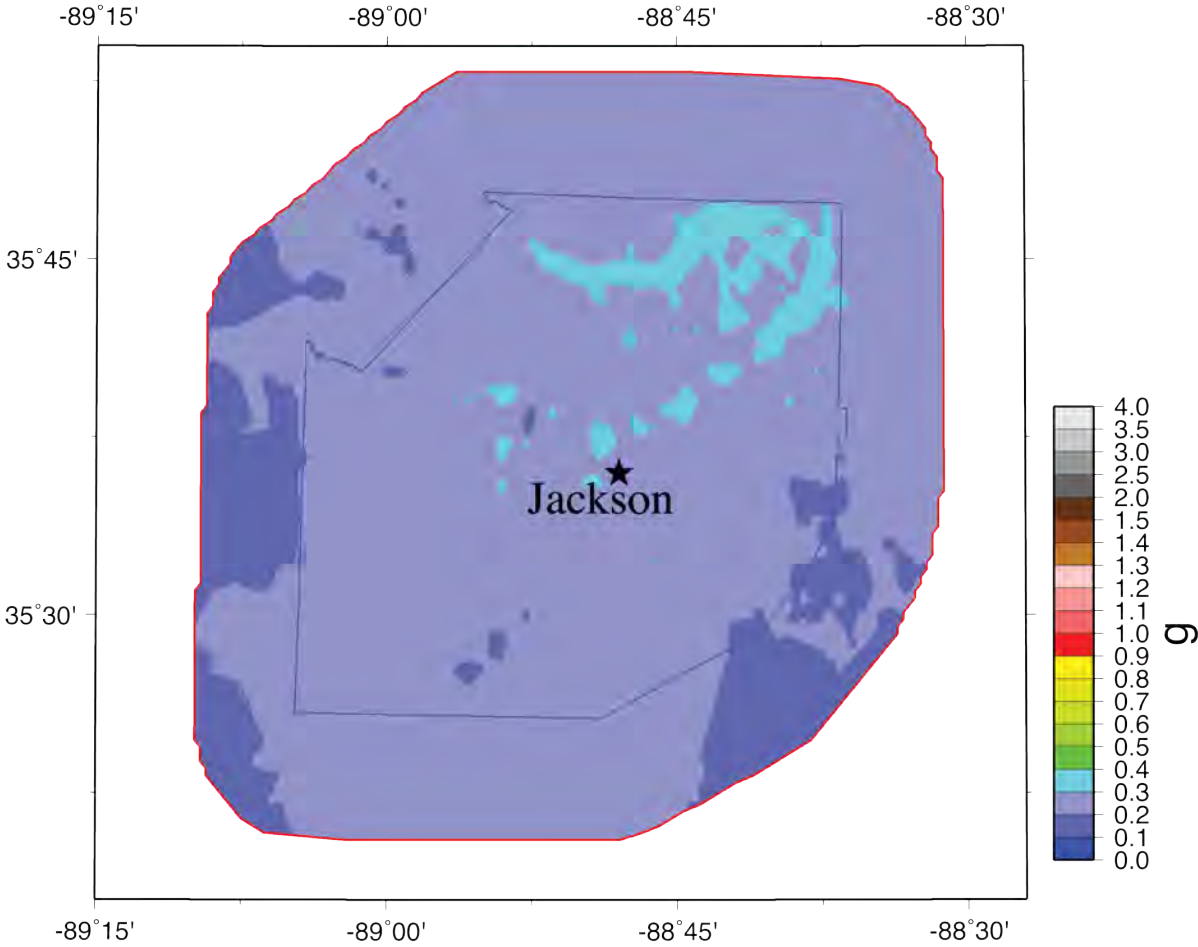


2% in 50 year, September 2021

Figure 45: 2%-in-50-year 1.0 s hazard map for Madison County with the effects of local geology inset on the U.S. Geological Survey's national seismic hazard map for BC boundary conditions.

Figures 46 - 52 present the PGA, 0.2 s, and 1.0 s seismic hazard maps for the seven scenarios of Table 7. There are no equivalent comparisons to the USGS probabilistic maps for these scenarios. At all periods shown, the M7 New Madrid scenario hazard maps range from 0.15 to 0.5 g for a repeat of the M7.7 February 1812 earthquake, from 0.15 to 0.4 g for the repeat of the M7.5 December 1811 earthquake, and 0.1 to 0.3 g for the repeat of the M7.3 January 1812 earthquake. The M6.9 largest aftershock hazard map alternatives range from 0.1 to 0.2 g if on the northern end of the SW arm and 0.1 to 0.3 g if on the east end of the Reelfoot thrust. The M6.2 1843 scenario ground motions are ~0.1 g, and the M5.8 hypothetical Madison County earthquake ground motions ranges from 0.1 – 1.3 g.

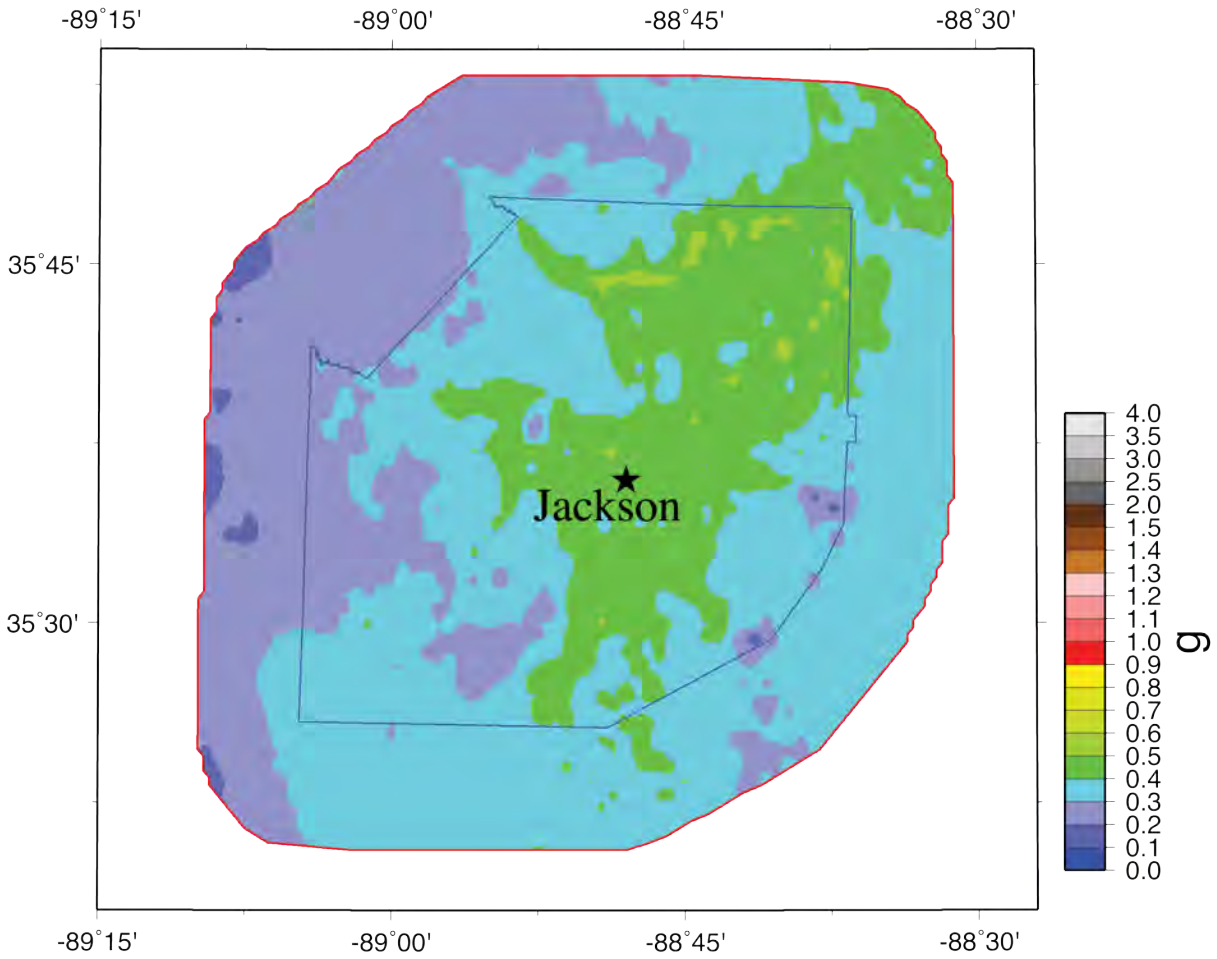
Madison Co PGA Hazard



NMRT M7.7, October 2021

Figure 46A: Scenario PGA hazard map for a M7.7 earthquake on the Reelfoot Thrust (central segment of NMSZ) for Madison County with the effects of local geology.

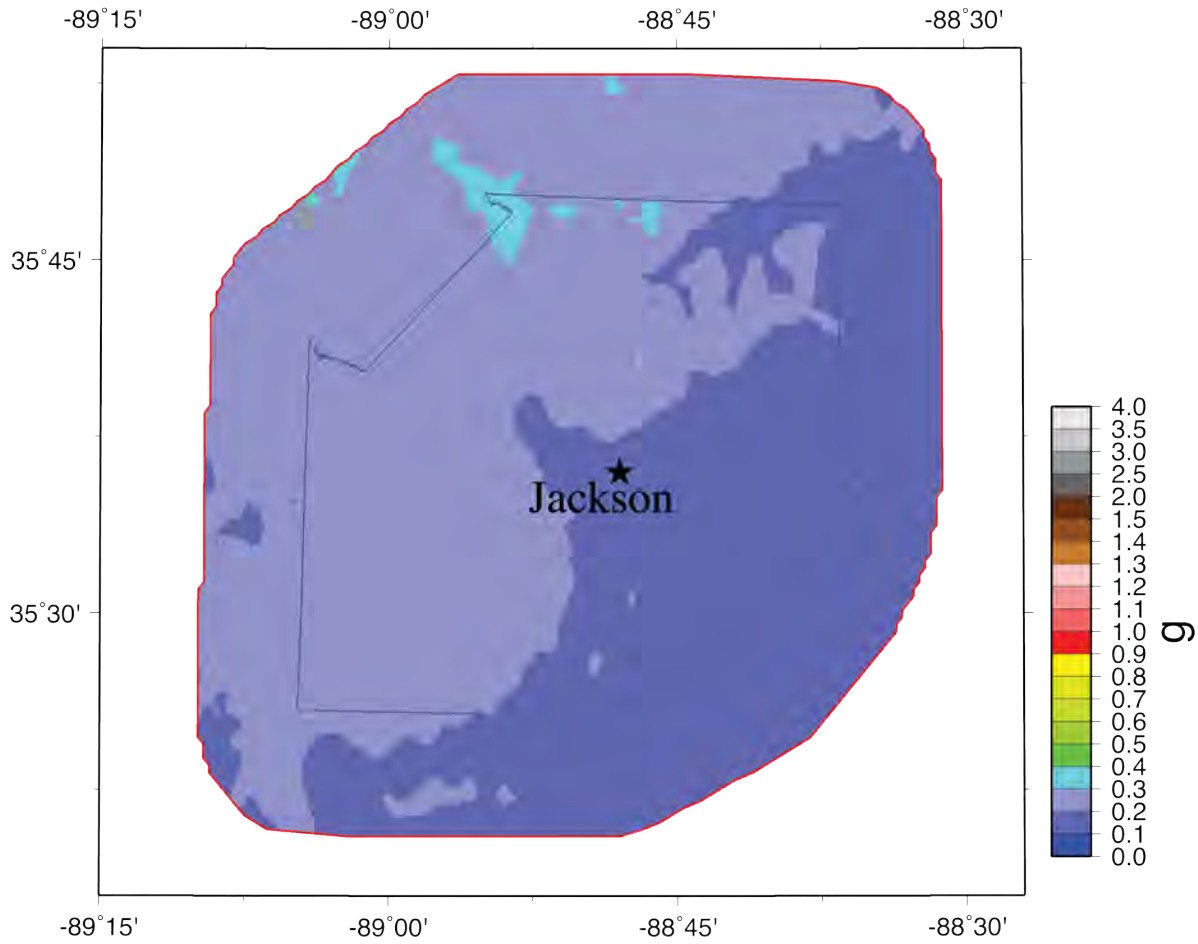
Madison Co 0.2s Hazard



NMRT M7.7, October 2021

Figure 46B: Scenario 0.2 s hazard map for a M7.7 earthquake on the Reelfoot Thrust (central segment of NMSZ) for Madison County with the effects of local geology.

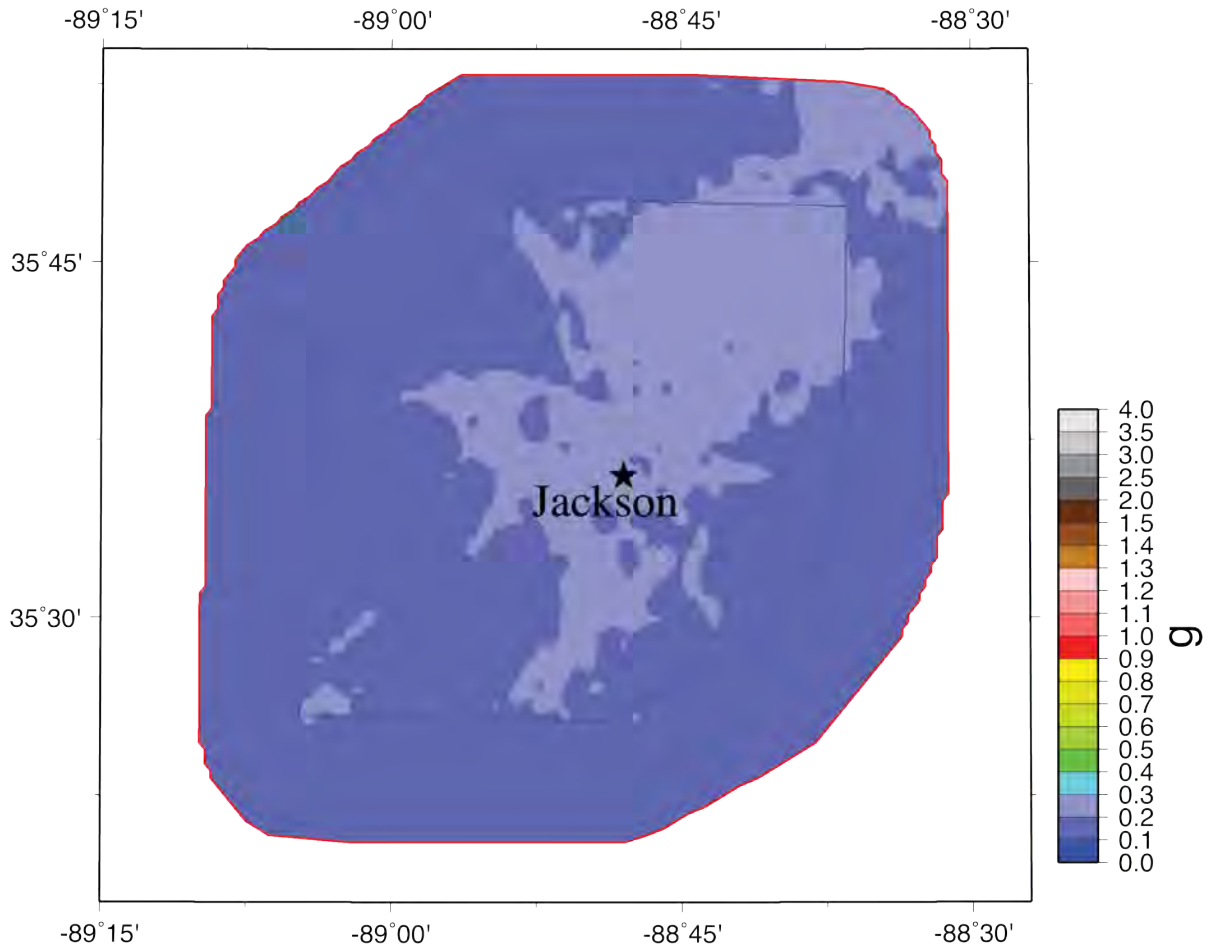
Madison Co 1.0s Hazard



NMRT M7.7, October 2021

Figure 46C: Scenario 1.0 s hazard map for a M7.7 earthquake on the Reelfoot Thrust (central segment of NMSZ) for Madison County with the effects of local geology.

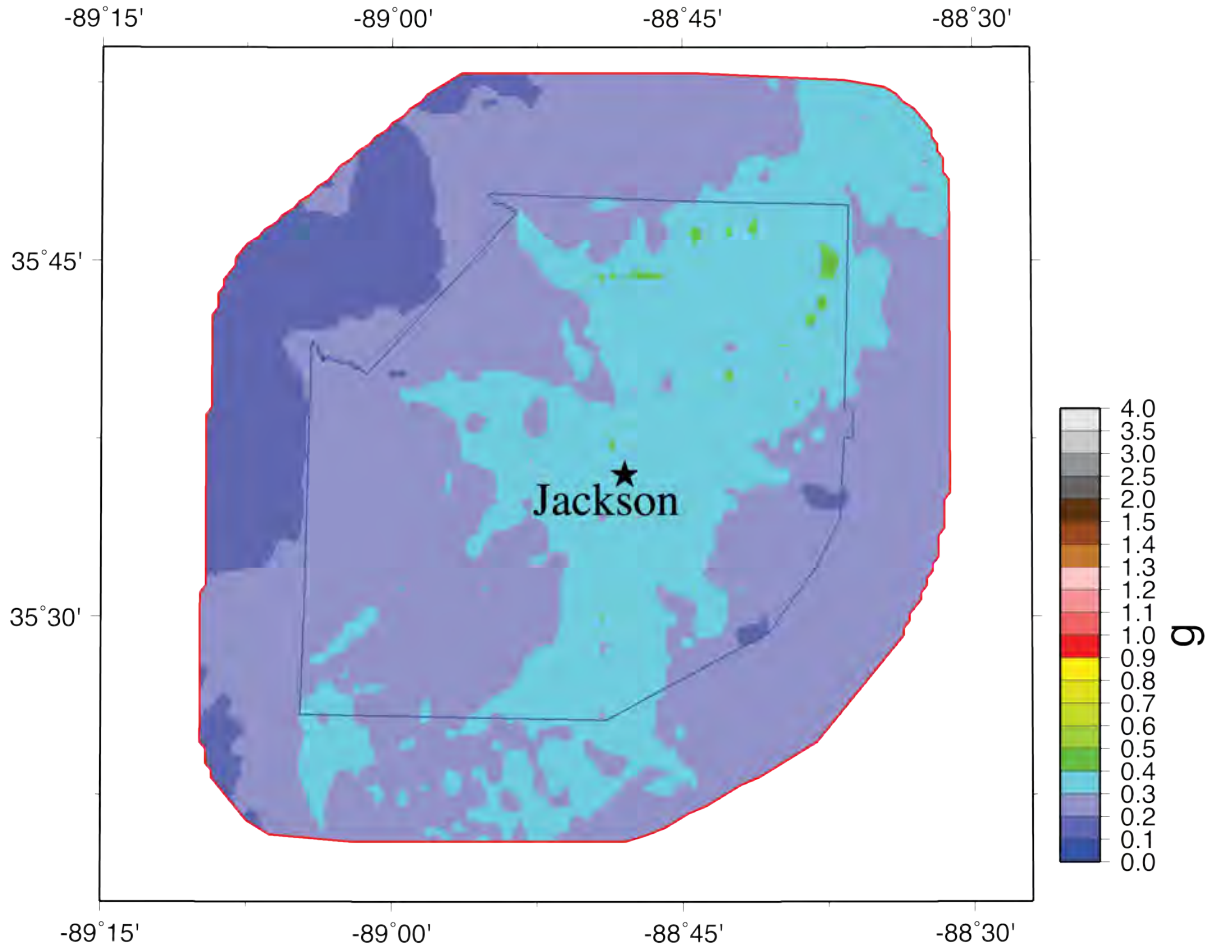
Madison Co PGA Hazard



NMSW M7.5, October 2021

Figure 47A: Scenario PGA hazard map for a M7.5 earthquake on the Cottonwood Grove Fault (SW segment of NMSZ) for Madison County with the effects of local geology.

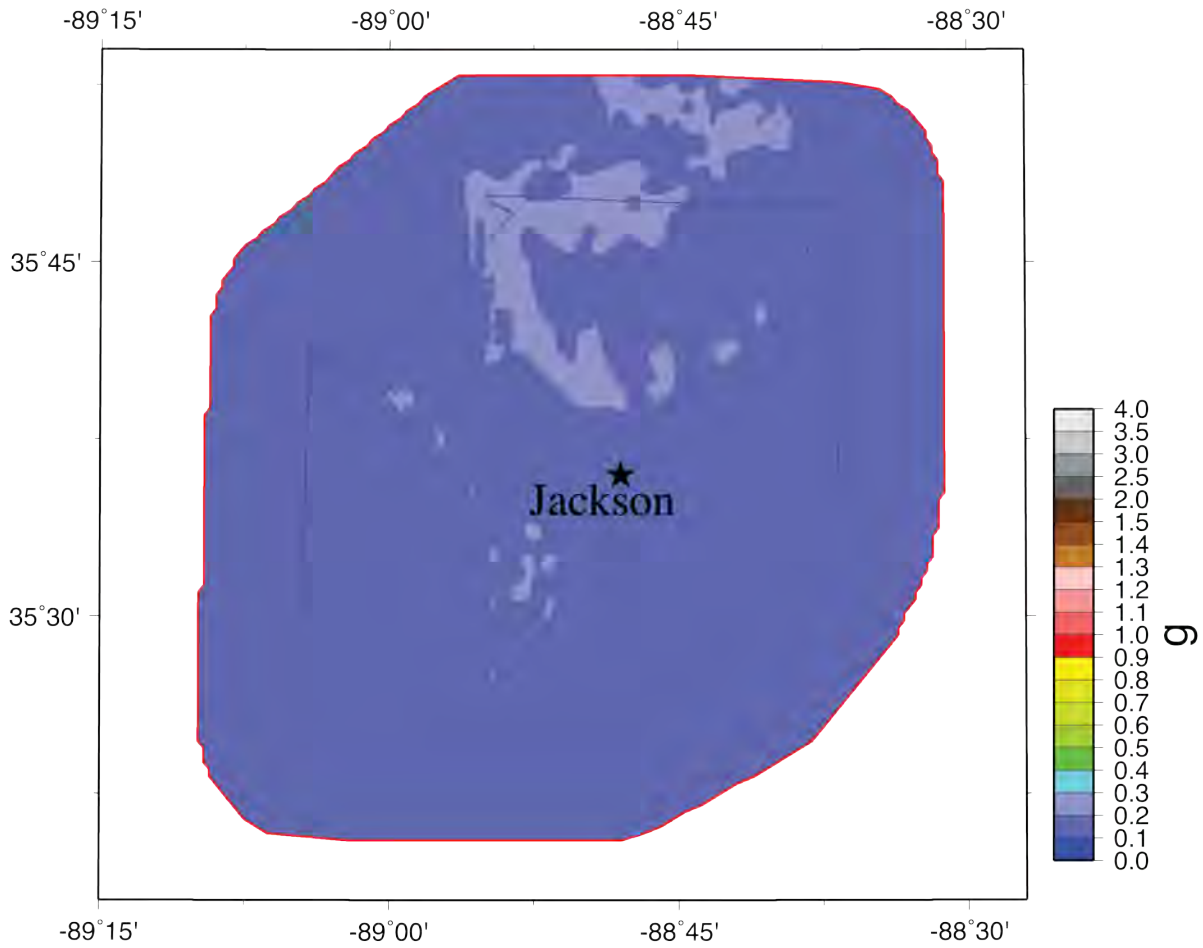
Madison Co 0.2s Hazard



NMSW M7.5, October 2021

Figure 47B: Scenario 0.2 s hazard map for a M7.5 earthquake on the Cottonwood Grove Fault (SW segment of NMSZ) for Madison County with the effects of local geology.

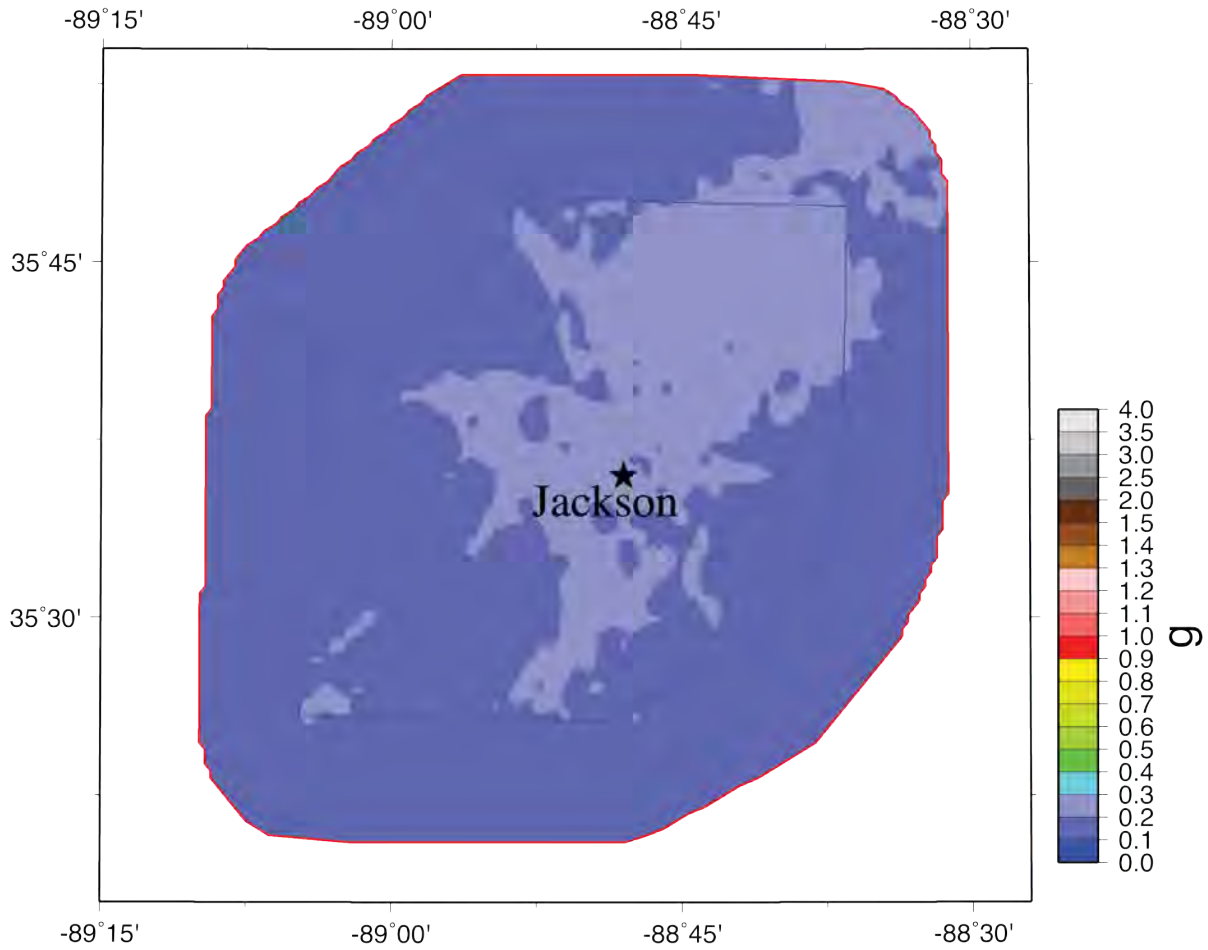
Madison Co 1.0s Hazard



NMSW M7.5, October 2021

Figure 47C: Scenario 1.0 s hazard map for a M7.5 earthquake on the Cottonwood Grove Fault (SW segment of NMSZ) for Madison County with the effects of local geology.

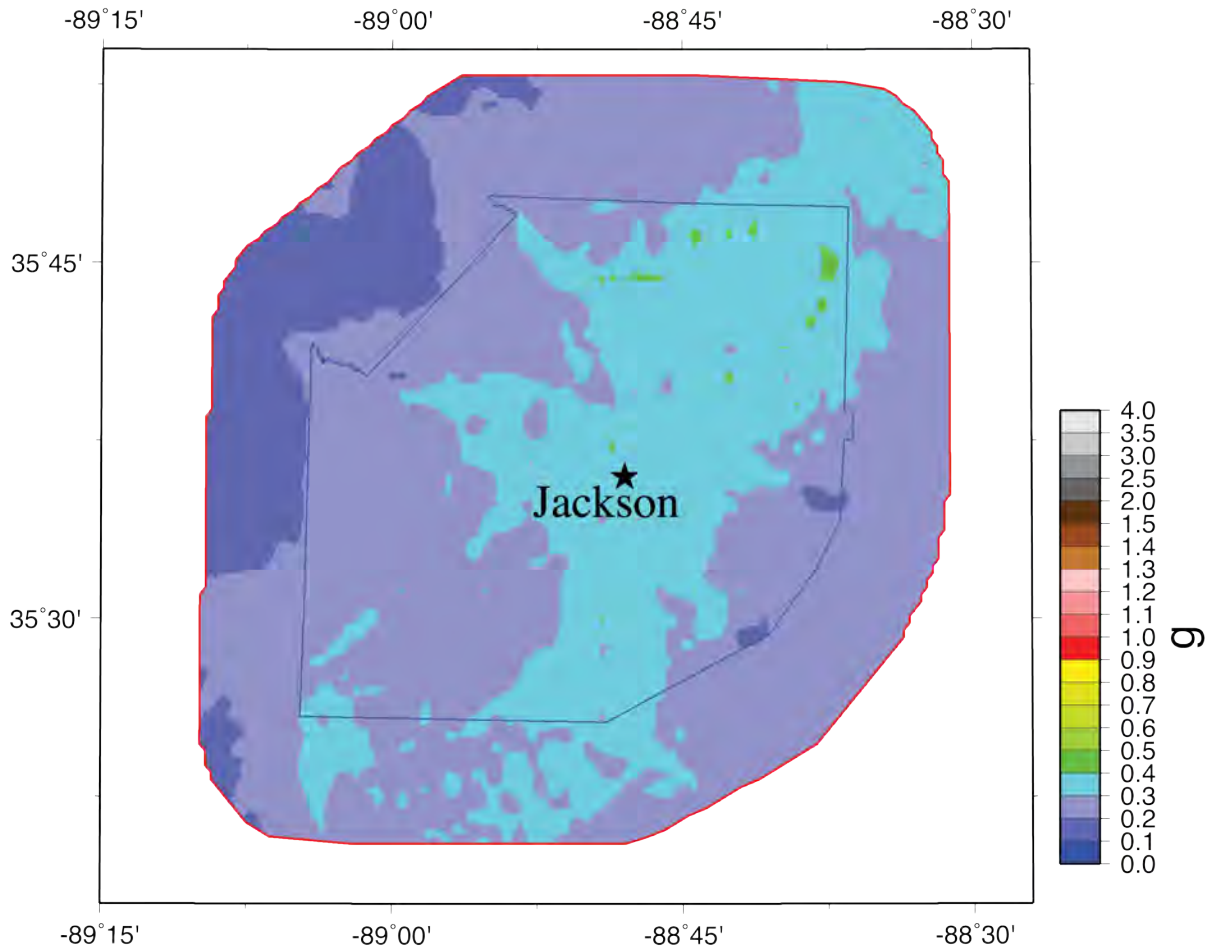
Madison Co PGA Hazard



NMSW M7.5, October 2021

Figure 48A: Scenario PGA hazard map for a M7.3 earthquake on the New Madrid North Fault (NE segment of NMSZ) for Madison County with the effects of local geology.

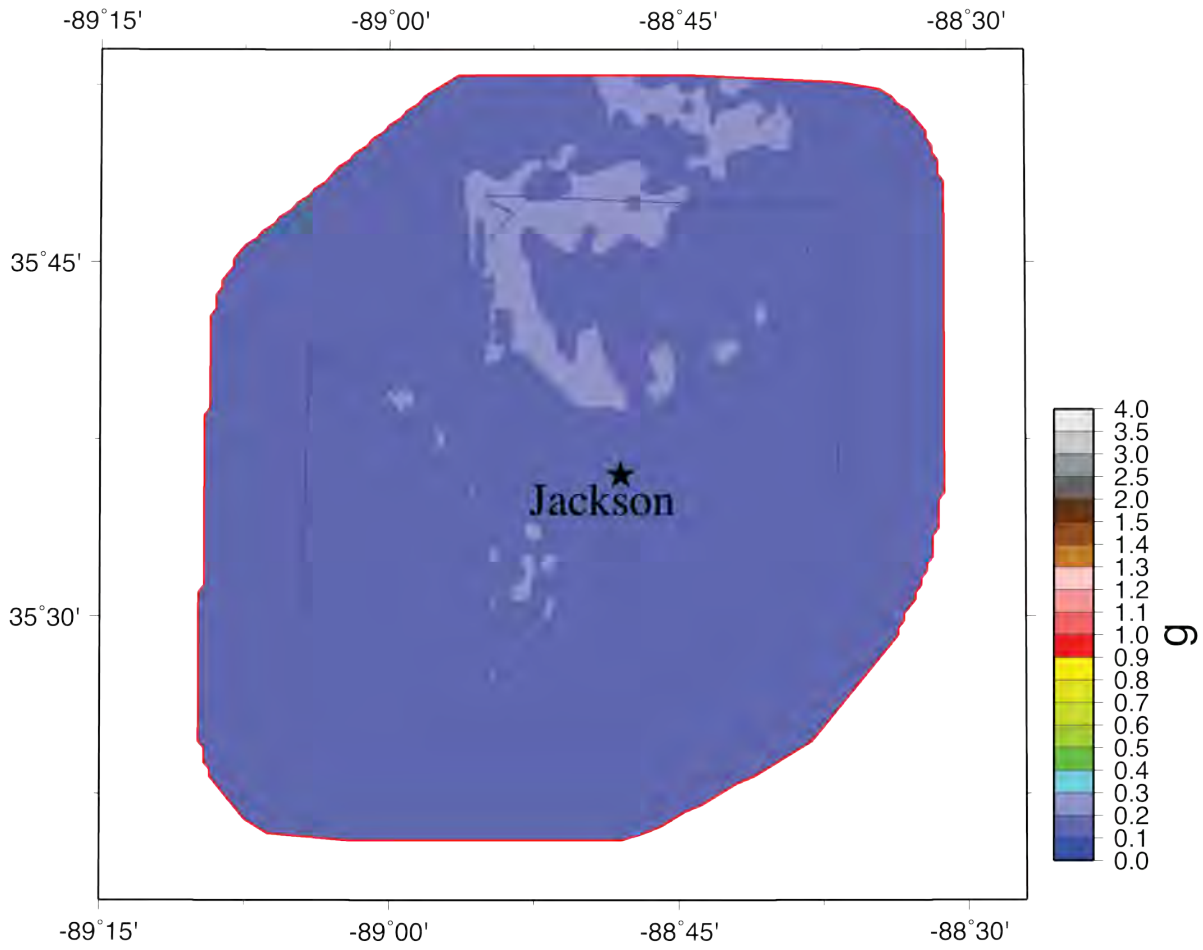
Madison Co 0.2s Hazard



NMSW M7.5, October 2021

Figure 48B: Scenario 0.2 s hazard map for a M7.3 earthquake on the New Madrid North Fault (NE segment of NMSZ) for Madison County with the effects of local geology.

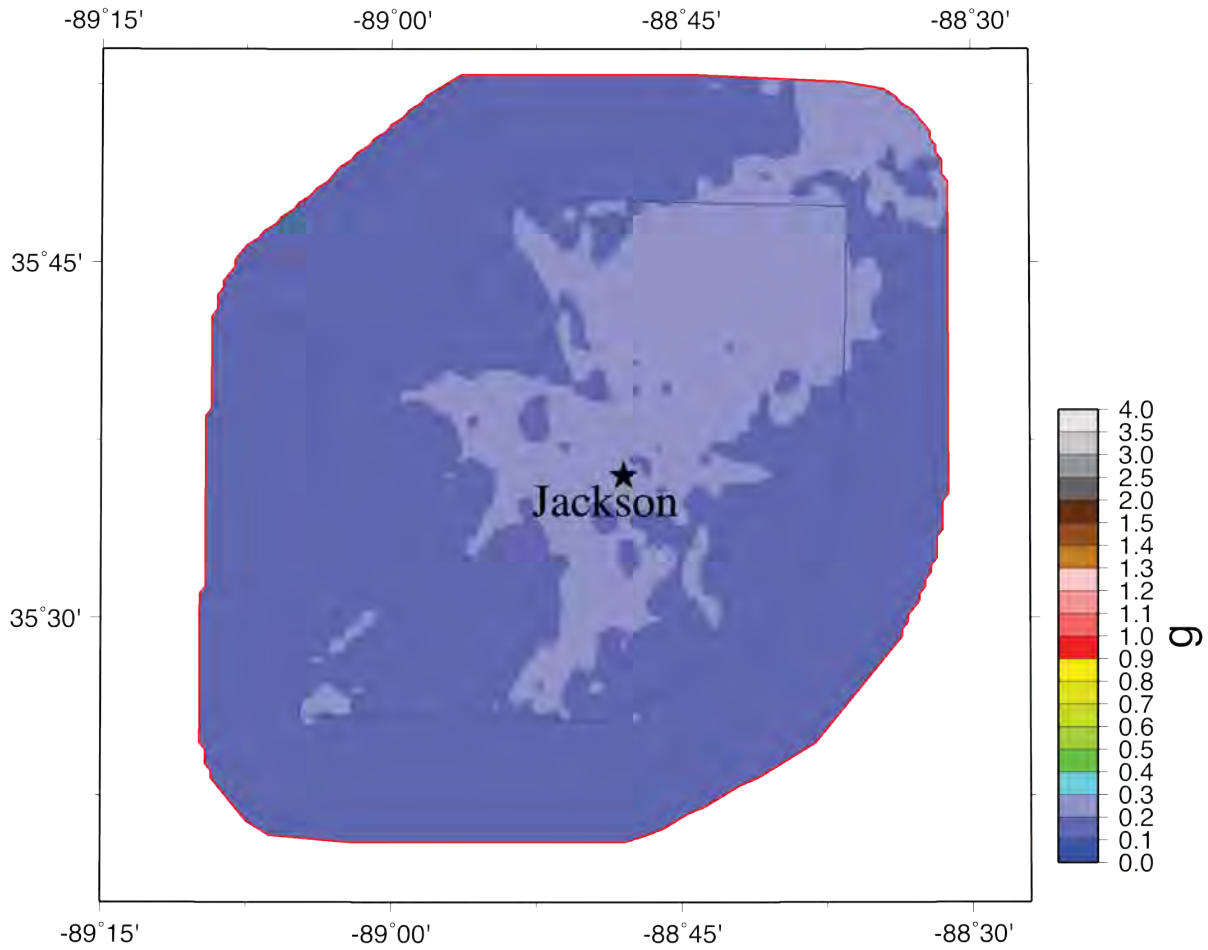
Madison Co 1.0s Hazard



NMSW M7.5, October 2021

Figure 48C: Scenario 1.0 s hazard map for a M7.3 earthquake on the New Madrid North Fault (NE segment of NMSZ) for Madison County with the effects of local geology.

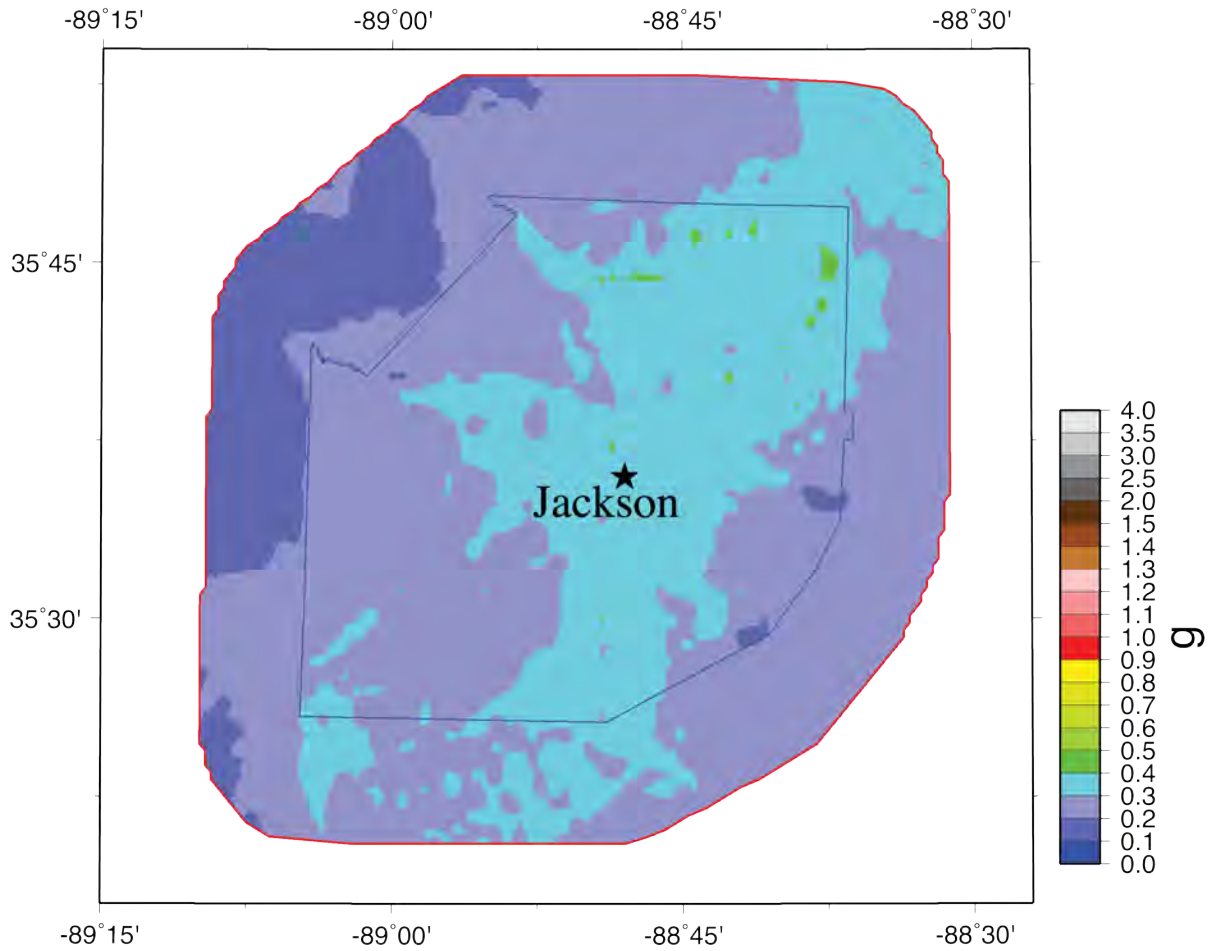
Madison Co PGA Hazard



NMSW M7.5, October 2021

Figure 49A: Scenario PGA hazard map for a M6.9 “Dawn” aftershock (alt. 1) on the Cottonwood Grove Fault (SW segment of NMSZ) for Madison County with the effects of local geology.

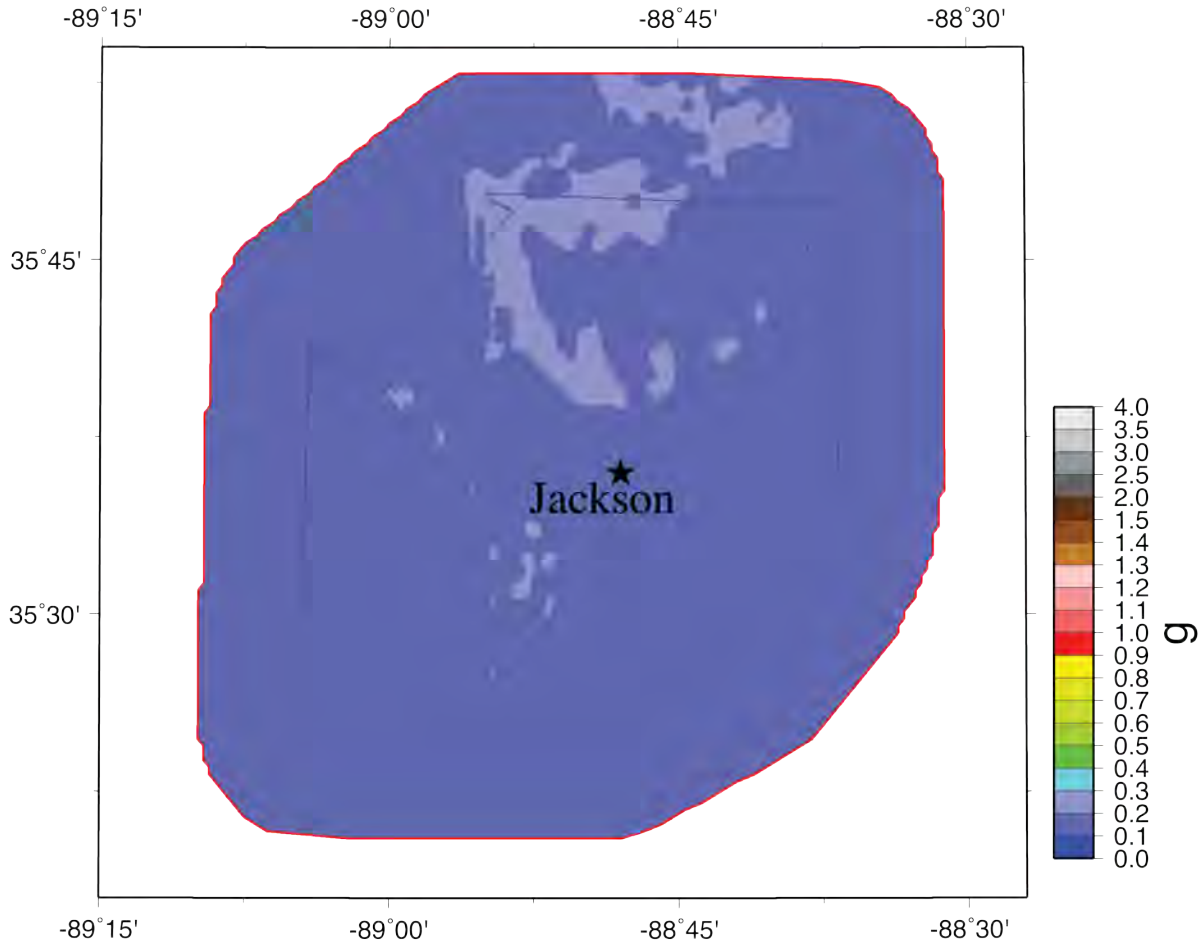
Madison Co 0.2s Hazard



NMSW M7.5, October 2021

Figure 49B: Scenario 0.2 s hazard map for a M6.9 “Dawn” aftershock (alt. 1) on the Cottonwood Grove Fault (SW segment of NMSZ) for Madison County with the effects of local geology.

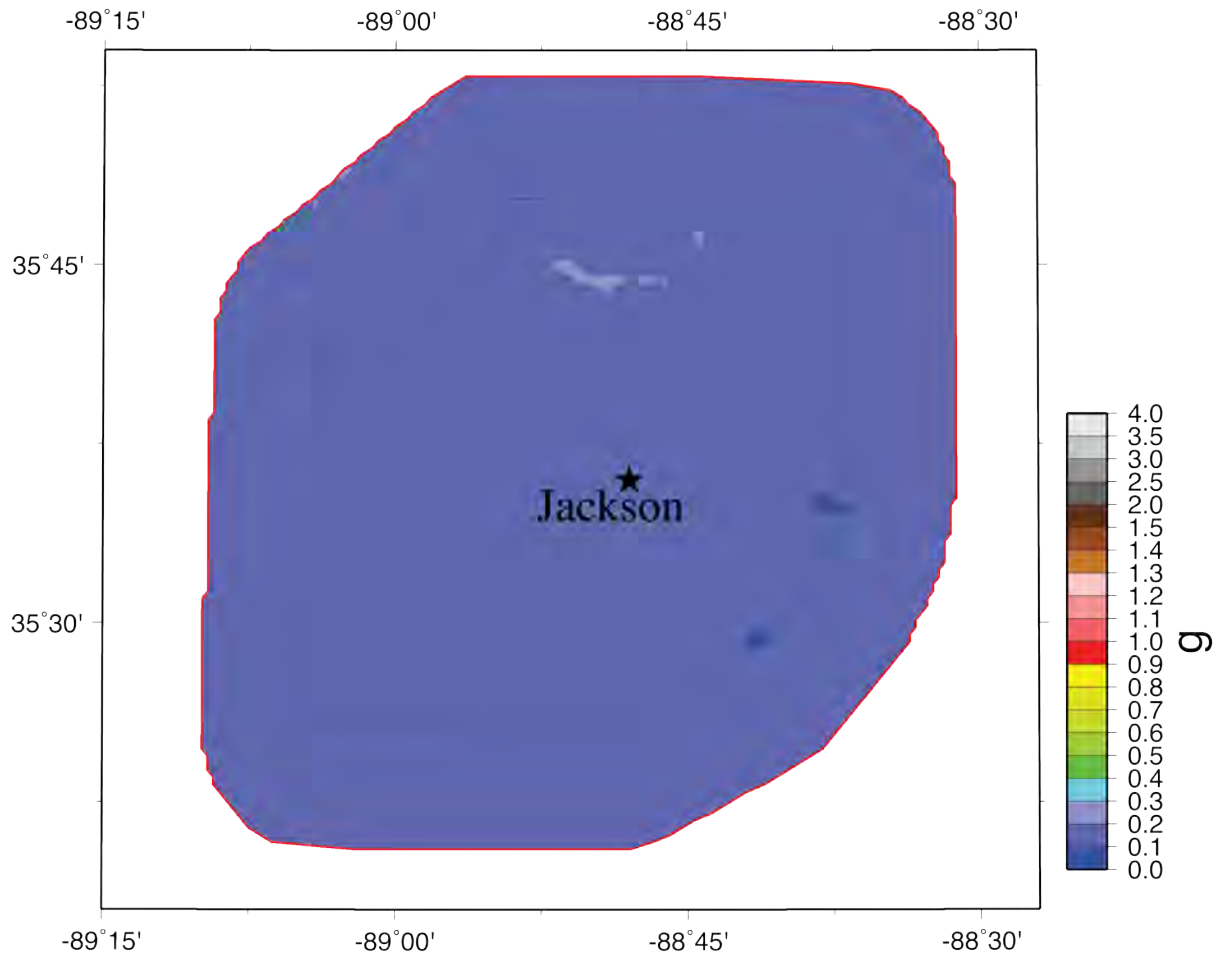
Madison Co 1.0s Hazard



NMSW M7.5, October 2021

Figure 49C: Scenario 1.0 s hazard map for a M6.9 “Dawn” aftershock (alt. 1) on the Cottonwood Grove Fault (SW segment of NMSZ) for Madison County with the effects of local geology.

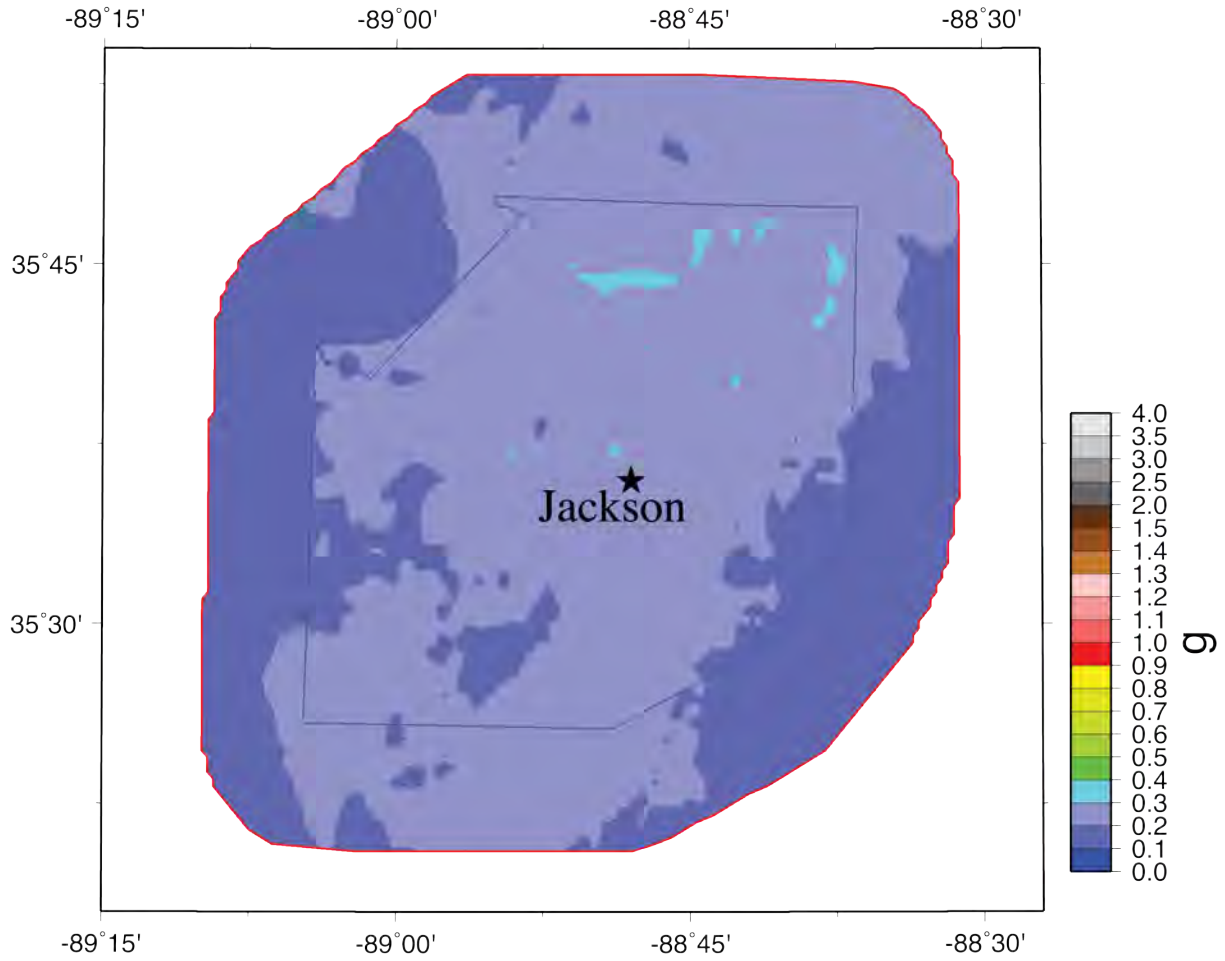
Madison Co PGA Hazard



NMRTA M6.9, October 2021

Figure 50A: Scenario PGA hazard map for a M6.9 “Dawn” aftershock (alt. 2) on the Reelfoot Thrust (central segment of NMSZ) for Madison County with the effects of local geology.

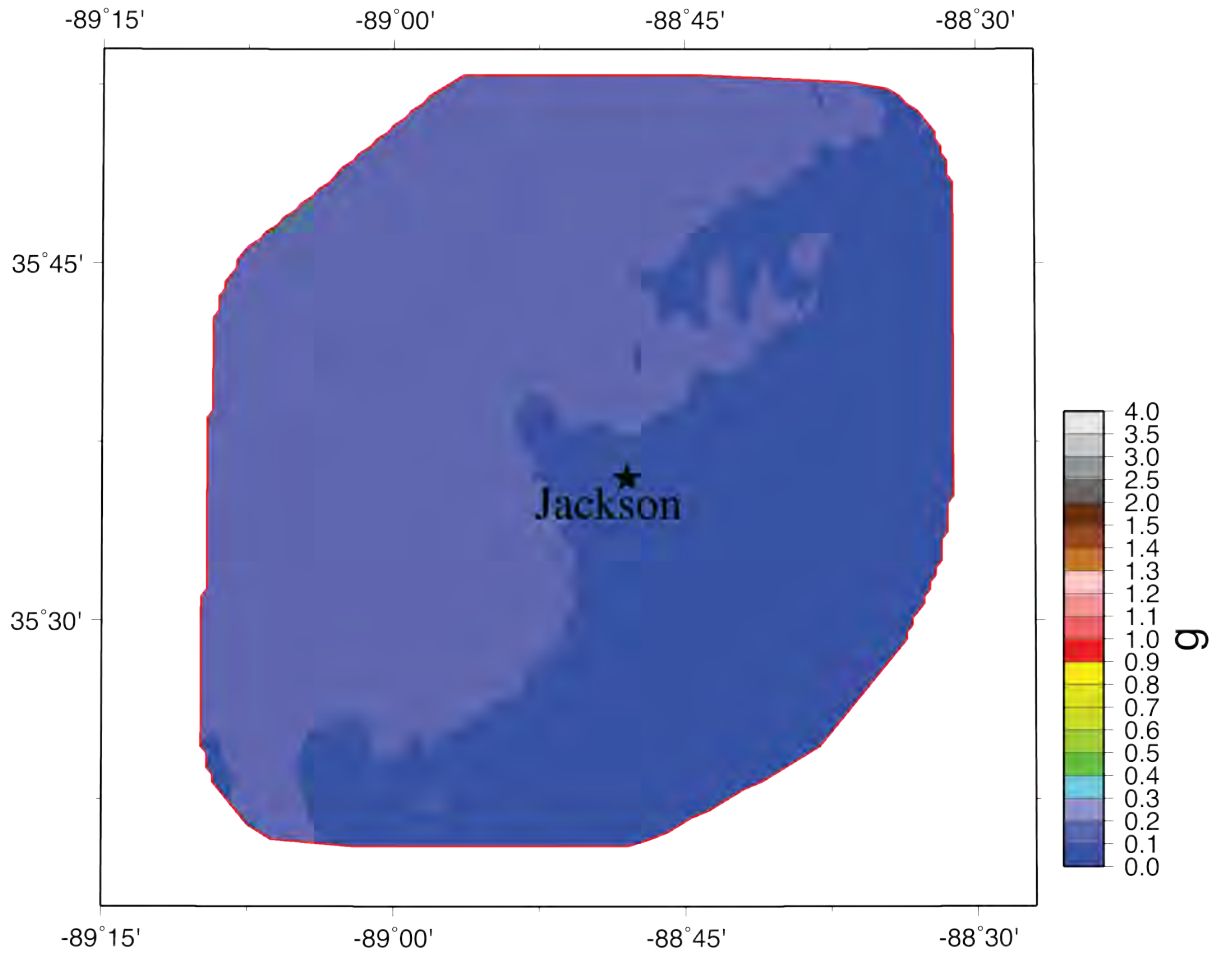
Madison Co 0.2s Hazard



NMRTA M6.9, October 2021

Figure 50B: Scenario 0.2 s hazard map for a M6.9 “Dawn” aftershock (alt. 2) on the Reelfoot Thrust (central segment of NMSZ) for Madison County with the effects of local geology.

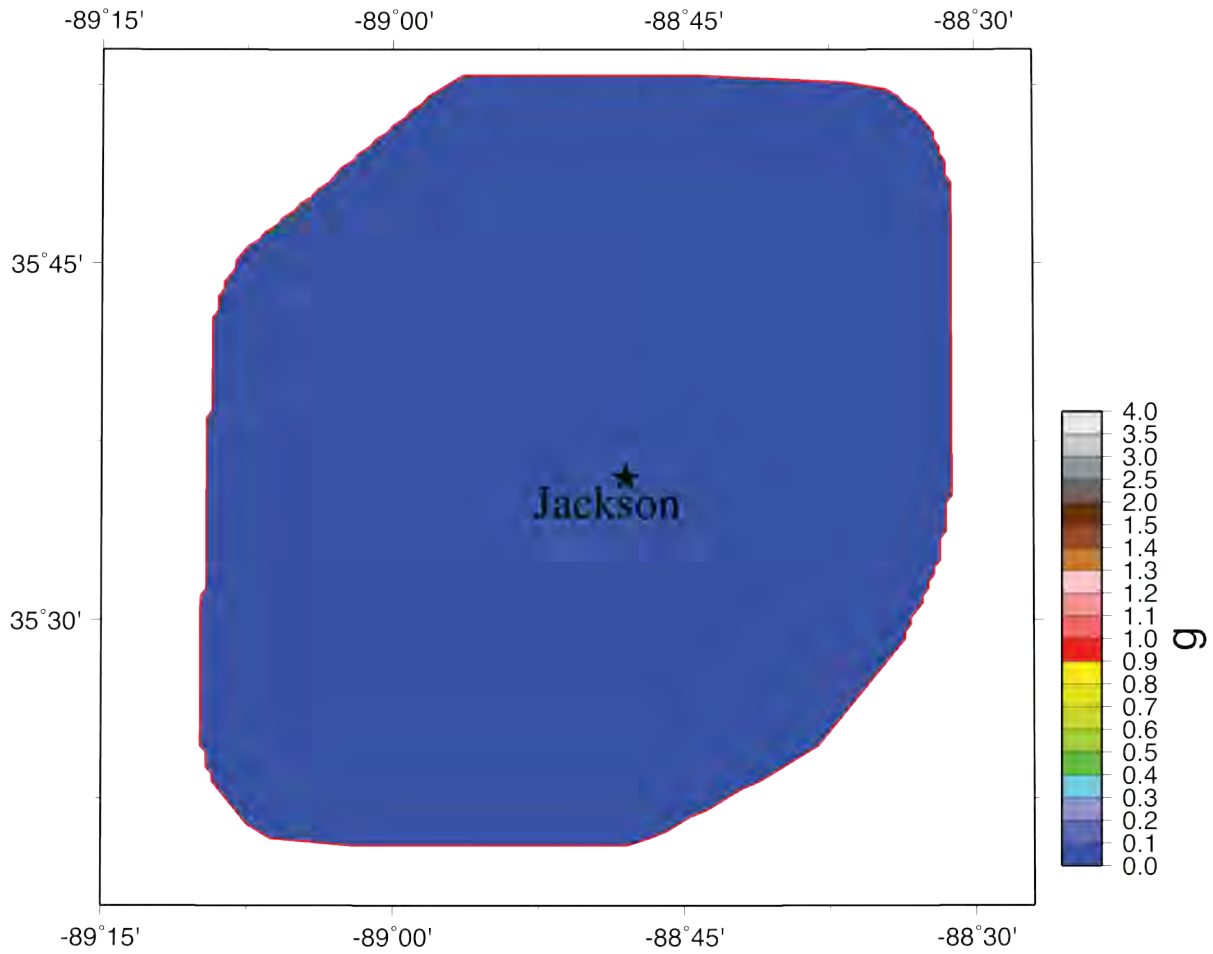
Madison Co 1.0s Hazard



NMRTA M6.9, October 2021

Figure 50C: Scenario 1.0 s hazard map for a M6.9 “Dawn” aftershock (alt. 2) on the Reelfoot Thrust (central segment of NMSZ) for Madison County with the effects of local geology.

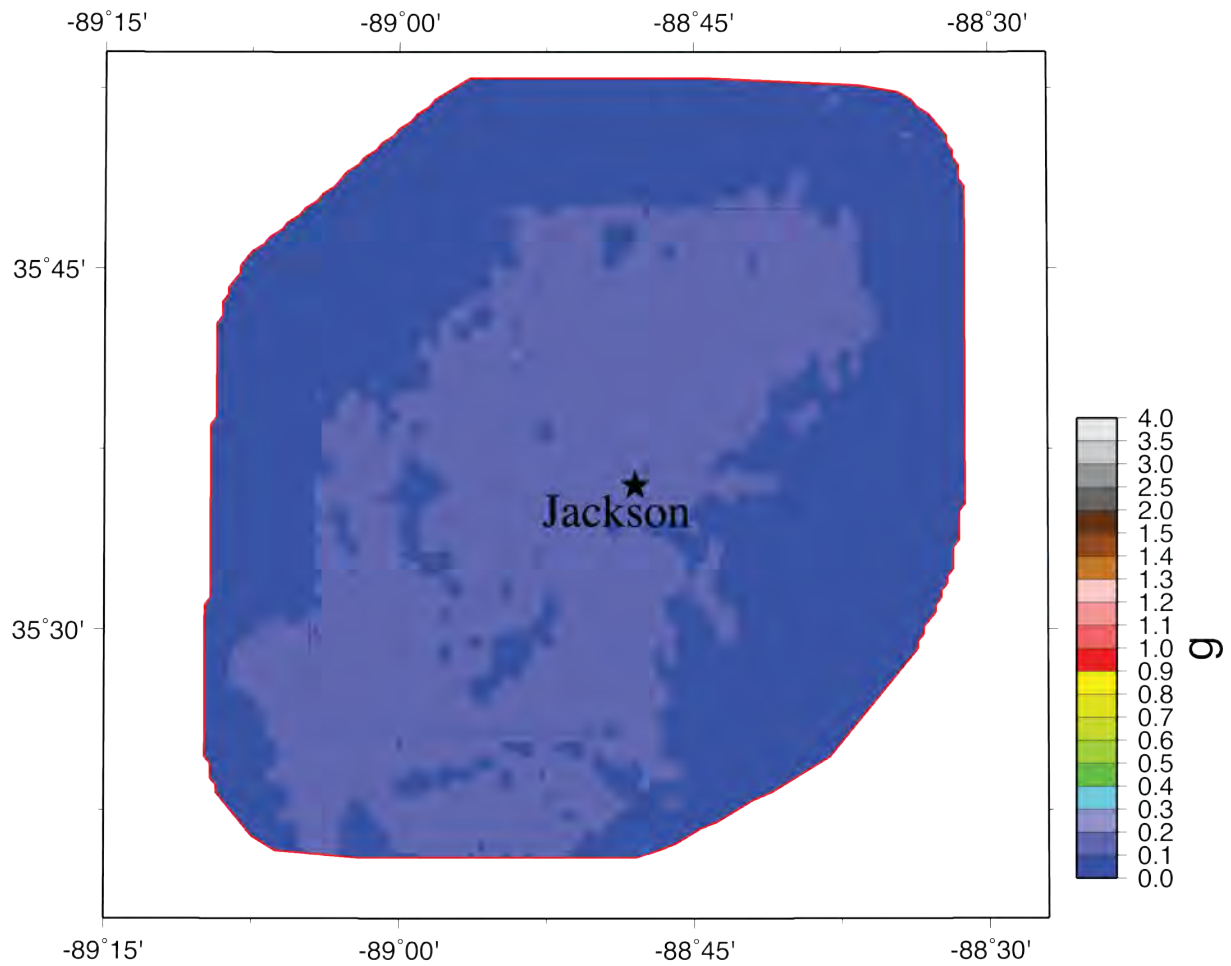
Madison Co PGA Hazard



NMMT M6.2, October 2021

Figure 51A: Scenario PGA hazard map for a M6.2 on the Cottonwood Grove Fault (1843 Marked Tree – SW segment of NMSZ) for Madison County with the effects of local geology.

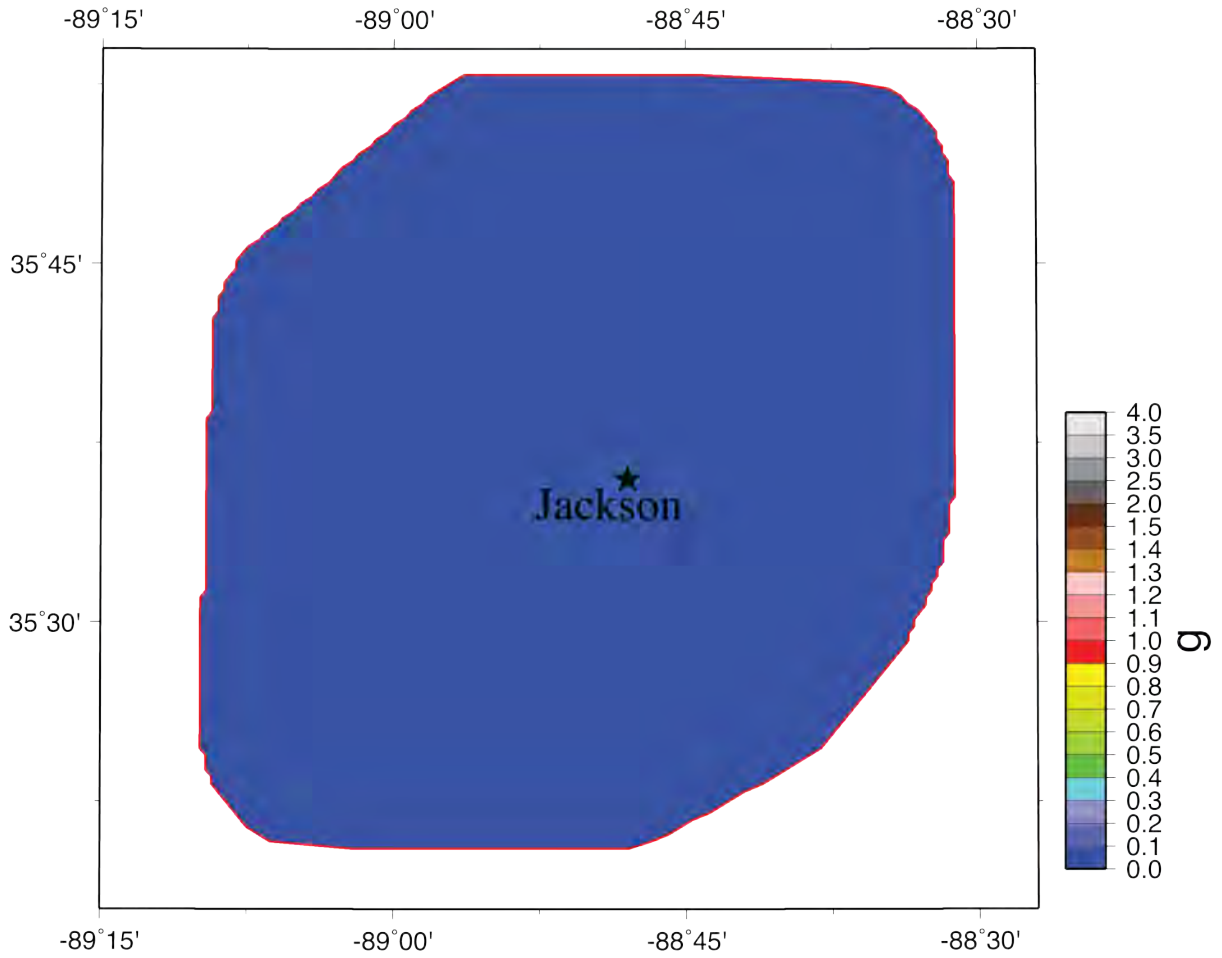
Madison Co 0.2s Hazard



NMMT M6.2, October 2021

Figure 51B: Scenario 0.2 s hazard map for a M6.2 on the Cottonwood Grove Fault (1843 Marked Tree – SW segment of NMSZ) for Madison County with the effects of local geology.

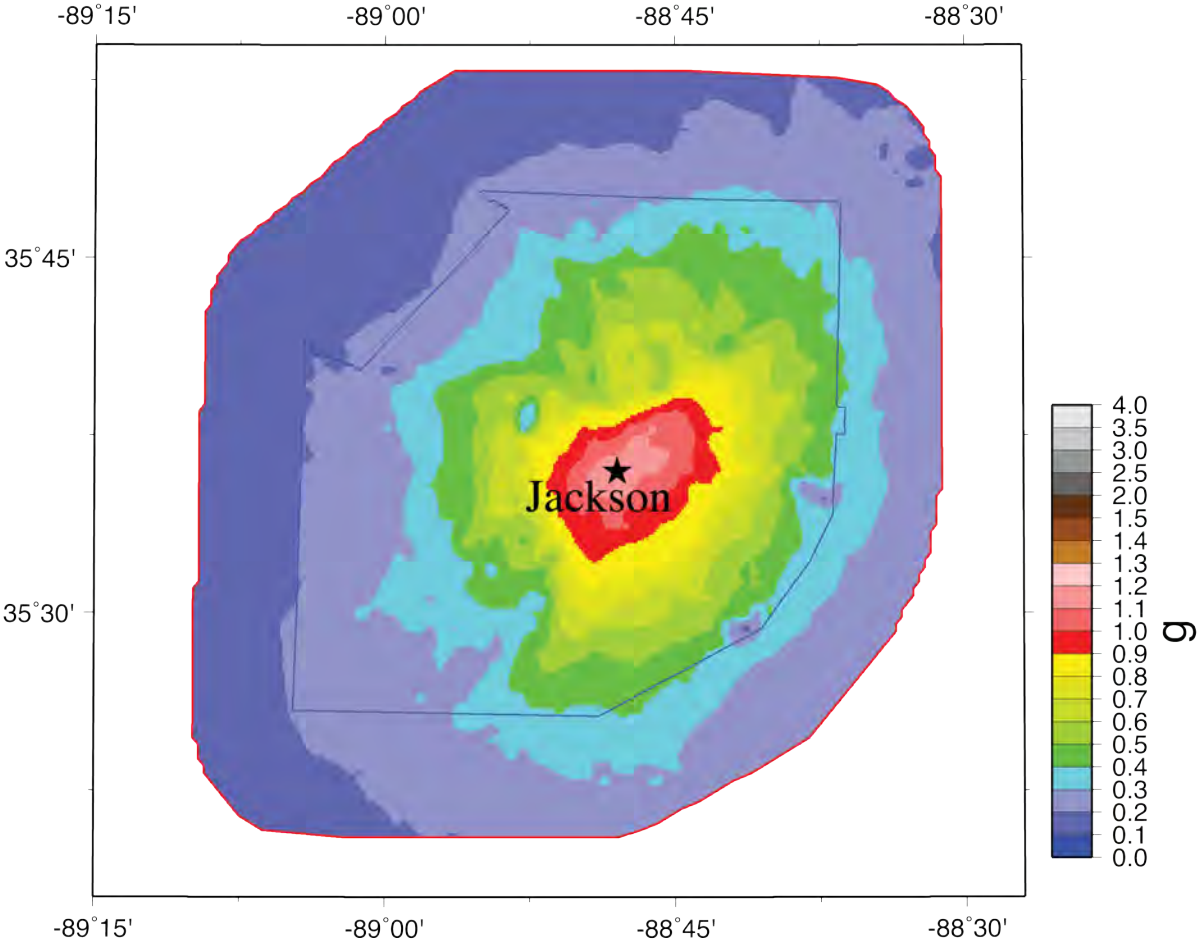
Madison Co 1.0s Hazard



NMMT M6.2, October 2021

Figure 51C: Scenario 1.0 s hazard map for a M6.2 on the Cottonwood Grove Fault (1843 Marked Tree – SW segment of NMSZ) for Madison County with the effects of local geology.

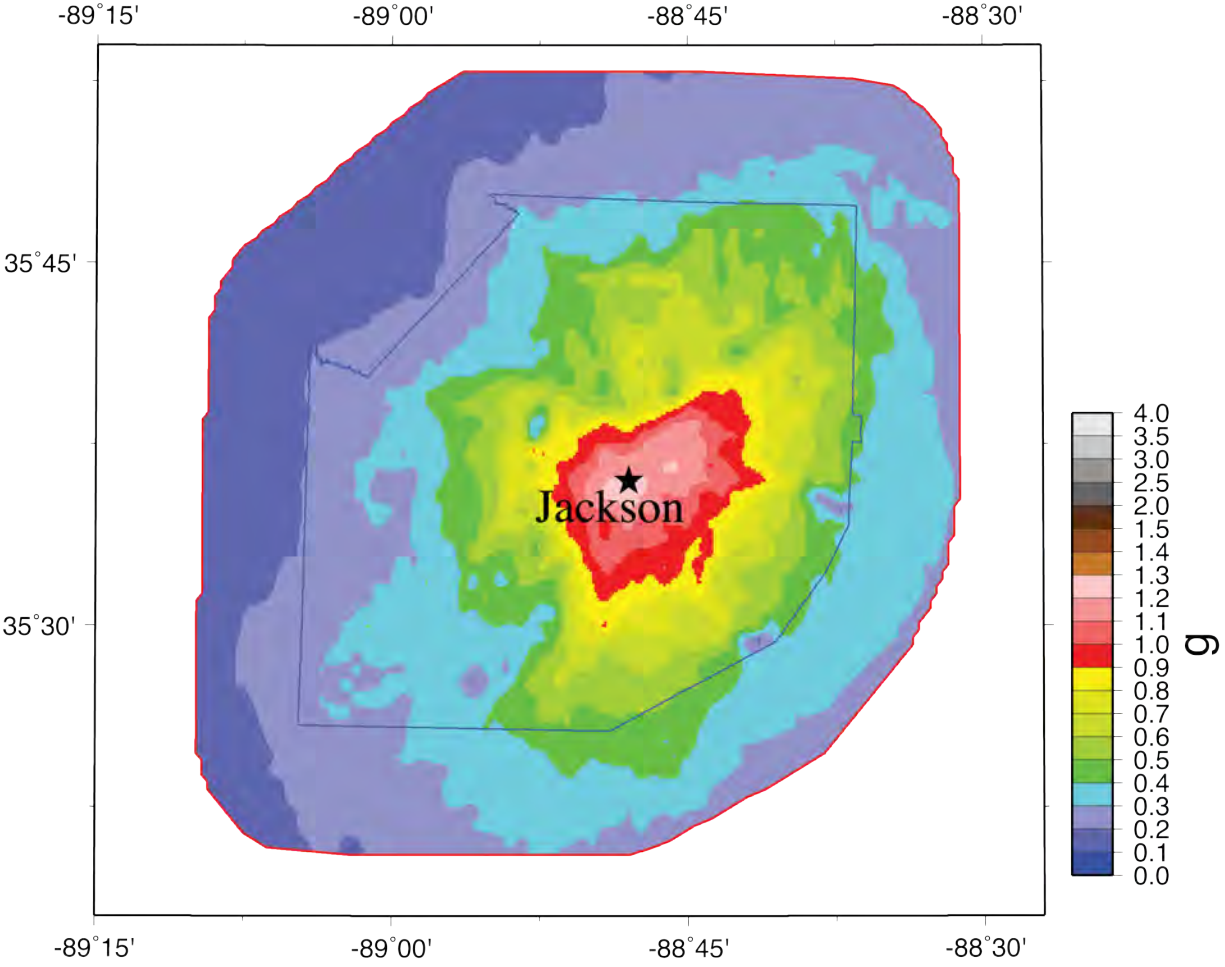
Madison Co PGA Hazard



MAD M5.8, October 2021

Figure 52A: Scenario PGA hazard map for a M5.8 hypothetical earthquake for Madison County with the effects of local geology.

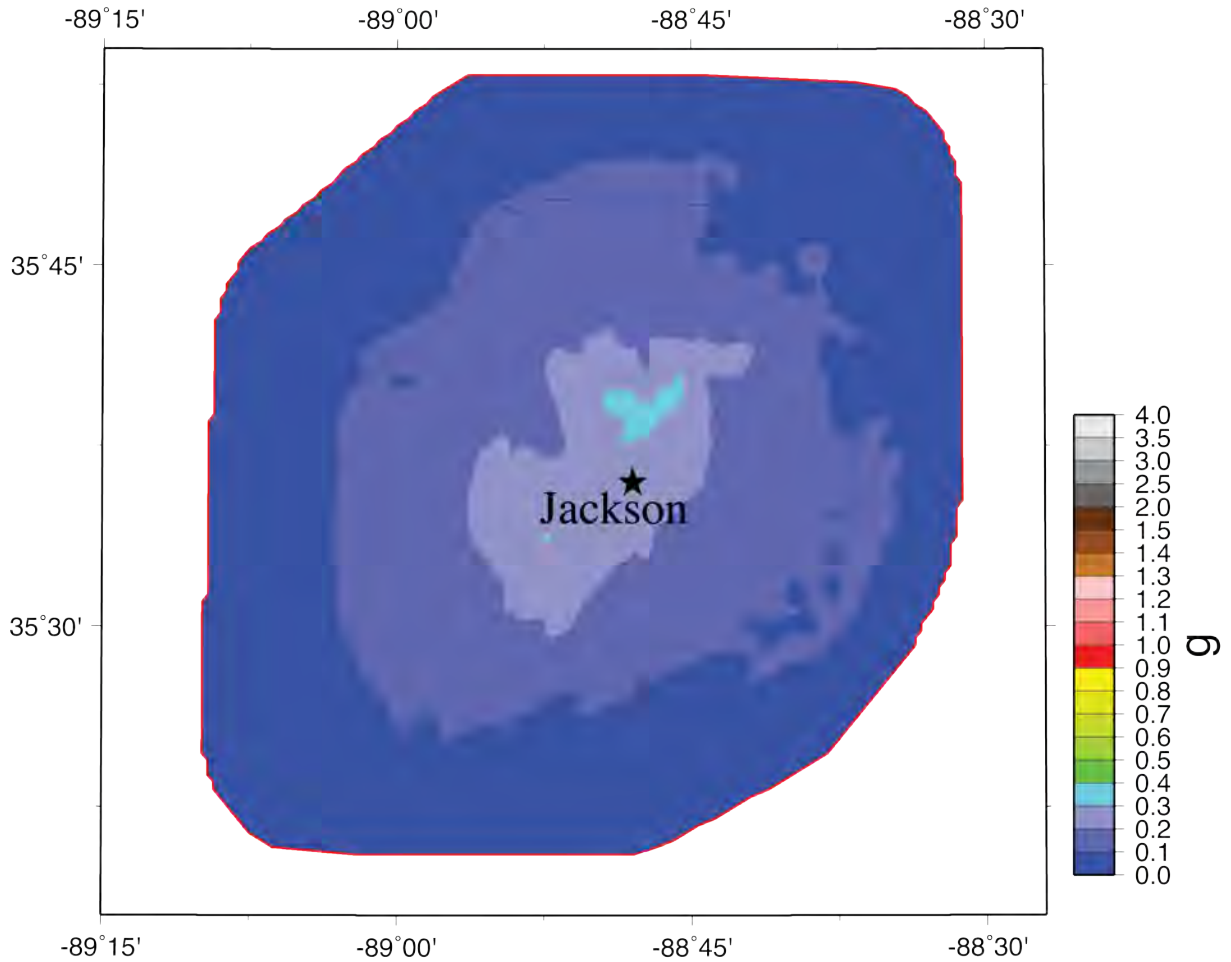
Madison Co 0.2s Hazard



MAD M5.8, October 2021

Figure 52B: Scenario 0.2 s hazard map for a M5.8 hypothetical earthquake for Madison County with the effects of local geology.

Madison Co 1.0s Hazard



MAD M5.8, October 2021

Figure 52C: Scenario 1.0 s hazard map for a M5.8 hypothetical earthquake for Madison County with the effects of local geology.

Liquefaction Hazard Maps

To generate the liquefaction hazard maps for Lauderdale County, we used the SPT-based liquefaction probability curves (LPCs) recommended above in Figures 25 and 26 for lowlands and non-lowlands, respectively. The LPCs are for Liquefaction Probability Index (LPI) exceeding 5, which is for the manifestation of liquefaction at the surface (moderate to severe liquefaction). These LPCs were used to maintain compatibility with the liquefaction maps we generated for Lake County (Cramer et al., 2019). Thus, our liquefaction hazard maps are for the probability of moderate to severe liquefaction. If the LPI_{ISH} moderate to severe liquefaction LPCs for the effects of non-liquefiable crust of Figures 27 and 28 are used, the liquefaction hazard would be reduced.

Figures 53 - 60 show the two probabilistic and six scenario liquefaction hazard maps derived from the equivalent PGA seismic hazard maps shown above. The probabilistic liquefaction hazard maps show 30 – 40% probability of liquefaction in the river flood plains and less than 10% in the non-river-flood-plains areas for 5%-in-50-years, and about 50 – 60% in the river flood plains and less than 10% in the non-river-flood-plains areas for 2%-in-50-years probability of liquefaction in Madison County. The M7.7 scenario on the Reelfoot Thrust liquefaction hazard map shows 30 – 40% probability of liquefaction in the flood plains and less than 10% in the other areas. For the M7.5 scenario on the SW arm, the liquefaction hazard map shows 20 – 30% in the flood plains and less than 10% in the other areas. The M7.3 scenario on the NE arm shows about 15 – 25% probability of liquefaction in the flood plains and less than 10% probability of liquefaction in the other areas. The largest aftershock alternatives show 10 – 20% probability of liquefaction in the flood plains and less than 10% in the other areas. And the M5.8 hypothetical Madison County earthquake shows 10 – 90% probability of liquefaction in the flood plains and about 10% or less probability in the other areas. The 1843 and 1895 M6.2 scenarios do not produce any significant liquefaction hazard and are not shown. The liquefaction hazard is low to moderate in the flood plains for the earthquake scenarios shown, except for the hypothetical M5.8 scenario where the flood plains near the epicenter have high liquefaction hazard.

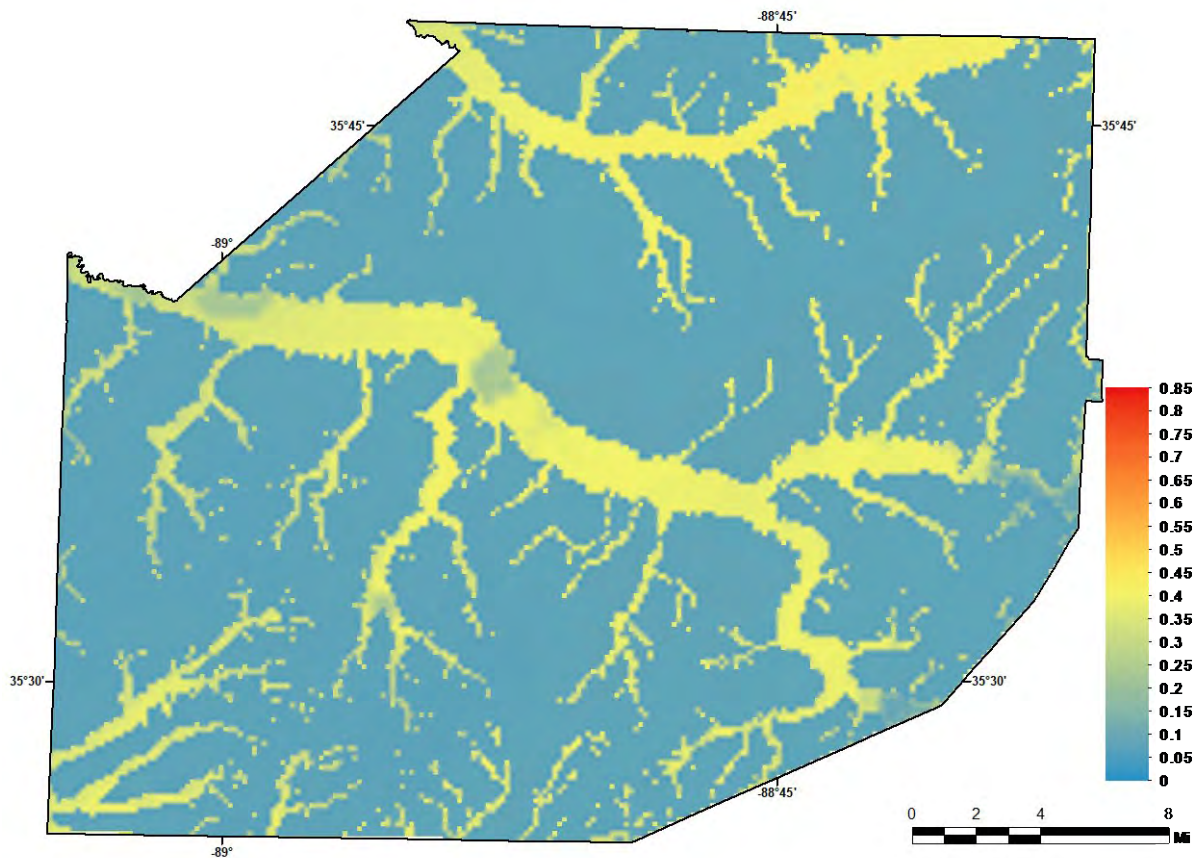


Figure 53: 5%-in-50-year liquefaction hazard map for moderate to severe liquefaction at the surface (LPI > 5) for Madison County including the effects of local geology.

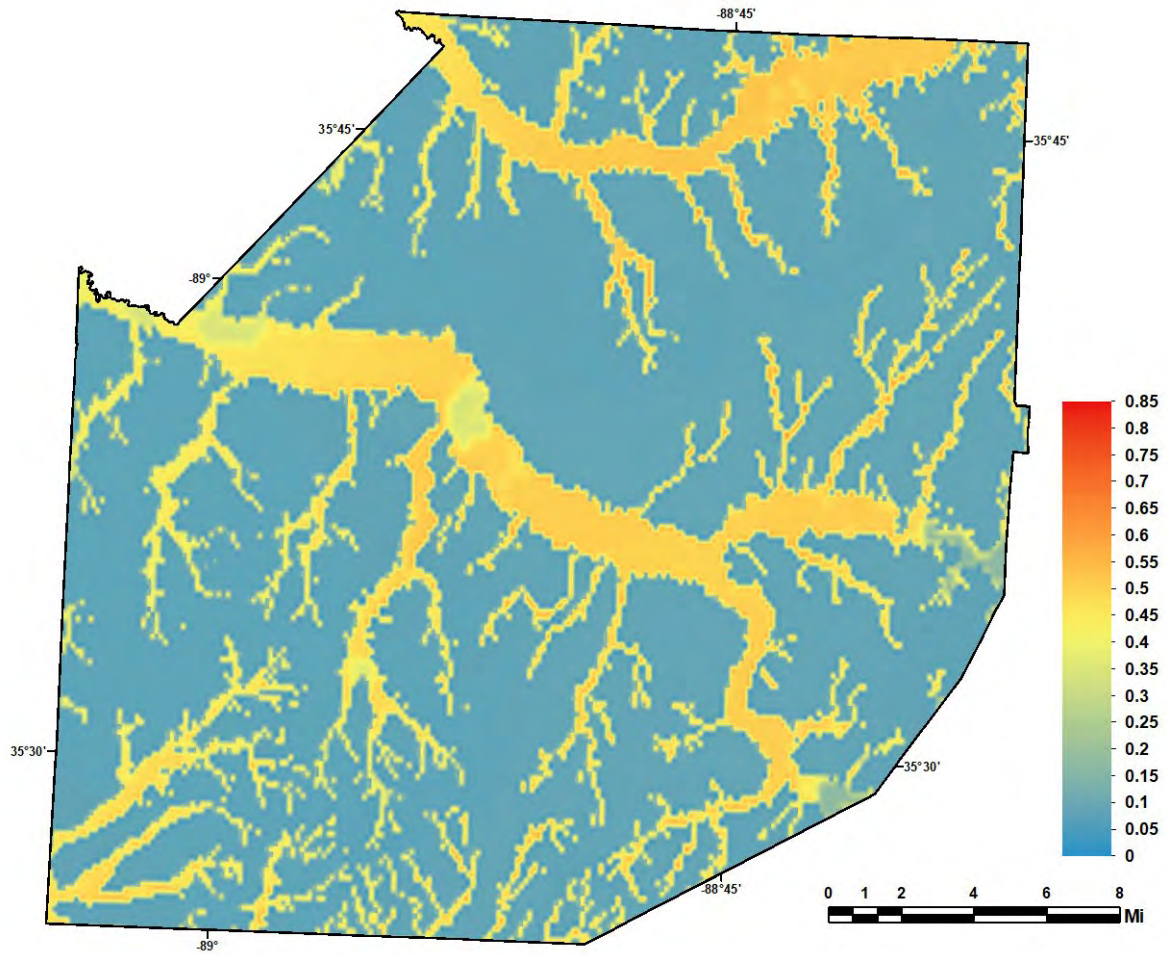


Figure 54: 2%-in-50-year liquefaction hazard map for moderate to severe liquefaction at the surface (LPI > 5) for Madison County including the effects of local geology.

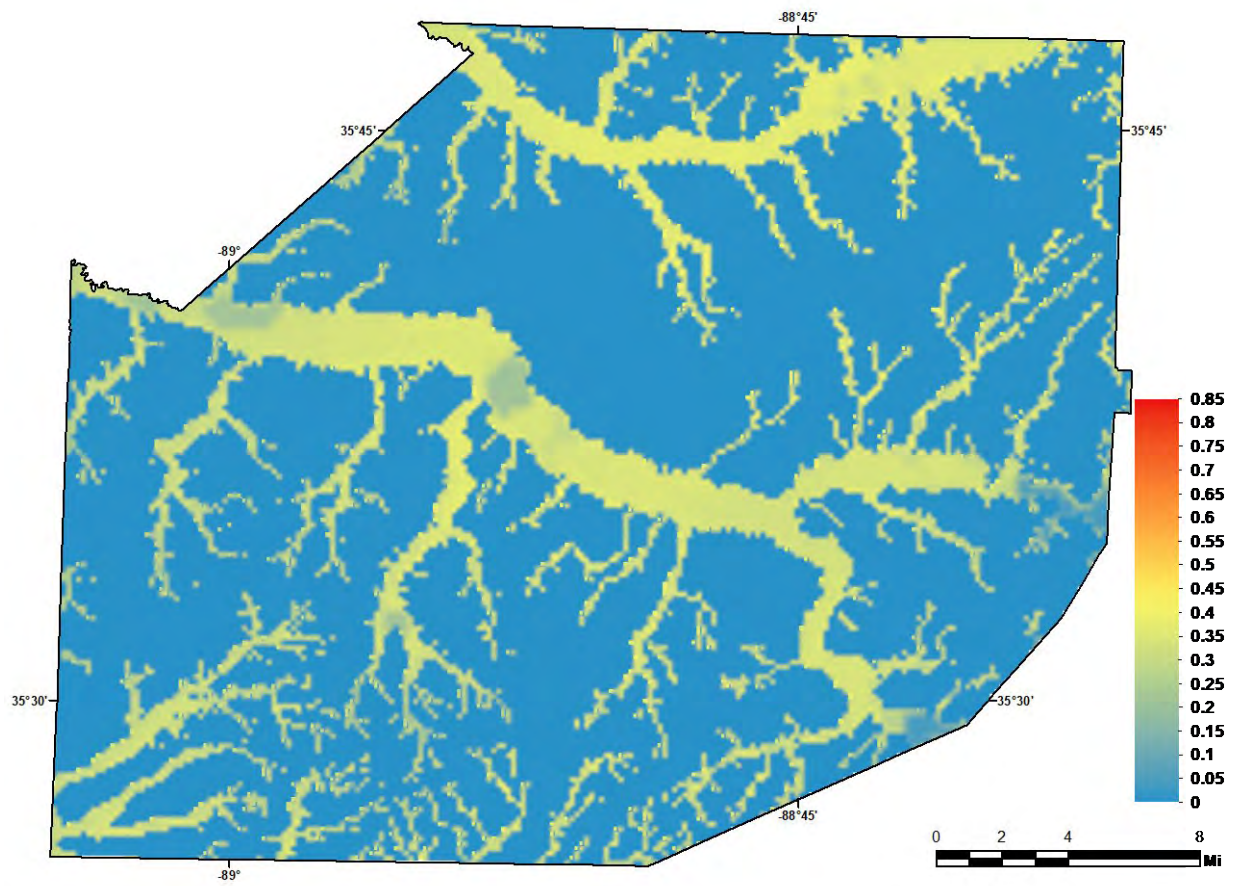


Figure 55: Scenario liquefaction hazard map for moderate to severe liquefaction at the surface (LPI > 5) for a M7.7 earthquake on the Reelfoot Thrust (central segment of NMSZ).

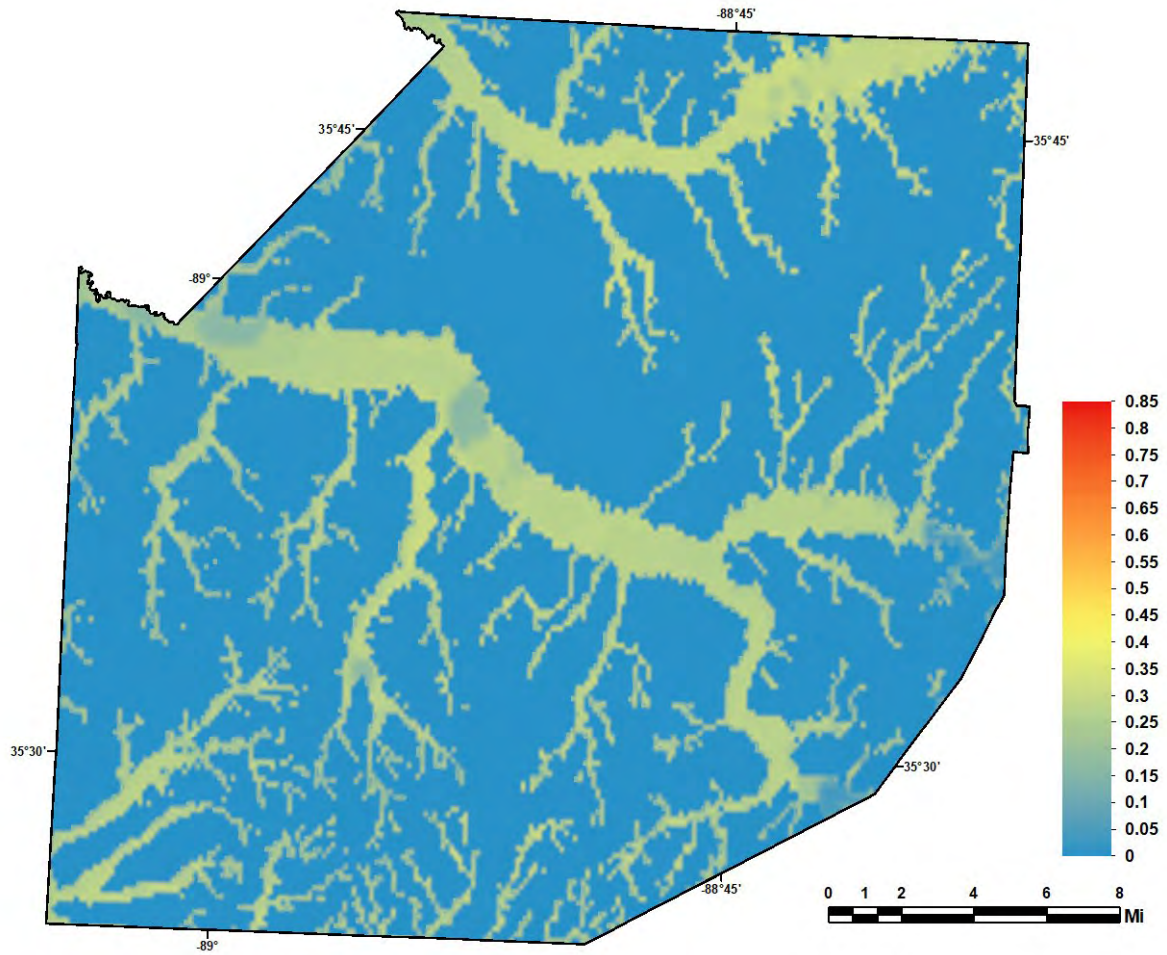


Figure 56: Scenario liquefaction hazard map for moderate to severe liquefaction at the surface (LPI > 5) for a M7.5 earthquake on the Cottonwood Grove Fault (SW segment of NMSZ).

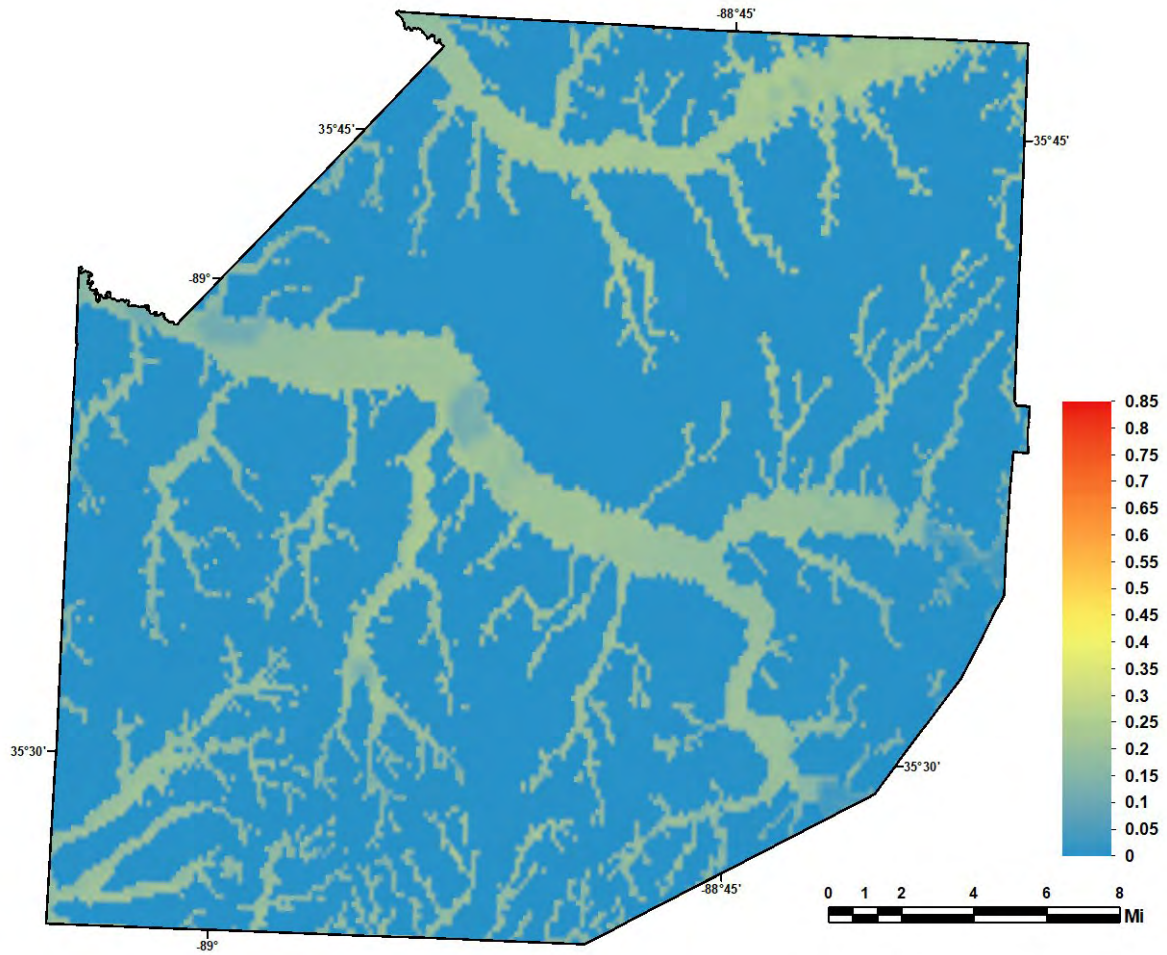


Figure 57: Scenario liquefaction hazard map for moderate to severe liquefaction at the surface (LPI > 5) for a M7.3 earthquake on the New Madrid North Fault (NE segment of NMSZ).

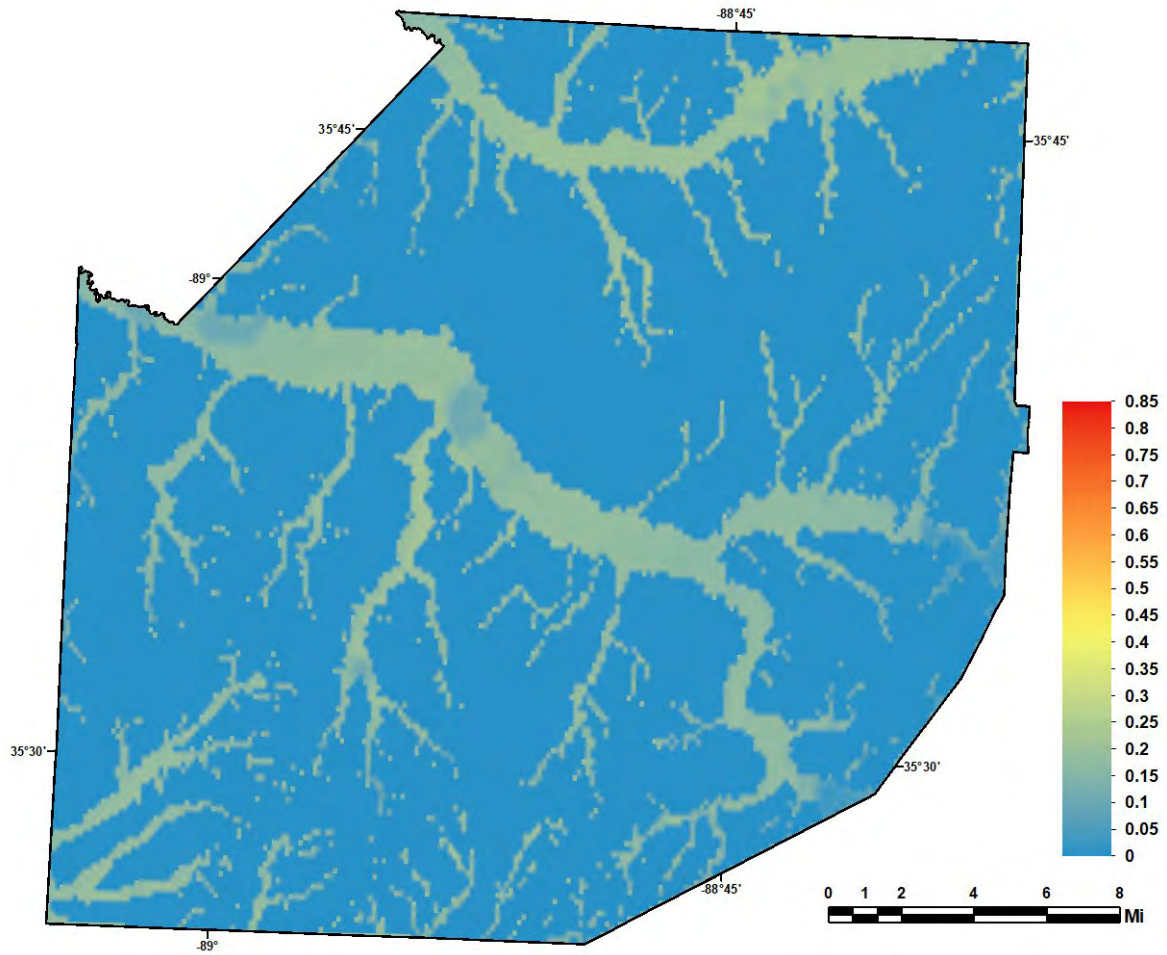


Figure 58: Scenario liquefaction hazard map for moderate to severe liquefaction (LPI > 5) for a M6.9 “Dawn” aftershock (alt. 1) on the Cottonwood Grove Fault (SW segment of NMSZ).

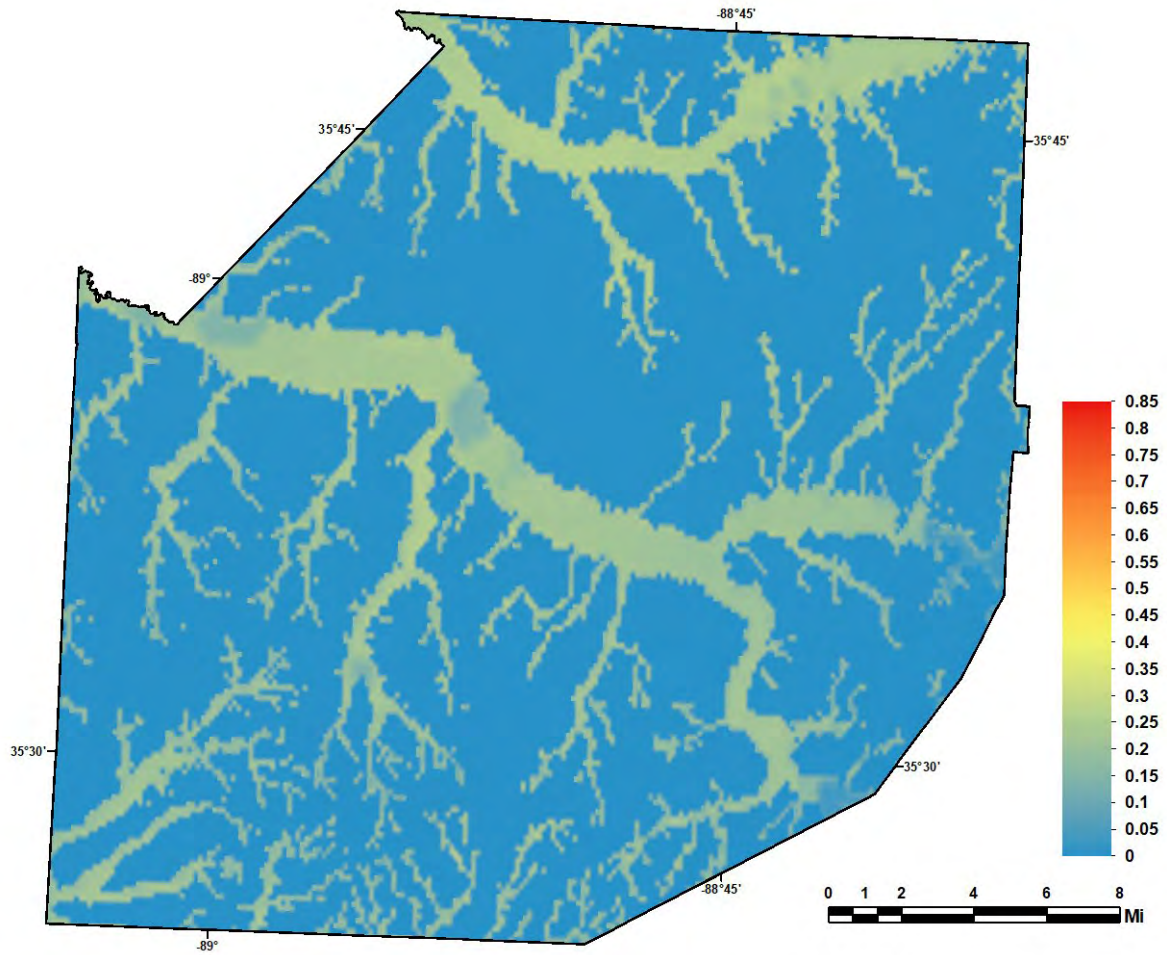


Figure 59: Scenario liquefaction hazard map for moderate to severe liquefaction (LPI > 5) for a M6.9 “Dawn” aftershock (alt. 2) on the Reelfoot Thrust (central segment of NMSZ).

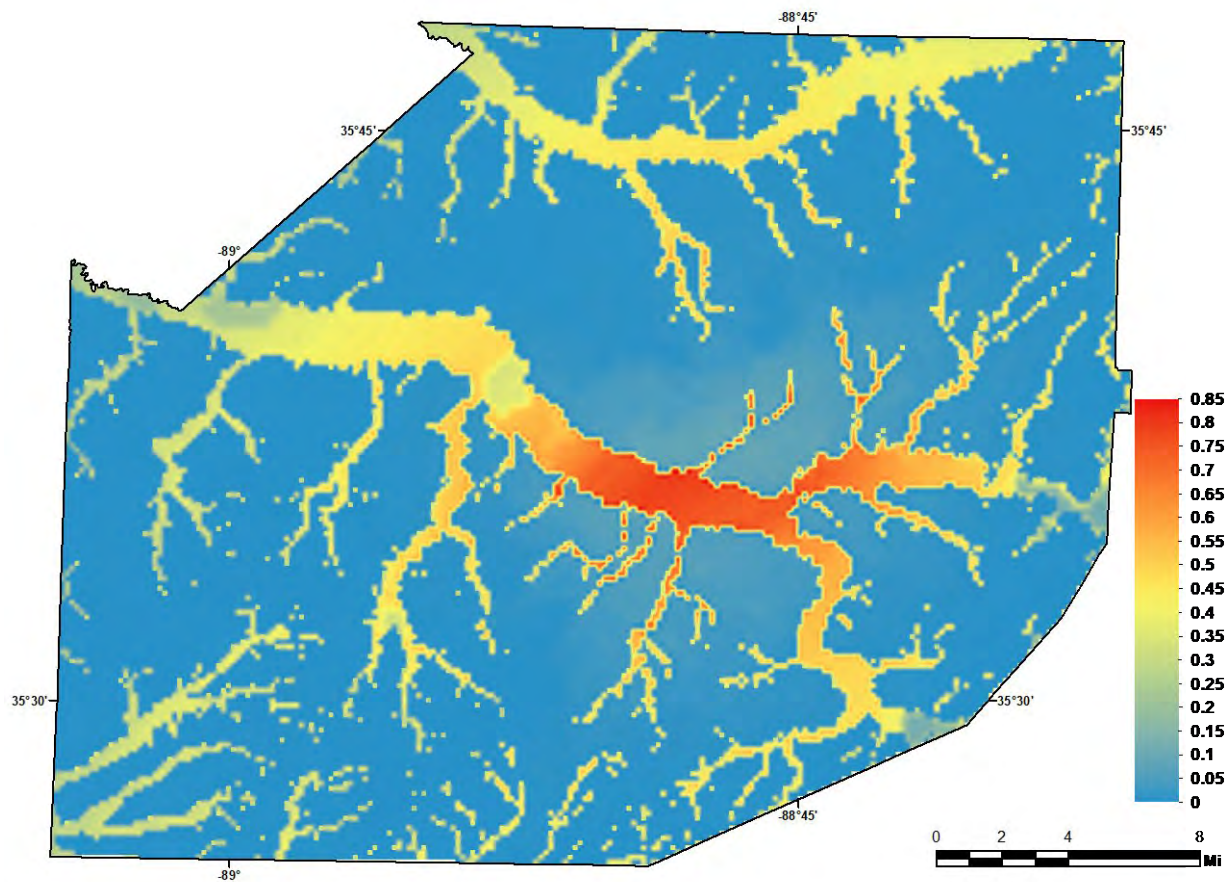


Figure 60: Scenario liquefaction hazard map for moderate to severe liquefaction (LPI > 5) for a M5.8 hypothetical Madison County earthquake (near Jackson).

Conclusions

We have produced seismic and liquefaction hazard maps that include the effects of local geology for Madison County. The products from this effort include a 3D geology database and model, a geotechnical database and liquefaction probability curves (LPCs), and probabilistic and scenario hazard maps for Madison County. The geology model is detailed for the River Alluvial and Terrace sediments down to depths of 100 ft (30 m) and more generalized for the Claiborne to Paleozoic formations. Paleozoic limestones form the bedrock of the model. The geotechnical database includes information on water table depths, and standard penetration tests (SPT). It was used to generate LPCs based on SPT measurements for river alluvium and other sediments. The liquefaction hazard maps for Madison County were based on our developed LPCs for river alluvium and terrace alluvium. The V_s measurements in Madison County were used to develop V_s values for river alluvium, terrace, and Claiborne sediments. Deeper published information from the region developed for Shelby County were used to extrapolate the Wilcox to Paleozoic V_s reference profile used in this study. Seismic and liquefaction hazard maps were generated that include the new geological, geotechnical, and

seismological information gathered. The hazard maps are both probabilistic (5% and 2% probability of being exceeded in 50 years) and for seven earthquake scenarios. Seismic hazard maps show a 50% decrease to 100% increase in hazard at short periods and a 0-100% increase at long periods compared with 2014 USGS NSHMP maps, which are for a uniform standard geology not found in western Tennessee. Liquefaction hazard maps show low to moderate hazard in Madison County for all five of the five M7 New Madrid scenarios and a low to high hazard for the M5.8 hypothetical Madison County earthquakes. The 1843 and 1895 M6.2 scenarios do not produce any significant liquefaction hazard due to more distant epicenters and a shorter duration of strong shaking.

Acknowledgements

We wish to thank those that provided data necessary for this project including Vince Antonacci, Luke Ewing and William Mann of TDEC, and the US Army Corps of Engineers. We also thank the landowners that allowed us to make geophysical measurements on their land: Deanne Ellis of Jackson City Parks Department (Fairgrounds site), Billy Ray Goldsby of the Lambuth Campus of the University of Memphis (Lambuth sites), Lisa Homes of the Tennessee Wildlife Resources Agency (Lake Graham sites), and Dr. Bob Hayes and Dr. Scott Stewart of the West Tennessee Research and Education Center, University of Tennessee (Agricultural Experimentation Station sites).

References

- Antonacci, V., and Hoyal, M., 2011, Geologic Map of the Medina Quadrangle, Tennessee. State of Tennessee Department of Environment and Conservation, Division of Geology. Scale 1:24000.
- Antonacci, V., and Hoyal, M., 2012a, Geologic Map of the Adair Quadrangle, Tennessee. State Of Tennessee Department of Conservation, Division of Geology. Scale 1:24000.
- Antonacci, V., and Hoyal, M., 2012b, Geologic Map of the Humboldt Quadrangle, Tennessee. State of Tennessee Department of Conservation, Division of Geology. Scale 1:24000.
- Antonacci, V., and Hoyal, M., 2014a, Geologic Map of the Bells Quadrangle, Tennessee. State of Tennessee Department of Conservation, Division of Geology. Draft Open File Map. Scale 1:24000.
- Antonacci, V., and Hoyal, M., 2014b, Geologic Map of the Beech Bluff Quadrangle, Tennessee. State of Tennessee Department of Conservation, Division of Geology. Draft Open File Map. Scale 1:24000.
- Atkinson, G.M., and I.A. Beresnev, 2002. Ground motions at Memphis and St. Louis from M 7.5–8.0 earthquakes in the New Madrid seismic zone, *Bull. Seism. Soc. Am.* **92**, 1-15-1024.
- Brown, D.L., 1968a, Geologic Map of the Henderson Quadrangle, Tennessee. State of Tennessee Department of Conservation, Division of Geology. Scale 1:24000.
- Brown, D.L., 1968b, Geologic Map of the Luray Quadrangle, Tennessee. State of Tennessee Department of Conservation, Division of Geology. Scale 1:24000.
- Chiu, J. M., Johnston, A. C., and Yang, Y. T., 1992. Imaging the active faults of the central New Madrid seismic zone using PANDA array data. *Seismological Research Letters* **63**, p. 375-93.
- Cox, R.T., Van Arsdale, R.B., Harris, J.B., and Larsen, D., 2001, Neotectonics of the southeastern Reelfoot Rift zone margin, central United States, and implications for regional strain accommodation. *Geology* **29**, p. 419-422.
- Cox, R.T., J. Cherryhomes, J. B. Harris, D. Larsen, R. B. Van Arsdale, S. L. Forman, 2006. Paleoseismology of the southeastern Reelfoot rift in western Tennessee and implications for intraplate fault zone evolution. *Tectonics* **25**, p. 1-17.
- Cox, R.T., Van Arsdale, R., Clark, D., Hill, A., and Lumsden, D., 2013, A revised paleo-earthquake chronology on the southeast Reelfoot rift margin near Memphis, Tennessee. *Seismological Research Letters*, v. 84, p. 402-408.

- Cox, R.T., Lumsden, D.N., and Van Arsdale, R.B., 2014. Possible relict meanders of the Pliocene Mississippi River and their implications. *Journal of Geology* **122**, p. 609-622.
- Cramer, C.H., J.S. Gomberg, E.S. Schweig, B.A. Waldron, and K. Tucker, 2006. First USGS urban seismic hazard maps predict the effects of soils, *Seism. Res. Lett.* **77**, 23-29.
- Cramer, C.H., 2006. Quantifying the uncertainty in site amplification modeling and its effects on site-specific seismic-hazard estimation in the Mississippi embayment and adjacent areas, *Bull. Seism. Soc. Am.* **96**, 2008-2020.
- Cramer, C.H., G. Rix, and K. Tucker, 2008. Probabilistic liquefaction hazard maps for Memphis, Tennessee, *Seis. Res. Lett.* **79**, 416-423.
- Cramer, C.H., and O.S. Boyd, 2014, Why the New Madrid earthquakes are M7–8 and the Charleston earthquake is ~M7, *Bull. Seism. Soc. Am.* **104**, 2884-2903.
- Cramer, C.H., J.S. Gomberg, E.S. Scheig, B. A. Waldron, and K. Tucker, 2004, *Memphis, Shelby County, Tennessee, seismic hazard maps*, U.S. Geological Survey, Open-File Report 04-1294, 41pp.
- Cramer, C.H., R.B. Van Arsdale, M.S. Dhar, D. Pryne, and J. Paul, 2014. Updating of urban seismic-hazard maps for Memphis and Shelby County, Tennessee: geology and Vs observations, *Seis. Res. Lett.* **85**, 986-996.
- Cramer, C.H., G. Patterson, and David Arellano, 2015. Final Technical Report, Updating Liquefaction Probability Curves, Seismic Hazard Model, and Urban Seismic Hazard Maps with Public Outreach for Memphis and Shelby County, Tennessee, USGS grant G14AP00099, October 30, 2015, 42 pp (available at <http://earthquake.usgs.gov/research/external/reports/G14AP00099.pdf>).
- Cramer, C.H., R.A. Bauer, J. Chung, J.D. Rogers, L. Pierce, V. Voigt, B. Michell, D. Gaunt, R.A. Williams, D. Hoffman, G.L. Hempen, P.J. Steckel, O.S. Boyd, C.M. Watkins, K. Tucker, and N. McCallister, 2017. St. Louis area earthquake hazards mapping projects: seismic and liquefaction hazard maps, *Seis. Res. Lett.* **88**, 206-223.
- Cramer, C.H., M.S. Dhar, and D. Arellano, 2018a. Update of the urban seismic and liquefaction hazard maps for Memphis and Shelby County, Tennessee: liquefaction probability curves and 2015 hazard maps, *Seis. Res. Lett.* **89**, 688-701.
- Cramer, C., R. Van Arsdale, D. Arellano, S. Pezeshk, S. Horton, T. Weathers, N. Nazemi, J.A. Jimenez, H. Tohidi, and L.P. Ogwen, 2018b, Seismic and liquefaction hazard maps for Lake County, northwestern Tennessee, (2018 SE-GSA abstract). Geological Society of America Abstracts with Programs 50. 10.1130/abs/2018SE-312570.

Cramer, C., R.B. Van Arsdale, V. Harrison, D. Arellano, S. Pezeshk, S.P. Horton, T. Weathers, N. Nazemi, J. Jimenez, H. Tohidi, and L.P. Ogweno, 2019. Lake County seismic and liquefaction hazard maps, CERl Report, 129 pp.

Cramer, C., R.B. Van Arsdale, R. Reichenbacher, D. Arellano, H. Tahidi, S. Pezeshk, S.P. Horton, R. Bhattarai, N. Nazemi, and A. Farhadi, 2020a. Dyer County seismic and liquefaction hazard maps, CERl Report, 90 pp.

Cramer, C. H., Van Arsdale, R. B., Harrison, V., Bouzeid, K., Arellano, D., Tohidi, H., Pezeshk, S., Horton, S. P., Bhattarai, R., Nazemi, N., and Farhadi, A., 2020b, Lauderdale County seismic and liquefaction hazard maps, CERl Report, 85 pp.

Cramer, C. H., Van Arsdale, R. B., Harrison, V., Arellano, D., Tohidi, H., and Bhattarai, R., 2021, Tipton County seismic and liquefaction hazard maps, CERl Report, 89 pp.

Csontos, R., and Van Arsdale, R., 2008. New Madrid seismic zone fault geometry. *Geosphere* **4**, p. 802-813.

Cupples, W., and Van Arsdale, R., 2014, The Preglacial “Pliocene” Mississippi River. *Journal of Geology* **122**, 1-15.

Dhar, M.S., and C.H. Cramer, 2018. Probabilistic seismic and liquefaction hazard analysis of the Mississippi embayment incorporating nonlinear effects, *Seis. Res. Lett.* **89**, 253-267, published online 13 December 2017.

Iwasaki, T., Tatsuoka, F., Tokida, K. and Yasuda, S., 1978. A practical method for assessing soil liquefaction potential based on case studies at various sites in Japan, Second International Conference on Microzonation for Safer Construction Research and Application 1978.

Iwasaki, T., Tokida, K., Tatsuoka, F., Watanabe, S., Yasuda, S., and Sato, H., 1982. Microzonation for soil liquefaction potential using simplified methods. Proceedings 3rd International Conference on Microzonation, Seattle, USA. 1319-1330.

Jewel, J.W., 2006, Geologic Map of the Jackson North Quadrangle, Tennessee. State of Tennessee Department of Environment and Conservation, Division of Geology. Scale 1:24000.

Louie, J.N., 2001. Faster, Better: Shear-Wave Velocity to 100 Meters Depth from Refraction Microtremor Arrays. *Bulletin of the Seismological Society of America* **91**, 347–364.

Lumsden, D.N., Cox, R.T., Van Arsdale, R.B., and Cupples, W.B., 2016, Petrology of Pliocene Mississippi River alluvium: provenance implications. *The Journal of Geology* **124**, 501-517.

Markewich, H. H., Wysocki, D. A., Pavich, M. J., Rutledge, E. M., Millard, H. T., Rich, F. J., et al. (1998). Paleopedology plus TL, 10Be, and 14C dating as tools in stratigraphic and paleoclimatic investigations, Mississippi River valley, U.S.A. *Quaternary International* **51**, 143–167. doi: 10.1016/s1040-6182(97)00041-4.

Maurer, B. W., Green, R. A., and Taylor, O.-D. S., 2015. Moving towards an improved index for assessing liquefaction hazard: Lessons from historical data, *Soils and Foundations* **55**, 778–787.

Odum, W., Hofmann, F., Van Arsdale, R., and Granger, D., 2020, New $^{26}\text{Al}/^{10}\text{Be}$ and (U-Th)/He constraints on the age of the Upland Complex, central Mississippi River Valley, *Geomorphology* **371**, 1-9, 107448.

Parks, W.B., 1968a, Geologic Map of the Beech Bluff Quadrangle, Tennessee. State of Tennessee Department of Conservation, Division of Geology. Scale 1:24,000.

Parks, W.B., 1968b, Geologic Map of the Cedar Grove Quadrangle, Tennessee. State of Tennessee Department of Conservation, Division of Geology. Scale 1:24,000.

Parks, W.B., 1968c, Geologic Map of the Medon Quadrangle, Tennessee. State of Tennessee Department of Conservation, Division of Geology. Scale 1:24,000.

Parks, W.B., 1968d, Geologic Map of the Juno Quadrangle, Tennessee. State of Tennessee Department of Conservation, Division of Geology. Scale 1:24,000.

Parks, W.B., 1968e, Geologic Map of the Jackson South Quadrangle, Tennessee. State of Tennessee Department of Conservation, Division of Geology. Scale 1:24,000.

Parks, W.B., 1968f, Geologic Map of the Claybrook Quadrangle, Tennessee. State of Tennessee Department of Conservation, Division of Geology. Scale 1:24,000.

Petersen, M. D., M. Moschetti, P. Powers, C. Mueller, K. Haller, A. Frankel, Y. Zeng, S. Rezaeian, S. Harmsen, O. Boyed, N. Field, R. Chen, K. Rukstales, N. Luco, R. Wheeler, R. Williams, and A. Olsen, 2014, *The 2014 update of the United States national seismic hazard models*, U.S. Geological Survey, OFR 2014-X1091, 255 p.

Pezeshk, S., C.V. Camp, L. Liu, J.M. Evens, and J. He, 1998. Seismic acceleration coefficients for West Tennessee and expanded scope of work for seismic acceleration coefficients for West Tennessee phase 2 – field investigations, Final Report to Tennessee Dept. of Transportation, 420 pp.

Rodbell, D. T., 1996, Subdivision, subsurface stratigraphy, and estimated age of fluvial-terrace deposits in northwestern Tennessee. U.S. Geologic Survey Bulletin, v. 2128, 24 pp.

Saucier, R.T., 1987, Geomorphological interpretations of late Quaternary terraces in western

Tennessee and their regional tectonic implication. U.S. Geologic Survey Professional Paper 1336-A, 19 pp.

Saucier, R.T., 1994, Geomorphology and Quaternary Geologic History of the Lower Mississippi Valley: Vicksburg, Mississippi. U.S. Army Engineer Waterways Experiment Station, v. 1, 364 p., and v. 2, map plates.

Schrader, T.P., 2008. Potentiometric surface in the Sparta-Memphis aquifer of the Mississippi embayment, Spring 2007, U.S. Geological Survey Scientific Investigations Map 3014.

Seed, H. B., and Idriss, I. M. (1971). "Simplified procedure for evaluating soil liquefaction potential." J. Soil Mechanics and Foundations Div., ASCE **97**(SM9), 1249–273. Seed, H. B., and Idriss, I. M. (1982). Ground Motions and Soil Liquefaction During Earthquakes, Earthquake Engineering Research Institute, Oakland, CA, 134 pp.

Stokoe II, K.H., and J.C. Santamarina, 2000. Seismic-wave-based testing in geotechnical engineering, International Conference on Geotechnical and Geological Engineering, GeoEng 2000, 1490–1536.

Tuttle, M. P., Schweig, E. S., Sims, J. D., Lafferty, R. H., Wolf, L. W., and Haynes, M. L., 2002. The earthquake potential of the New Madrid seismic zone, *Bulletin Seismological Society of America* **92**, 2080–2089, doi: 10.1785/01200 10227.

Tuttle, M. P., M. P., Wolf, L. W., Starr, M. E., Villamor, P., Mayne, P. W., Lafferty, R. H., et al., 2019, Evidence for large New Madrid earthquakes about A.D. 0 and B.C. 1050, Central United States, *Seismological Research Letters*, v. 90, n. 3, p. 1393-1406.

Van Arsdale, R.B., Bresnahan, R.P., McCallister, N.S., and Waldron, B., 2007. The Upland Complex of the central Mississippi River Valley: Its origin, denudation, and possible role in reactivation of the New Madrid seismic zone, in Stein, S., and Mazzotti, S., eds., *Continental Intraplate Earthquakes: Science, Hazard, and Policy Issues*. Geological Society of America Special Paper 425, p. 177-192.

Appendices (separate files)

Please see accompanying files in APPENDIX_A and APPENDIX_B folders.